Title
Understanding species and community responses to past and future climate change

Author
Williams, John Eric

Publication Date
2018

UNIVERSITY OF CALIFORNIA, MERCED

Understanding species and community responses to past and future climate change

A dissertation submitted in partial satisfaction of the requirements
for the degree Doctor of Philosophy

in

Environmental Systems

by

John Eric Williams

Committee in charge:

Professor Michael N. Dawson, Chair
Professor Jessica L. Blois
Professor Jenny L. McGuire
Professor Jason Sexton

2018

Copyright

The Dissertation of John Eric Williams is approved, and it is acceptable in quality and form for publication on microfilm and electronically:

Jessica L. Blois, Advisor

Michael N. Dawson, Chair

Jenny L. McGuire

Jason Sexton

Table of Contents

List of Tables

List of Figures

Acknowledgements

First and foremost, I would like to thank my family. My wife Tiffany has stuck by my side throughout my master’s and Ph.D. programs and has been my rock and foundation, allowing me to make it through the grind that is graduate school; without her I doubt I would be where I am today.

Secondly, I would like to thank Dr. Jessica L. Blois. She has served as an amazing mentor and while my wife was my personal foundation through these years, Jessica has served as my educational foundation. Putting her students before herself, it has been a blessing to work with her. She has spent countless hours mentoring and guiding me throughout my time at UC Merced and has pushed me to be the best scientist and graduate student that I could be. Her guidance has allowed me to reach milestones in my career that I never thought were possible and at some points seemed impossible to attain. Thank you for all your hard work and dedication over the past five and a half years.

I would also like to thank my committee members, Dr. Michael N. Dawson, Dr. Jenny L. McGuire, and Dr. Jason Sexton for their invaluable comments, guidance, and direction during my time at UC Merced. I am grateful for your time and support.

Finally, I would like to acknowledge all of the past and current members of the Blois lab during my time here, all of whom have been some of my greatest assests over the last several years. Their conversations, advice, guidence, and expertise have been invaluable and guided me through some difficult tasks and problems. Thank you all for support, insight, and time.

Chapter 2 is a full reprint of the material as it appers in Journal of Biogeography 2018. The dississertation author is the primary investigator and primary author of this paper. Jessica L. Blois aided in development of the project, analyses, and provided substantial edits to the main manuscript. Jessica L. Blois was the advisor throughout.

Curriculum Vitae

Education

Ph.D., 2018	Environmental Systems, University of California, Merced
M.S., 2013	Biology, University of North Carolina Wilmington
B.S., 2010	Biology, University of North Carolina Wilmington

Publications

Williams, J.E. and WM. D. Webster (accepted). Noteworthy record of the woodland jumping mouse (*Napaeozapus insignis*) in western South Carolina. Journal of the North Carolina Academy of Sciences.

Williams, J.E. and J.L. Blois (submitted). Determining patterns of community assembly over the last 17,000 years using species distribution models and Late Quaternary fossil assemblages.

Williams, J.E. & Blois, J.L. (2018) Range shifts in response to past and future climate change: Can climate velocities and species' dispersal capabilities explain variation in mammalian range shifts? *Journal of Biogeography*, **45**, 2175–2189.

Blois, J.L. and **J.E. Williams** (2016). Quaternary biogeography and climate change. In: Kliman, R.M. (ed.), The Encyclopedia of Evolutionary Biology. vol. 3, pp. 395-405. Oxford: Academic Press.

Honors/Awards

2018	Graduate Dean's Dissertation Fellowship
2017	Environmental Systems Travel Award, UC Merced
2016	Environmental Systems Travel Award, UC Merced
2015	School of Engineering Dean's Travel Fellowship, UC Merced
2015	UC Merced Natural Reserve System Scholarship, UC Merced
2014-2016	Environmental Systems Summer Fellowship, UC Merced
2011-2012	Parnell Biology Fellowship, UNC-Wilmington
2010	Magna Cum Laude, UNC-Wilmington
2009-2010	National Science and Math Talent Grant, UNC-Wilmington

Teaching Experience

Fall 2018	Teaching Assistant for Intro to Earth Systems Science, UC Merced

Spring 2018	Teaching Assistant for Contemporary Biology and Intro to Earth Systems Science, UC Merced
Fall 2017	Teaching Assistant for Terrestrial Ecosystem Ecology, UC Merced
Fall 2015	Teaching Assistant for Contemporary Biology, UC Merced
Fall 2014	Teaching Assistant for Contemporary Biology, UC Merced
Spring 2014	Teaching Assistant for Ecosystems of California, UC Merced
Fall 2013	Teaching Assistant for Contemporary Biology, UC Merced
Spring 2013	Teaching Assistant for General Biology, UNC-Wilmington
Fall 2011	Teaching Assistant for General Biology, UNC-Wilmington

Research Experience

2014	International PhD course: Species Distribution Models
2013-2014	Methods in Paleoecology
2013	Acoustical Bat Surveys
2013, 2015	Mammal Trapping Surveys
2011	Sonobat Field Techniques Workshop

Presentations

June 2018	Oral Presentation, American Society of Mammalogists Meeting
July 2017	Poster, American Society of Mammalogists Meeting
January 2017	Poster, International Biogeography Society Meeting
June 2016	Poster, The American Quaternary Association
March 2016	Oral Presentation, Environmental Systems Castle Seminar Series, UC Merced
August 2015	Oral Presentation, Ecological Society of America
January 2015	Poster, International Biogeography Society Meeting
August 2014	Oral Presentation, Ecological Society of America
October 2013	Oral Presentation, Environmental Systems Castle Seminar Series, UC Merced
March 2012	Oral Presentation, The North Carolina Academy of Science Annual Meeting

Professional Service

Journal Article Reviewer (2016 – Present): I have reviewed articles for the following journals: Frontiers of Biogeography.

Synergistic Activities

2017-Present	International Biogeography Society Social Media Intern
2016	STEM Day, Cub Scouts of America, Merced CA
2014-2017	Mammal Research Presentation/Owl Pellet Dissections UC Merced naturalist course
2012	Night at the Museum, Cape Fear Museum, Wilmington NC

Abstract of the Dissertation

Understanding species and community responses to past and future climate change

by

John Eric Williams

Doctor of Philosophy, Environmental Systems
University of California, Merced 2018
Dr. Jessica L. Blois, Graduate Advisor
Dr. Michael N. Dawson, Chair

Successful conservation depends on a solid understanding of how climate change and biological interactions regulate biodiversity across both space and time, so that the distribution of species, communities, and ecosystems can be accurately predicted in responses to future climate change. Because species tend to respond to environmental changes in an idiosyncratic manner, it is difficult to generalize and predict biodiversity patterns for the future. The main goal of this dissertation is to increase our understanding of the effects that climate change had on species and communities in the past so that we can use the observed and estimated responses (from models and empirical data) to better inform our predictions of how species and communities may respond to climate change in the future. To complete this goal, I first examined the patterns of mammalian range shifts during the late Quaternary and estimated how the velocity of climate change and the dispersal ability of a species affects the magnitude of species range shifts in response to climate change. Findings from this research show that the broad pattern of species range shifts are poleward, but overall, species respond to climate change with a multidirectional response. Species are also projected to shift their ranges at a much faster rate in the future when compared to estimated past range shifts. The factors estimated to increase past rates of range shift are the velocity of temperature and precipitation change, while species traits appear to determine shift rates in the future. I next examined the factors associated with the assembly of small mammal communities since the Last Glacial Maximum and determined if those factors changed over time in relation to climate change. Using species distribution models and the fossil record, I determined if small mammal communities preserved in a fossil deposit in northern California at various time periods in the past assembled as a function of environmental filtering or competition. Results suggest that climate (environmental filtering) plays a large role in determining the species composition of a community in any given time period, but under certain scenarios competition could be an additional determinant for the integration of single species into the community. Lastly, I examined how mammalian communities in North America are expected to change in the future as a response to anthropogenic climate change. I examined this question using stacked species distribution models and projected these models into two future time periods and under two different representative concentration pathways. Results from this study suggests that large areas of the southeastern US and the deserts of the southwest will lose species, on average, while the Rocky Mountains and the interior portion of Canada will gain species. I also determined that large areas of Canada are expected to harbor novel mammalian communities as species respond individualistically to climate change. Overall, by examining the factors that drive specie range shifts, examining processes important to community assembly patterns, and estimating species responses to future climate change, I have generated findings that are valuable for efforts to develop conservation strategies around the globe. Research from this dissertation is also one of first examinations of the development of novel mammalian communities in North America as a response to future climate change over a large spatial scale, and the results from this study will be important in providing conservation managers with areas of potential diversity loss and change in the coming future.

1 Introduction

1.1 Background

Climate patterns across the globe have fluctuated throughout Earth's history ranging from periods of extreme cold, which contained large ice sheets, to extreme warm periods where ice-caps were not present even at the poles (Zachos et al. 2001). Currently, we are faced with an anthropogenic warming event that is predicted to warm the globe at rates equal to or faster than those observed over the last millennia (Allen et al. 2000; IPCC 2014). Determining how species, both flora and fauna, are going to respond to the increased rates of climate change is a key concern as scientists and managers attempt to conserve and mitigate species, ecological and functional diversity, and ecosystem loss due to anthropogenic climate change. Unfortunately, our understanding of potential species responses to future climate change is limited, making it difficult to develop efficient conservation management strategies.

Overall, species exhibit multiple responses to environmental change (Blois and Hadly 2009). A species can undergo changes in its local population abundances due to climate change (Andrewartha and Birch 1954), which can then lead to other changes at the population and genetic levels of the species. Changes in populations can lead to extirpation of individuals in one portion of a species' range and/or lead to the establishment of individuals in a previously unoccupied portion of their range, resulting in a shift of the species' range (Blois and Hadly 2009; Hewitt 2000; Lundberg et al. 2000). Species can also alter their phenology in response to climate change, leading to loss or establishment of new species interactions due to changes in daily or seasonal activity times (Parmesan and Yohe 2003; Root et al. 2003; Walther et al. 2002; Winder and Schindler 2004). The aggregate effect of individual species responses to climate change can and will lead to changes in the overall community structure, diversity, and ecosystem function of an area (Blois et al. 2010; Grayson 2006; Lyman 2014). The aggregate of individual species changes can also lead to the development of 'no-analog' assemblages, which are assemblages that are compositionally different from any observed today (Graham et al. 1996; Williams and Jackson 2007). These no-analog communities have been observed to occur during periods of significant climate transitions (Shuman et al. 2009; Williams and Jackson 2007). While we know and understand how species have responded to climate change overall, the detailed understanding needed to effectively predict species responses and generate effective conservation strategies for species regarding their responses future climate change is still lacking.

By understanding and quantifying the patterns of species response to past episodes of climate warming and cooling, we can transfer the gained knowledge and use it to more accurately predict how species and communities will respond during similar future climate change. The late Quaternary serves as a unique time period to examine the responses of species and communities to climate and other kinds of environmental changes. Since the Last Glacial Maximum (LGM) 21-18,000 years ago, the earth has experienced several abrupt and significant climate change events such as the Bølling-Allerød warming episode and the rapid cooling that occurred during the Younger Dryas (Liu et al. 2009). The late Quaternary also experienced periods of relative climatic stability (Dansgaard et al. 1993). Beause all of the extant species experienced the climatic episodes of the late Quaternary, we can examine their responses to those climate change events to gain insight on how they may respond to future climate change.

1.2 Purpose of Dissertation

With access to climate and species data that span from the LGM to the present day, the purpose of this dissertation is to examine, analyze, and interpret extant species and community responses to past climate change and predict their responses to future climate. Data obtained from this dissertation will increase our insight and expectations for how species and communities will respond to future climate change. I approached this question from several angles: I examined local to regional to continental scales, I examined responses seen in the past and anticipated for the future, and I focused on a variety of responses (range shifts, community assembly, and macroecological attributes such as richness and dissimilarity).

First, in order to understand how species will respond to future climate change, I estimated how they responded to past and future climate change events, focusing on range shifts across western North America. I did this by estimating species range shifts for 122 North American mammal species throughout five time periods during the late Quaternary and two time periods in the future. This allowed me to estimate the overall patterns (direction and rate) of species range shifts. I then determined if dispersal distance, body size, and climate velocities explained the estimated variation in species range shifts using generalized additive models.

After determining the patterns of species range shifts, I then examined the mechanisms that drive community assembly patterns of small mammals at the local scale. I did this by predicting the species that would be present at one site in northern California, Samwell Cave, throughout the late Quaternary using species distribution models, which served as a climate-based community hypothesis. I then compared the climate-based hypotheses and a stochastic community hypothesis against empirical data for the site to determine which assembly mechanism more accurately predicted the community comoposition of Samwell Cave over the previous 18,000 years. Determining that neither climate nor stochastic mechanisms perfectly predict community composition, I then performed a community trait analysis to estimate the potential importance of competition in structuring the Samwell Cave communities since the LGM.

After examining single species responses to climate change and estimating the importance of climate in structuring local communities, I then estimated the effect that future climate change may have on North American mammalian communities. I did this by generating stacked species distribution models for 390 mammalian species in the contemporary time period and forecasting those models to two different representative concentration pathways (rcp 4.5 and 8.5) for AD 2050 and AD 2070. This allowed me to determine how species richness, community composition, and community dissimilarity may change across North America in response to future climate change. The aggregated results of my dissertation provide an overview of expectations, responses, and mechanisms that drive mammalian species and community response to climate change.

1.3 References

Allen, M.R., Stott, P.A., Mitchell, J.F., Schnur, R., & Delworth, T.L. (2000) Quantifying the uncertainty in forecasts of anthropogenic climate change. *Nature*, **407**, 617–620.

Andrewartha, H.G. & Birch, L.C. (1954) *The distribution and abundance of animals.* University of Chicago Press, Chicago.

Blois, J.L. & Hadly, E.A. (2009) Mammalian Response to Cenozoic Climatic Change. *Annual Review of Earth and Planetary Sciences*, **37**, 181–208.

Blois, J.L., McGuire, J.L., & Hadly, E.A. (2010) Small mammal diversity loss in response to late-Pleistocene climatic change. *Nature*, **465**, 771–4.

Dansgaard, W., Johnsen, S.J., Clausen, H.B., Dahl-Jensen, D., Gundestrup, N.S., Hammer, C.U., Hvidberg, C.S., Steffensen, J.P., Sveinbjörnsdottir, A.E., Jouzel, J., & Bond, G. (1993) Evidence for general instability of past climate from a 250-kyr ice-core record. *Nature*, **364**, 218–220.

Graham, R., Lundelius, E., Graham, M., Schroeder, E., Toomey, R., Anderson, E., Barnosky, A., Burns, J., Churcher, C., Grayson, D., Guthrie, R., Harington, C., Jefferson, G., Martin, L., McDonald, H., Morlan, R., Semken, H., Webb, S., Werdelin, L., & Wilson, M. (1996) Spatial Response of Mammals to Late Quaternary Environmental Fluctuations. *Science*, **272**, 1601–6.

Grayson, D.K. (2006) The Late Quaternary biogeographic histories of some Great Basin mammals (western USA). *Quaternary Science Reviews*, **25**, 2964–2991.

Hewitt, G. (2000) The genetic legacy of the Quaternary ice ages. *Nature*, **405**, 907–13.

Liu, Z., Otto-Bliesner, B.L., He, F., Brady, E.C., Tomas, R., Clark, P.U., Carlson, A.E., Lynch-Stieglitz, J., Curry, W., Brook, E., Erickson, D., Jacob, R., Kutzbach, J., & Cheng, J. (2009) Transient simulation of last deglaciation with a new mechanism for Bolling-Allerod warming. *Science*, **325**, 310–4.

Liu, Z., Carlson, A.E., He, F., Brady, E.C., Otto-Bliesner, B.L., Briegleb, B.P., Wehrenberg, M., Clark, P.U., Wu, S., Cheng, J., Zhang, J., Noone, D., & Zhu, J.

(2012) Younger Dryas cooling and the Greenland climate response to CO2. *Proceedings of the National Academy of Sciences of the United States of America*, **109**, 11101–4.

Parmesan, C., Yohe, G., & Andrus, J.E. (2003) A globally coherent fingerprint of climate change impacts across natural systems. *Nature*, **421**, 37–42.

Root, T.L., Price, J.T., Hall, K.R., Schneider, S.H., Rosenzweig, C., & Pounds, J.A. (2003) Fingerprints of global warming on wild animals and plants. *Nature*, **421**, 57–60.

Shuman, B.N. & Newby, P. (2009) Abrupt climate change as an important agent of ecological change in the Northeast U.S. throughout the past 15,000 years. *Quaternary Science Reviews*, **28**, 1693–1709.

Williams, J.W. & Jackson, S.T. (2007) Novel climates, no-analog communities, and ecological surprises. *Frontiers in Ecology and the Environment*, **5**, 475–482.

Winder, M. & Schindler, D.E. (2004) Climatic effects on the phenology of lake processes. *Global Change Biology*, **10**, 1844–1856.

Zachos, J., Pagani, M., Sloan, L., Thomas, E., & Billups, K. (2001) Trends, rhythms, and aberrations in global climate 65 Ma to present. *Science*, **292**, 686–93.

2 Range shifts in response to past and future climate change: can climate velocities and species' dispersal capabilities explain variation in mammalian range shifts?

2.1 Abstract

Range shift is a relatively well-understood response to climate change, but our ability to predict shifts is limited. Two factors that may cause variation in range shifts across species are dispersal ability and varying rates of climate change through time and across space. Here, we assess patterns of range shifts during the late Quaternary and estimate how the velocity of climate change and the dispersal ability of a species affect the magnitude of species range shifts in response to climate change. We hindcast species distribution models for 122 North American mammals to five times over the past 17,000 years and forecast them to two future times given two emissions scenarios. Generalized additive models were constructed to quantify the importance of dispersal ability and the velocity of temperature and precipitation in determining the magnitude of range shift expected for individual species. Hindcasted and forecasted ranges demonstrate the variety of responses to climate change. In general, species shifted their ranges in a northerly direction (NW, N, NE) regardless of the type of climate change (i.e., warming vs. cooling). The highest rates of range shifts during the past occurred during periods of relatively rapid climate change (Last Glacial Maximum/Bølling-Allerød and Bølling-Allerød /Younger Dryas transitions). Rates of range shifts for the future are projected to be significantly higher than any of the past intervals. The velocity of climate change is significantly associated with the magnitude of range shifts during climate transitions that occur over longer time scales, while maximum dispersal distance is important during periods of rapid climate change. Our results suggest that both the dispersal ability and the velocity of climate change are significantly associated with species' range shifts. However, the importance of these two factors is context dependent and depends on the interaction of the rate of climate change and the length of time over which the change occurs.

2.2 Introduction

Future rates of climate change are projected to be as fast as or faster than those observed in the late Quaternary (IPCC, 2014). Species have shown a variety of responses to past and contemporary climate change, such as changes in behavior, phenology, and abundance (Blois & Hadly, 2009; Parmesan et al., 1999; Parmesan & Yohe, 2003). These local ecological responses integrate to biogeographic (geographic distribution shifts as species track their preferred habitats and climatic niches) or evolutionary (*in situ* adaptation to new climate regimes) responses. If rates of range shift or *in situ* adaptation are insufficient to track rates of climate change, then species risk local extirpation or extinction (Moritz & Agudo, 2013). Given the high estimated rates of future climate change, both range shifts and local adaptation could be difficult for most species, leading to increased extinction rates in the future (Thomas et al., 2004). Thus, understanding how species respond to changes in climate—both natural and anthropogenic—and accurately predicting those responses is essential if we are to develop effective conservation strategies for species.

Of the possible responses species could have to climate change, range shifts have been examined extensively in both fossil and contemporary systems (Lyons, 2003; Ordonez & Williams, 2013; Sexton et al., 2009; Walther et al., 2002). Ranges have shifted in all directions and at varying rates and magnitudes across species (Lyons, 2003; Schloss et al., 2012). While the general cause of such individualistic range shifts is thought to be the unique environmental niches of each species, which results in each species tracking different aspects of their environmental niche across space (Lyons, 2003; Jackson & Overpeck, 2000), environmental niches alone cannot fully predict range shifts (Rubidge et al. 2011, Santos et al. 2015). Further, due to overlap in the niche requirements of co-occurring species, there are some similarities in how ranges shift in response to climate change (Lyons, 2003). This suggests that the nature of climate change or aspects of species biology may improve predictions of range shifts.

A species geographic distribution is broadly based on its physiological tolerance to environmental factors (i.e., temperature, precipitation), such that species are found where the local environmental conditions are within their physiological limits (Brown et al., 1996). As Earth's climate changes, the geographic distributions of species will correspondingly change. In the absence of adaptation, if a species were to perfectly track climate change, the rate of range shift should equal the velocity of climate (i.e., the rate of isotherm movement across the landscape; Loarie et al., 2009). Thus, the direction and rate at which a species shifts its range should correlate with the overall velocity of climate. Biologically, tracking changes in climate niches across the landscape will be facilitated by dispersal (Schloss et al., 2012; Tingley et al., 2009), so dispersal distance should also be correlated with the magnitude of range shift. However, some populations may respond to climate change through *in situ* mechanisms such as phenotypic or behavioral plasticity or adaptation (Reale et al. 2003), which, together with the influence of local species interactions, may influence the overall correlation between climate and range shifts (e.g., Valladares et al. 2014 Wisz et al. 2013). Overall, the influence of climate velocity and dispersal capability on variation in range shifts is unknown.
Here, we investigate projected past range shifts for western North American mammals to interpret the nature and drivers of future projected range shifts. First, we focus on estimating and understanding the pattern of projected shifts (i.e., direction, rate, and magnitude of range shift) since the Last Glacial Maximum (LGM). We then examine the correlates of projected range shifts to determine if climate velocity or species traits—specifically traits related to dispersal ability—explain the estimated variation of past range shifts. Finally, we extend these analyses to the future by predicting range shifts in

response to two scenarios of future climate change and determining whether those shifts will also be associated with climate velocity and dispersal ability (Fig. 2.1).

2.3 Methods

2.3.1 Estimating species distributions

Occurrence data: Contemporary occurrence data for 242 mammals were downloaded from the Global Biodiversity Information Facility (GBIF; www.GBIF.org). Species were included in this study if any part of their geographic distribution overlapped the western United States, west of the Rocky Mountains. Due to data quality issues and the potential for spatial bias in GBIF data (Beck et al., 2014), all occurrences were inspected to validate their spatial accuracy. Occurrences were removed if they occurred substantially outside of the known modern range of the species, based on the NatureServe distributions (Patterson et al., 2007) or if their basis of record was labeled as either "unknown" or "fossil specimen". Occurrences were spatially thinned to match the resolution of the climate rasters by determining which grid cells contained at least one occurrence for a given species. This prevented pseudoreplication during the modeling process (Guisan & Zimmermann, 2000). Only species with > 20 occurrences after spatial thinning (189 species) were included in the dataset due to issues with modelling species with small sample sizes (Wisz et al., 2008). Sixty-seven additional species were excluded because they did not have sufficient trait data for this study. The final dataset contained occurrences for 122 species (see Appendix Table 2.10.1), ranging from 34 – 2890 spatially thinned observations for each species. These occurrences served as presence-only data and were used to construct species distribution models for the contemporary time period.

Climate simulations: Climate simulations are from the Community Climate System Model version 3 (CCSM3) transient simulation (Liu et al., 2009; Liu et al., 2012). The climate variables in this simulation were debiased and downscaled to a 0.5° x 0.5° resolution grid (~50 x 50 km) based on contemporary (1901-2011) Climate Research Unit time-series (CRU TS3.20) data (Lorenz et al., 2016). The downscaled simulations represent the average North American climate at every 500 years from 21,000 years ago to present (i.e., the variables are 200-year averages centered on the 500-year time slices for most times, though the contemporary simulations represent the average climate from 1850 to 1990 CE). At the same grid resolution, future climate simulations based on 12 Earth system models from CMIP5 (Taylor et al., 2012) were available every 10 years from the present to 2090 CE for two Representative Concentration Pathways (RCPs; RCP 4.5 and RCP 8.5) of greenhouse gas concentrations; in this case, the variables are 20-year averages centered on the 10-year time slices (Lorenz et al., 2016). Out of a possible 54 climate variables, we relied on the same six variables as Maguire et al. (2016) (maximum precipitation of the wettest quarter, mean yearly potential evapotranspiration, maximum temperature of the warmest quarter, mean yearly water deficit index, mean yearly actual evapotranspiration, and minimum precipitation of the driest quarter) because these variables were minimally correlated across space and time for the late Quaternary and represent a range of biologically important measures of temperature and precipitation. All climate layers contained paleoshorelines and estimated species distributions were clipped to represent the presence or absence of ice sheets during each time period. We note that our analyses are based on one climate simulation only, and that all climate simulations have associated uncertainty and biases (Harrison et al. 2014), which reinforces that we are exploring *potential* rather than actual range shifts and their correlates. CCSM3, however, has been shown to capture the broad-scale features of spatiotemporal climate change across the late Quaternary (Liu et al., 2009; Liu et al., 2012) and model-data comparisons that include CCSM3 have shown substantial consistency among different climate models (Harrison et al. 2014).

Our approach of modeling species ranges with only climatic variables implicitly assumes that there is only a direct influence of climate on mammal distributions. Climate could also act indirectly on mammal distributions by modifying the composition and/or structure of the habitat supporting mammal populations. Indirect effects could be particularly strong for precipitation, which may strongly influence vegetation composition and structure (Haxeltine et al., 1996). However, Ordonez and Williams (2013) found that biotic velocities in fossil pollen assemblages closely (but not perfectly) matched climate velocities at both northern and southern pollen distribution boundaries over the late Quaternary, suggesting that discrepancies between the direct and indirect influences of climate on mammal distributions should be minimal, especially at the timescales utilized in this study.

Species distribution models (SDMs): The contemporary distributions of all 122 mammals were generated using the R package ‘BIOMOD2’ (v. 3.3-7; Thuiller et al., 2009). Because the occurrence data were presence only and studies have shown that a k-fold random cross-validation analysis can lead to inflated performance estimates of SDMs (Bahn and McGill, 2012) we evaluated our SDMs using a geographically structured k-fold cross-validation approach (Radosavljevic and Anderson, 2013). This approach spatially partitions the occurrences into four quadrants of equal size. We then constructed the models for each species using an iterative process, where each model is generated using occurrences from three quadrants and the model is then evaluated in the fourth quadrant. This procedure is repeated for all possible iterations, resulting in four models. Area under the receiver operating characteristic curve (AUC) values were generated for each of the four models and then averaged together across all iterations to generate an average AUC value for the species. Random pseudoabsence points were generated for each quadrant equaling up to half of the grid cells not occupied by the focal species. Five models were constructed for each species using different model algorithms (maxent, artificial neural networks, generalized linear models, multiple adaptive regression splines, and boosted regression trees) and each algorithm underwent the geographically structured k-fold evaluation process. The chosen algorithms were among the best performing algorithms from an analysis by Elith et al. (2009) and represent a range of approaches for modeling distributions.

An ensemble distribution model was generated for each species using predictions from each of the five algorithms and their associated averaged AUC values from the evaluation process (Araújo & New, 2007), providing a probability distribution that is a function of the five underlying statistical models. By generating the SDMs through the ensemble process, the process is not relying on a single algorithm for its predictions and more robust predictions can be made for each species by weighting the useful information from each individual forecast into a single consensus model (Araújo & New, 2007). Ensemble predictions for the contemporary distributions were evaluated using the Boyce index. The Boyce index ranges from -1 to 1, where values of zero indicate that a model is similar to a random distribution, positive values represent predicted presences that are consistent with the evaluation dataset, and negative values indicate a poor performing model (Hirzel et al., 2006). We calculated the Boyce index using the R package 'ecospat' (v. 2.2.0; Broennimann et al., 2016) with a moving window of 0.1 of the habitat suitability range to determine the habitat suitability bins. This alleviates the sensitivity of this index to low numbers of suitability classes and provides a method of model evaluation that is similar to AUC, but is more appropriate for presence-only data (Hirzel et al., 2006).

Projecting SDMs: Ensemble models were both hindcasted and forecasted to generate predicted distributions for all species at eight time periods representing climatically unique periods during the late Quaternary and the future: 17 thousand years before present (ka BP) (representative of early deglaciation), 14.5 ka BP (Bølling-Allerød), 12 ka BP (Younger Dryas), 10.5 ka BP (Pleistocene-Holocene transition), 6 ka BP (mid-Holocene), 0 ka BP (contemporary period, 1950 CE), 2050 CE (for both RCP 4.5 and RCP 8.5), and 2090 CE (for both RCP 4.5 and RCP 8.5) (Fig. 2.2). All hindcasts from the past time periods were clipped using the location of ice sheets during the time period to account for unhospitable habitats. For the future time slices, the ensemble model for each species was projected for each of the 12 different Earth System Models; the resulting 12 ensemble models were then averaged together to generate a single ensemble prediction of the species distribution given the time period and greenhouse gas concentration scenario. These time periods provide a mechanism for testing if the dominant influences on range shifts vary during different climatic scenarios.

Validating hindcasted SDMs with fossil data: We validated the hindcasted SDMs with independent fossil occurrences from all of the past time periods (17, 14.5, 12, 10.5, and 6 ka BP), adding a buffer of +/- 1000 years to increase available sample sizes but remain in a climatically similar time. All available occurrences were downloaded from the Neotoma Paleoecology Database (Williams et al. 2018) using the R package 'neotoma' (v. 1.7.0; Goring et al., 2015). For each of the time periods, the occurrences were overlaid onto the hindcasted distribution maps and the predicted probability of presence for each species occurrence record was extracted and averaged to provide a general indication of model performance for that time. We also validated hindcasted models for each time period by calculating the AUC of each hindcasted model (Appendix Fig. 2.10.2). For these calculations, we used fossil assemblages (i.e., sites with >5 taxa found) at which the species being modeled was not found to serve as absence points.

Given the very limited sample sizes for the presence points, however, which appeared to overestimate model performance and resulted in inflated AUC values (Appendix Fig. 2.10.2), we present results from the first approach only in the main paper.

2.3.2 **Calculating range shifts**

To determine the magnitude of range shift that occurred for each species between adjacent time periods, we focused on shifts in the core projected distribution, i.e., those locations where the estimated probability of presence was 0.7 or higher. We conducted a sensitivity analysis to determine the effects of varying suitability thresholds on our predicted range shift results using two other probability thresholds (0.6, 0.8; Appendix Fig. 2.10.3). No significant difference in observed range shifts between these three probability thresholds were found. We then determined the unweighted centroid of the core distributional area using the 'gCentroid' function in the R package 'rgeos' (v. 0.3-26; Bivand et al., 2014) for each species at each time. We calculated range shift in two ways, standardizing for area and for time separately. First, the magnitude of range shift was calculated as the linear distance and direction between the centroids in each adjacent time period (17 – 14.5 ka BP, 14.5 – 12 ka BP, 12 – 10.5 ka BP, 10.5 – 6 ka BP, 6 – 0 ka BP/1950 CE, 1950 –2050 CE, 2050 – 2090 CE). Because the magnitude of range centroid shift may be constrained by the overall range size and available area, we standardized the range shift estimates by dividing the linear shift distance by the area (km^2) of the estimated core species distribution from the older time period. The standardized linear shift distance (SLSD) served as our metric to describe the magnitude of range shift for a species between two time periods. For each time period we determined the estimated rate of range shift for a species by dividing the unstandardized linear shift distance by the elapsed time between adjacent time periods.

To determine if species shifted their ranges in conjunction with the direction of climate velocity, we extracted the velocity of temperature and precipitation from the range centroids of the older time period. We then calculated the difference in bearing between the direction of estimated species range shift and the direction of each of the climate velocities. We determined whether the bearing difference was significantly different from zero using a one-sided t-test. Finally, to determine whether species exhibited consistent rates of range shift through time relative to one another, we rank ordered the species based on their range shift, then correlated species ranks between adjacent time comparisons.

2.3.3 **Testing correlates of range shifts**

Once we determined the magnitude and direction of range shifts, we tested whether several factors were associated with variation in range shift and determined if their relative importance changed through time. We considered four variables, all of which should be significantly correlated with range shifts: two that characterize climate velocity and two that characterize dispersal ability.

Climate velocity: Climate velocity can serve as a surrogate measure for how fast a species must be able to disperse and shift its distribution to track its preferred climatic niche (Serra-Diaz et al., 2014). We calculated the climate velocity associated with each species distribution shift across all time periods using methods similar to Loarie et al. (2009), separately for two variables representing average climate change: maximum yearly average temperature and yearly average precipitation. Neither of these variables was used to generate the SDMs. Briefly, we divided the temporal gradient of change at a focal grid cell for each time comparison (e.g., °C/year for temperature) by the local spatial gradient of change at the older time period based on the 3x3 matrix of grid cells centered on the focal cell (e.g.,, °C/km for temperature). The velocities of temperature and precipitation associated with each species range shift were then determined by extracting the velocity values at the range centroid during the older time period.

Dispersal ability: Direct estimates of the dispersal ability of mammals are lacking for most species. However, a species ability to disperse is positively correlated with both body size and home range area (Whitmee & Orme, 2013). For body size, larger species tend to disperse greater distances than smaller species (Whitmee & Orme, 2013). Bowman et al. (2002) and Whitmee & Orme (2013) determined that the home range area of a species is directly related to its maximum dispersal distance. We obtained home range area and body size for all 122 species from the PanTHERIA database (Jones et al., 2009), then transformed the estimates of home range area into direct estimates of maximum dispersal distance for each species (Bowman et al., 2002). Thus, one variable (maximum dispersal distance) is a direct estimate of dispersal ability, and an additional variable (body size) serves as a surrogate for dispersal ability and other life history attributes.

Predicting dispersal limitation: The amount of time to complete a range shift varies between the different focal times, and species with different generation times could have higher or lower potential to complete the range shift given the elapsed time. Therefore, we determined the potential for individual species to be limited by dispersal ability. We use the age at first birth served as a surrogate measure for the generation time of a species, relying on data in PanTHERIA (Jones et al. 2009). The maximum dispersal distance (originally in units of km/generation) was standardized across species based on their generation times to km/yr. The standardized maximum dispersal distance was then compared to the estimated shift rate (km/yr) for a species in a given time period. If the estimated shift rate was larger than maximum dispersal distance, then the species was predicted to be dispersal limited for that time period.

GAMs: To test which factors are associated with the magnitude of range shift and whether the importance of those factors varied through time, we constructed generalized additive models (GAMs). Generalized additive modelling does not rely on linear relationships or normally-distributed data and provides a model that is easily interpretable with flexible predictor and smoothing functions (Hastie & Tibshirani, 1986). The GAMs included the following variables as predictors: maximum dispersal distance (MD, km), body size (BS, g), velocity of temperature (temp velocity, km/yr), and velocity of precipitation (prcp velocity, km/yr) (equation 2.1):

$$SLSD = \log(BS) + \log(MD) + \text{temp velocity} + \text{prcp velocity} \quad \text{Eq. (2.1)}$$

Models were constructed using the *gam* function from the R package ‘mgcv’ (v. 1.8-23; Wood, 2011), after log-transforming body size and maximum dispersal distance to normalize the data. All models were generated using a gamma family distribution with a log link function and a cubic regression smoothing function was applied to each variable.

For each time comparison, GAMs were generated for all 16 possible combinations of predictor variables. The best model for the time comparison was determined based on the model with the lowest Akaike Information Criterion (AIC) score. If any models were within two AIC units of the model with the lowest AIC score, then in most cases the model with the highest deviance explained out of those models was chosen as the best model. However, when the top-ranked model based on AIC was the full model (a model containing all four predictor variables) but there were other models within two AIC units, the simplest model was chosen as ‘best’ as long as the deviance explained was similar to that of the full model (Arnold, 2010; Burnham & Anderson, 2001). To further confirm that our final models were the best models for the data, Akaike weights were determined for each model in all time periods. Akaike weights describe the probability that a model is the best model given the data, and are dependent upon the data and the models generated *a priori* (see Burnham & Anderson, 2001). In all cases, our final model was the best model given the data.

All analyses were completed in R (v. 3.4.3; R Development Core Team, 2017).

2.4 Results

2.4.1 Species distribution models and range shifts

Contemporary distributions: The Boyce index indicates that all SDMs were reconstructed within an acceptable level of accuracy, though accuracy of the SDMs varied across species. The mean Boyce index was 0.954 (± 0.04; see Appendix Table 2.10.1), ranging from 0.733 for the Mazama pocket gopher (*Thomomys mazama*) to 0.998 for American Red Squirrel (*Tamiascurus hudsonicus*) and the American deer mouse (*Peromyscus maniculatus*).

Hindcasted distributions: Between 38 (17 ka BP) and 154 (12 ka BP) fossil occurrences were downloaded for the 17, 14.5, 12, 10.5 and 6 ka BP time periods, ranging from 1 – 10 occurrences per species per time period. Thus, even with a +/- 1000 year buffer, few occurrences were found for most species since many mammal fossil assemblages are imprecisely dated and/or time-averaged (e.g., some localities were reconstructed as ‘Glacial’, which ranged from 20,500 – 9,500 years ago). Average predicted probability of presence for fossil occurrences was 74.995.28% (s.d. = 22.38) during the mid-Holocene (6 ka BP), 69.58% (s.d. = 25.04) at the Pleistocene-Holocene transition (10.5 ka BP), 61.91% (s.d. = 26.39) during the Younger Dryas (12.5 ka BP), 50.94% (s.d. = 33.32) during the Bølling-Allerød (14.5 ka BP), and 44.38% (s.d. = 32.50) during early deglaciation (17 ka BP; Fig. 2.3), indicating hindcasted distributions for some times should be interpreted with caution.

Rate and magnitude of range shifts: Based on the hindcasted and forecasted SDMs and subsequent range shift calculations, species are projected to have shifted their ranges in all directions and at varying rates across the previous 17,000 years and as we move into the future (Figs. 2.4 & 2.5; Table 2.1; Table 2.2). Across each time comparison, on average 71% of all species shifted their ranges in a northward direction (i.e.,, NW, N, or NE) regardless of the nature of climate change during that time (Table 2.1, Fig. 2.3). The largest percentage of species shifted their ranges northward (95%) during the warming transition from the LGM into the Bølling-Allerød (17 – 14.5 ka BP in our hindcasted comparison). The second largest pulse of northward range shifts occurred during the Pleistocene/Holocene warming transition from 12 – 10.5 ka BP (79.3%) and between 1950 – 2050 RCP 8.5 (80.2%) in our comparison (Table 2.1, Fig. 2.4). Very few species are estimated to have shifted their ranges in a southward direction (i.e., SW, S, or SE) across any past time period: the percentage of species that potentially shifted southward ranged from 0.8% (17 – 14.5 ka BP) to 22.8% (6 ka BP – 1950 CE). Lastly, comparisons between the direction of species range shifts and the direction of change in climate isotherms suggests that estimated species shifts are significantly different from the direction that temperature ($t = -15.7$; $df = 987$; $p = 0$) and precipitation ($t = -5.62$; $df = 952$; $p = 0$) isotherms are predicted to have shifted (Fig. 2.6).

The predicted distributions of species shifted at a much slower rate (0.05 km/yr and 0.01 km/yr; Table 2.2) during the Holocene (10.5 – 6 ka BP and 6 – 0 ka BP time periods, respectively) when climates were relatively stable, than in the late Pleistocene (0.20 km/yr from 17 to 14.5 ka BP, 0.19 km/yr from 14.5 to 12 ka BP, and 0.17 km/yr from 12 to 10.5 ka BP), when rates of climate change were much higher (Fig. 2.2; Table 2.2). No species are predicted to be dispersal limited in the past based on the elapsed time between range projections and their maximum dispersal distances (Table2.2)

Rates of projected range shifts for the future are expected to be significantly higher than any of the rates from the late Quaternary, regardless of time period or greenhouse gas concentration scenario (Table 2.2). The future scenarios are also the only scenarios where species are predicted to be dispersal limited (between 19 – 32% of examined species; Table 2.2). Species are predicted to shift their ranges at an average rate of 2.89 km/yr between 1950 – 2050 CE and 3.25 km/yr between 2050 – 2090 CE under the RCP 4.5 scenario. Under the RCP 8.5 scenario, species are predicted to shift their ranges at a slightly higher average rate of 3.35 km/yr between 1950 – 2050 CE and a substantially higher rate of 7.86 km/yr from 2050 – 2090 CE.

Species overall had a weak, but significant correlation in their range shift ranks between adjacent time periods, suggesting that species were consistent in the distance that they shifted their distributions between time periods (Appendix Fig. 2.10.4). One species was estimated to have the largest range shift in four of the nine examined time periods. The Arctic shrew (*Sorex arcticus*) had the largest predicted shift for the time periods 17 – 14.5 ka BP (1.53 km/yr), 14.5 – 12 ka BP (1.70 km/yr), 12 – 10.5 ka BP (0.74 km/yr) and 1950 – 2050 CE for RCP 8.5 (37.2 km/yr). Other species that had large estimated shifts in the other examined time periods were the brown bear (*Ursus arctos*; 10.5 – 6 ka BP; 0.51 km/yr), the wolverine (*Gulo gulo*; 6 ka BP – 1950 CE; 0.08 km/yr); the gray wolf (*Canis* lupus, 1950 – 2050 CE for RCP 4.5; 11.03 km/yr), the Canada lynx (*Lynx canadensis*, 1950 – 2050 CE for RCP 8.5; 14.97 km/yr), and the San Joaquin pocket mouse (*Perognathus inornatus*, 2050 – 2090 CE for RCP 4.5; 20.68 km/yr).

2.4.2 Generalized additive models

Even though the predicted distributions were based solely on climate variables, climate velocity only partially explained differences in the magnitude of range shifts across species. Final GAMs (see Appendix Table 2.10.5 for list of models) for each time comparison in the past explained at most 42% of the model deviance (17 – 14.5 ka BP) and as little as 25.3% (14.5 – 12 ka BP; Table 2.3). Models explaining variation in future range shifts fared similarly, ranging from 22.5% to 45.5% explained deviance depending on time period and RCP (Table 2.3). Akaike model weights for the top models also varied substantially, ranging from 0.15 to 0.81 depending on time comparison. For all time comparisons, at least one of the climate velocity variables was present in the top model. The one exception was the 1950 – 2050 CE, RCP 4.5 time period (Table 2.3), when neither of the climate velocity variables was included in the top model. However, only the velocity of precipitation change was significantly correlated with the estimated range shift of species, during three out of nine time periods. Either the body size of a species or its maximum dispersal distance were also included in the top models explaining SLSD patterns for past time comparisons. Body mass was significantly correlated with SLSD during the transition from the Bølling-Allerød into the Younger Dryas, 14.5 – 12 ka BP, and MDD was significant during the transition from the LGM into the Bølling-Allerød, 17 – 14.5 ka BP (Table 2.3). For the future, body mass was important in all of the future climate scenarios and MDD was important only in 2050 – 2090 CE for both RCPs (Table 2.3).

2.5 Discussion

2.5.1 Geographic patterns of species range shifts

Many species respond to climate change in the form of poleward (north or south) and elevational (upward or downward in elevation) range shifts (Chen et al., 2011; Davis & Shaw, 2001; Parmesan & Yohe, 2003; La Sorte & Thompson, 2007), reflecting the influence of temperature on species distributions (Parmesan & Yohe, 2003). Not all species are strongly limited by temperature (VanDerWal et al., 2012), however, and a more refined expectation is that the direction of a range shift will depend upon how climate changes relative to the climatic constraints on the species range; distribution shifts are the result of species tracking the movement of their preferred climatic variable(s), such as temperature, precipitation, and/or some other climatic (or correlated habitat) variable important to the species survival (Tingley et al., 2009; Walther et al., 2002). Indeed, species responses to past changing climates and habitats were individualistic (e.g.,, Jackson & Overpeck, 2000; Ordonez & Williams, 2013), and species are shifting their distributions in all directions in response to recent climate change (Pinsky et al., 2012; VanDerWal et al., 2012).

North American mammals have also responded to climate change in an individualistic manner over the late Quaternary (Graham et al., 1996; Lyons, 2003). Previous studies have focused on broad-scale responses due to the nature of the time-averaged fossil record, detecting changes in species ranges from the Glacial (20,500 – 9,500 years ago) to the Holocene period (10,500 years ago to present) from fossils, for example (Graham et al., 1996; Lyons, 2003). The broad temporal windows across which a species range is being inferred in these previous studies could mask finer temporal dynamics in ranges associated with deglaciation, as climate did not change smoothly from a glacial to an interglacial state. For example, the Glacial time period examined in Lyons (2003) potentially includes fossil localities recorded from the LGM, the warm Bølling-Allerød, and the colder Younger Dryas, thus missing the effects of rapid climate transitions. Other studies have estimated the past range shift patterns for only one or a few species of mammal (e.g., Nogues-Bravo et al., 2008, Davis et al., 2014).

In this paper, we instead use SDMs to project range shifts that may have occurred (similar to Lawing and Polly 2011) as the Earth system transitioned from a glacial to an interglacial, and then we examine the responses expected in the future, focusing on two aspects of range shifts: direction and rate. Validation of species shifts with fossil data is inconclusive (see Appendix Fig. 2.10.2) especially during the earliest time periods (similar to Davis et al., 2014), in part due to the low number of radiocarbon-dated occurrences available to accurately validate the projected ranges and because the models have been constructed with assumption that the relationship between species occurrence and climate is constant through time and the only factor determining range. In addition, we rely on one climate model only (CCSM3) to capture past paleoclimates. Therefore, our results outline only the potential scenarios of past and future range shifts, but allow us to examine the potential fine-scale dynamics that accompanied range shifts. Our validation results agree with other studies showing that SDMs predict species ranges more accurately in time periods that are more climatically similar (i.e., 6 ka BP) to the time period in which the SDMs were constructed (e.g., Maguire et al., 2016). Therefore, model interpretations must be carefully considered for future predictions, especially as future climate becomes more novel.

The hindcasted range shifts, like the results from many other studies (Graham et al., 1996; Lyons, 2003; Moritz et al., 2008; Pinsky et al., 2012), show that mammals likely responded to climate change in individualistically, with species predicted to have shifted their distributions at various rates and directions over the previous 17,000 years (Tables 2.1 & 2.2; Fig. 2.4). The individualistic pattern of species shifts is also demonstrated by the fact that the same species does not exhibit consistently large or small distances in any given climate change scenario (except for *Sorex arcticus*), making it difficult to predict the pattern of range shifts in the future. However, all species are expected to have increased shift rates in the future regardless of the greenhouse gas concentration scenario (Tables 2.1 & 2.2; Fig. 2.5).

Directionality: Based on climate-only hindcasted and forecasted SDMs, the overall estimated pattern of species range shifts is generally in the northward (poleward) direction (NW, N, or NE), with a minority of species estimated to have shifted their distributions in other directions across all time periods. This strong northward directionality in species shifts has been observed in multiple studies and largely results from the latitudinal temperature gradient across North America (Lyons, 2003; Ordonez & Williams, 2013). The past time periods in which the largest percentage of the species shifted northward were periods of rapid climate warming such as the transition into the Bølling-Allerød and the Pleistocene/Holocene transition from the Younger Dryas into the interglacial (Table 2.1). During these two time periods, approximately 25 to 40% more species shifted their distributions northward than during other periods in the past. However, fewer species are projected to shift their ranges northward in the future than in the past, even though we anticipate higher rates of future climate warming (Marcott, et al., 2013, Table 2.1). Further, past species ranges were predicted to have shifted farther (average: 300.5 km; maximum: 2885 km) than they are expected to in the future (average: 267.1 km; maximum: 1497 km). One possible explanation is that during the past, when the Cordilleran and Laurentide ice sheets were still present over northern North America, there was less habitable area and species mostly resided in what is now the contiguous United States and Central America. As ice sheets retreated following the LGM, more land area became exposed, allowing species to shift northward. In contrast, for contemporary and future range shifts, most land area in North America has already been available to species for 1000s of years (excluding Greenland, outside the geographic scope of this study) and several species have already shifted as far north as geographically possible. Therefore, it is plausible that the estimated percentage of species shifting northward in the future will continue to decline. Our results emphasize the importance of studying the interactions of multiple climate variables, geography, topography, and other species and how these variables dictate the direction a species will shift in response to climate change.

While these results recover the main pattern of poleward shifts and echo the findings of other studies that species respond to warming climates by shifting their ranges poleward (La Sorte & Thompson, 2007; Parmesan & Yohe, 2003), our projections suggest there is significant multidirectionality in species responses to climate change (Figs. 2.4 & 2.5). Recently, VanDerWal et al. (2012) also observed similar multidirectionality, but found that bird species were generally shifting their ranges towards the equator or longitudinally as they followed changes in precipitation. Similarly, Fei et al. (2017) found more westward than poleward shifts in trees over the last few decades, likely related to changes in moisture rather than temperature. However, the direction of Quaternary mammal species shifts is not strongly related to the overall movement of the climate isotherms, at least at the range centroid. Therefore, the direction a species shifts its range is most likely the result of multiple climate factors, combined with geographic barriers and species interactions, which this study did not address. It is also possible that species ranges track climate more closely at the range margins rather than the range centroids. For example, Ordonez and Williams (2013) found stronger correlations between biotic and climatic velocities at northern versus southern boundaries.

Rates: Species ranges are projected to shift very quickly in the future regardless of RCP scenario, much higher than rates of range shift seen in the past (e.g., compare the scale of range shift rates in Fig. 2.4 vs. Fig. 2.5). Average past range shift rates are 30 - 250 times lower than average estimated rates for the future (Table 2.2). The species exhibiting the largest shifts were different across time periods, though the arctic shrew is predicted to consistently have large shift rates across many time periods. Results from this study are within the range of estimates for woody taxa from Davis and Shaw (2001; 0.01 – 1 km/yr) and Ordonez and Williams (2013; -0.17 – 0.27 km/yr and -0.15 – 2.7 km/yr for northern vs. southern boundaries, respectively), but are higher than rattlesnake range shift rates from Lawing and Polly (2011; 0.002 km/yr). While some of the difference in rates of range shifts is likely due to differences in the time interval over which rates are calculated (e.g.,, Barnosky et al., 2003; Ordonez & Williams 2013), rates of future climate change are projected to be much faster than seen for the past in our averaged data, indicating that faster range shifts will be necessary for species to track future climate change (Lawing & Polly, 2011; Malcom et al., 2002). The effect of differing interval lengths also influences the amount of time that a species has to accomplish a range shift. The warming event that occurred during the transition from the LGM into the Bølling-Allerød spans approximately 2,500 years in our study (17 – 14.5 ka BP) while the Holocene time periods span 4,500 and 6,000 years (for 10.5 – 6 ka BP and 6 – 0 ka BP, respectively). If range shifts lagged behind fast climate changes, however, these fine-scale dynamics may be undetectable due to the broad spatial and temporal scales employed in this study. Other studies have also reported that species had sufficient shift rates to track their climatic niches in the past. Ordonez and Williams (2013) showed that rates of range shift for 30 woody taxa were as fast or faster than estimated rates of climate velocity from 16 kya to the present. However, all of the future intervals are significantly shorter than the past time intervals (100 years for 1950 – 2050 CE and 40 years for 2050 – 2090 CE). Our data suggest that the high rates of climate change over shorter time scales will lead to species being limited by dispersal as they attempt to track their climate niches in the future (Table 2.3), and they may need hundreds to thousands of years in the future to catch up to the lags caused by dispersal limitation.

The median rates of future range shifts estimated in this study (from 2.49 – 6.18 km/yr among time comparisons and RCPs) are slightly higher than the median rate of 1.69 km/yr reported in a recent meta-analysis of historical latitudinal range shifts (Chen et al., 2011), though note that our calculations of range shift encompass both latitudinal and longitudinal shifts, exacerbating any mismatch among studies. These historical observations (Chen et al., 2011) indicate a significant amount of variation in the rate at which species shifted their ranges, and species may need to shift their ranges at substantially higher rates in the future to keep pace with climate change (our results: 0.01 – 37.23 km/yr across all species (Table 2.2); Lawing & Polly, 2011: 1.61 – 7.90 km/yr). However, the estimated extent of species range shifts in the future could possibly be an over-estimation of actual species shifts, since our models do not account for local adaptation. Therefore, the number of species at risk of becoming dispersal limited in the future may not be as high as our estimates suggest.

2.5.2 Drivers of species range shifts

Given the climate-based projected distributions, the velocity of climate change should be strongly correlated with the direction and rate of range shifts. Our results show, however, that while either temperature or precipitation velocity is present in the final models, for six out of the nine time periods neither variable is significantly correlated to SLSD. In fact, the velocity of temperature change is not significantly correlated with SLSD in any time period (Table 2.3), which is counter to results from Pinsky et al. (2013) showing that climate velocity was a better predictor of range shifts than life histories. Species traits may better describe variation in species responses to climate change, as body mass and MDD are significantly correlated with SLSD in six out of the nine time periods, especially in the future (Table 2.3). Body mass was generally significant in more models than MDD, echoing its usefulness as a trait that reflects a broad range of ecological and evolutionary processes (Brown, 1995). Future studies should consider incorporating species traits and life histories into their modelling framework, as they attempt to describe and determine species response patterns to future climate change (Kearney and Porter, 2009; Kearney et al., 2010). Determining which factor is likely most limiting in different times is one framework for interpreting these results. In the past, species had enough time to track their climatic niche at millennial scales, thus a species dispersal ability was adequate for facilitating range shifts and not important in determining SLSD; climate velocity emerged as the strongest factor associated with SLSD during these periods. As the magnitude of climate change lessened and the extent of range shifts became very small in the Holocene (Fig. 2.4), the importance of any variable in explaining the pattern of SLSD is removed and no variables are significantly correlated with SLSD. However, in the future, high rates of climate change are expected over short time scales (IPCC, 2014; Marcott et al., 2013) and the estimated rates of shift required for species to track their climatic niches are significantly larger (Fig. 2.4 & 2.5; Table 2), so dispersal ability may become the limiting factor (Table 2.3).

Overall, our results suggest that maximum dispersal ability is a good indicator for how far a species may shift its range, but only during periods of rapid climate change. However, the models did not explain all of the observed variation in the extent of range shifts – ranging from 22.5% - 45.5% explained variation– and for three of the times, none of the variables were significantly correlated with SLSD. Other factors that could be driving species distribution shifts are biotic interactions, geographic barriers (or lack thereof), local adaptation, or climatic or environmental factors that were not included in our original set of predictors. Further, we did not allow interactions between variables in the GAMs, and there may be interactions between temperature and precipitation velocity or between body mass and MDD, for example, pointing to the need for further model refinement.

2.6 Conclusions

Overall, a better understanding of the factors that explain the magnitude, direction, and rate of range shifts can be used to guide management practices and goals for protecting species and their habitats as climate continues to change in the future. The observation that species potentially shifted their distributions in multiple directions in response to past climate change, and will continue this pattern as climate changes in the future, is important if we are to effectively manage future populations and account for likely scenarios of species range shifts. The potential influence of factors other than temperature and precipitation is apparent by the fact that temperature velocity was not significant in any time period and precipitation velocity was important in only three out of the nine time periods, therefore suggesting that future studies should incorporate multivariate climate velocity simulations (see Dobrowski et al., 2013) in their models to accurately estimate the effect of climate on species range shifts. We are beginning to converge on similar rates of range shifts across studies for some taxonomic groups, but a large amount of unexplained variation remains; much more influences the distributions of species than just simple climate relationships, as shown by the significance of dispersal ability in our models. Instead, the combination of climate, traits, species interactions, and topography is most important for determining range shifts (Lenoir & Svenning, 2015). Because species are expected to shift their ranges at highly variable rates, our forecasts need to be able to incorporate species interactions and associations, physiology, and fine-scale environmental factors in order to guide effective conservation strategies in the future.

2.7 References

Arnold, T.W. (2010) Uninformative parameters and model selection using Akaike’s information criterion. *Journal of Wildlife Management*, **74**, 1175-1178.

Arujo, M.B. & New, M. (2007) Ensemble forecasting of species distributions. *Trends in Ecology and Evolution*, **22**, 42-47.

Barnosky, A.D., E.A., Hadly and C. J., Bell. (2003) Mammalian response to global warming on varied temporal scales. *Journal of Mammalogy*, **84**, 354–368.

Beck, J., Boller, M., Erhardt, A. & Schwanghart, W. (2014) Spatial Bias in the GBIF Database and its Effect on Modeling Species’ Geographic Distributions. *Ecological Informatics*, **19**, 10-15.

Blois, J.L. & Hadly, E.A. (2009) Mammalian response to Cenozoic climatic change. *Annual Review of Earth and Planetary Sciences*, **37**, 181–208.

Bivand, R., Rundel, C., Pebesma, E. & Hufthammer, K.O. (2014) Interface to geometry engine- open source (GEOS). R-cran repository. http://cran.r-project.org/web/packages/rgeos/index.html.

Bowman, J., Jaeger, J.A.G. & Fahrig, L. (2002) Dispersal distance of mammals is proportional to home range size. *Ecology*, **83**, 2049-2055.

Broennimann, O., Di Cola, V. & Guisan, A. (2016) Ecospat: spatial ecology miscellaneous methods. R package version 2.1.1. http://www.unil.ch/ecospat/home/menuguid/ecospat-resources/tools.html.

Brown, J. H. (1995) *Macroecology*. Chicago, IL: University of Chicago Press.

Brown, J. H., Stevens, G. & Kaufman, D. (1996) The Geographic Range: Size, Shape, Boundaries, and Internal Structure. *Annual Review of Ecology and Systematics*, **27**, 597–623.

Burnham, K.P. & Anderson, D.R. (2001) Kullback-Leibler information as a basis for strong inference in ecological studies. *Wildlife Research*, **28**, 111-119.

Chen, I-C., Hill, J.K., Ohlemüller, R., Roy, D.B. & Thomas, C.D. (2011) Rapid range shifts of species associated with high levels of climate warming. *Science*, **333**, 1024-1026.

Davis, E. B., McGuire, J. L. & Orcutt, J. D. (2014) Ecological niche models of mammalian glacial refugia show consistent bias. *Ecography*, **37**, 1133-1138.

Davis, M. B. & Shaw, R. G. (2001) Range shifts and adaptive responses to Quaternary climate change. *Science*, **292**, 673-679.

Dobrowski, S. Z., Abatzoglou, J., Swanson, A. K., Greenburg, J. A., Mynsberge, A. R., Holden, Z. A. & Schwartz, M. K. (2013). The climate velocity of the contiguous United States during the 20th century. *Global Change Biology*, **19**, 241-251.

Elith, J., Graham, C.H., Anderson, R.P., Dudík, M., Ferrier, S., Guisan, A., Hijmans, R.J., Huettmann F., Leathwick, J.R., Lehmann, A., Li, J., Lohmann, L.G., Loiselle, B.A., Manion, G., Moritz, C., Nakamura, M., Nakazawa, Y., McC, J., Overton, M., Peterson, A.T., Phillips, S. J., Richardson, K., Scachetti-Pereira, R., Schapire, R.E., Soberón, J., Williams, S., Wisz, M.S. & Zimmermann, N.E. (2006) Novel methods improve prediction of species' distributions from occurrence data. *Ecography*, **29**, 129-151.

Fei, S., Desprez, J.M., Potter, K.M., Jo, I., Knott, J.A., & Oswalt C.M. (2017) Divergence of species responses to climate change. *Science Advances*, **3**, e1603055.

Goring, S., Dawson, A., Simpson, G.L., Ram, K., Graham, R.W., Grimm, E.C. & Williams, J.W. (2015). Neotoma: a programmatic interface to the Neotoma Paleoecological Database. *Open Quaternary,* **1**, 1-17.

Graham, R., Lundelius, E., Graham, M., Schroeder, E., Toomey, R., Anderson, E., Barnosky, A., Burns, J., Churcher, C., Grayson, D., Guthrie, R., Harington, C., Jefferson, G., Martin, L., McDonald, H., Morlan, R., Semken, H., Webb, S., Werdelin, L. & Wilson, M. (1996) Spatial response of mammals to late Quaternary environmental fluctuations. *Science,* **272**, 1601–1606.

Guisan, A. & Zimmermann, N.E. (2000) Predictive habitat distribution models in ecology. *Ecological Modelling,* **135**, 147-186.

Harrison S.P., Bartlein P.J., Brewer S., Prentice I.C., Boyd M., Hessler I., Holmgren K., Izumi K., & Willis K. (2014) Climate model benchmarking with glacial and mid-Holocene climates. *Climate Dynamics,* **43**, 671–688.

Hastie, T. & Tibshirani, R. (1986) Generalized additive models. *Statistical Science*, **1**, 297-318.

Haxeltine, A., Prentice, I.C., & Creswell, I.D. (1996) A coupled carbon and water flux model to predict vegetation structure. *Journal of Vegetation Science,* **7**, 651–666.

Hirzel, A.H., Lay, G.L., Helfer, V., Randin, C. & Guisan, A. (2006) Evaluating the ability of habitat suitability models to predict species presences. *Ecological Modelling*, **199**, 142-152.

IPCC, (2014) Climate change 2014: synthesis report. Contribution of Working Groups I, II, and III to the Fifth Assessment Report of the Intergovernmental Panel on Climate Change [Core Writing Team, Pachauri, R.K. & Meyer, L.A. (eds.)]. IPCC, Geneva, Switzerland, 151 pp.

Jackson, S.T. & Overpeck, J.T. (2000) Responses of plant populations and communities to environmental changes of the late Quaternary. *Paleobiology*, **26**, 194-220.

Jones, K.E., Bielby, J., Cardillo, M., Fritz, S., O'Dell, J., Orme, C.D.L., Safi, K., Sechrest, W., Boakes, E.H., Carbone, C., Connolly, C., Cutts, M.J., Foster, J. K., Grenyer, R., Habib, M., Plaster, C.A., Price, S.A., Rigby, E.A., Rist, J., Teacher, A., Bininda-Emonds, O.R.P., Gittleman, J. L., Mace, G.M. & Purvis, A. (2009) PanTHERIA: a species-level database of life history, ecology, and geography of extant and recently extinct mammals. *Ecology*, **90**, 2648.

Kearney, M. & Porter, W. (2009) Mechanistic niche modelling: combining physiological and spatial data to predict species' ranges. *Ecology Letters*, **12**, 334-350.

Kearney, M., Simpson, S. J., Raubenheimer, D. & Helmuth, B. (2010) Modelling the ecological niche from functional traits. *Philosophical Transactions of the Royal Society of London B: Biological Sciences*, **365**, 3469-3483.

La Sorte, F.A. & Thompson III, F.R. (2007) Poleward shifts in winter ranges of North American birds. *Ecology*, **88**, 1803-1812.

Lenoir, J. & Svenning, J.-C. (2015) Climate-related range shifts – a global multideminsional synthesis and new research directions. *Ecography*, **38**, 15-28.

Loarie, S.R., Duffy, P.B., Hamilton, H., Asner, G.P., Field, C.B. & Ackerly D.D. (2009) The velocity of climate change. *Nature*, **462**, 1052–1055.

Lorenz, D.J., Nieto-Lugilde, D., Blois, J.L., Fitzpatrick, M.C. & Williams, J.W. (2016) Downscaled and debiased climate simulations for North America from 21,000 years ago to 2100AD. *Scientific Data*, **3**, 1-19.

Liu, Z., Otto-Bliesner, B.L., He, F., Brady, E.C,. Tomas, R, Clark, P.U., Carlson, A.E., Lynch- Stieglitz, J., Curry, W, Brook, E., Erickson, D., Jacob, R., Kutzbach, J. & Cheng, J. (2009) Transient simulation of last deglaciation with a new mechanism for Bølling-Allerød warming. *Science*, **325**, 310-314.

Liu, Z., Carlson, A.E., He, F., Brady, E.C., Otto-Bilesner, B.L., Briegleb, B.P., Wehrenberg, M., Clark, P.U., Wu, S., Cheng, J., Zhang, J., Noone, D. & Zhu, J. (2012) Younger Dryas cooling and the Greenland climate response to CO_2. *Proceedings of the National Academy of Sciences of the United States of America*, **109** 11101- 11104.

Lyons, S.K. (2003) A quantitative assessment of the range shifts of Pleistocene mammals. *Journal of Mammalogy*, **84**, 385-402.

Maguire, K.C., Nieto-Lugilde, D., Blois, J.L., Fitzpatrick, M.C., Williams, J.W., Ferrier, S. & Lorenz, D. (2016) Controlled comparison of species- and community-level models across novel climates and communities. *Proceedings of the Royal Society B*, **283**, 2015287.

Malcom, J. R., Markham, A., Neilson, R. P. & Garaci, M. (2002) Estimated migration rates under scenarios of global climate change. *Journal of Biogeography*, **29**, 835-849.

Marcott, S.A., Shakun, J.D., Clark, P.U. & Mix, A.C. (2013) A reconstruction of regional and global temperature for the past 11,300 years. *Science*, **339**, 1198-1201.

Moritz, C. & Agudo, R. (2013) The future of species under climate change: resilience or decline? *Science,* **341,** 504-508.

Moritz, C., Patton, J.L., Conroy, C.J., Parra, J.L., White, G.C. & Beissinger, S.T. (2008) Impact of a century of climate change on small-mammal communities in Yosemite National Park, USA. *Science*, **322**, 261-264.

Ordonez, A. & Williams, J.W. (2013) Climatic and biotic velocities for woody taxa distributions over the last 16000 years in eastern North America. *Ecology letters*, **16**, 773–781.

Parmesan, C., Ryrholm, N., Stefanescu, C., Hill, J.K., Thomas, C.D., Descimon, H., Huntley, B., Kaila, L., Kullberg, J., Tammaru, T., Tennent, J.W., Tomas, J.A. & Warren, M. (1999) Poleward shifts in geographical ranges of butterfly species associated with regional warming. *Nature*, **399**, 579-583.

Parmesan C. & Yohe, G. (2003) A globally coherent fingerprint of climate change impacts across natural systems. *Nature*, **421**, 37-42.

Patterson, B.D., Ceballos, G., Sechrest, W., Tognelli, M.F., Brooks, T., Luna, L., Ortega, P., Salazar, I. & Young, B.E. (2007) Digital distribution maps of the mammals of the western hemisphere, version 3.0. NatureServe, Arlington, Virginia, USA.

Pinsky, M.L., Worm, B., Fogarty, M.J., Sarmiento, J.L. & Levin, S.A. (2012) Marine taxa track local climate velocities. *Science*, **341**, 1239– 1242.

R Development Core Team (2017). R: A language and environment for statistical computing. R Foundation for Statistical Computing, Vienna, Austria. Available from http://www.R-project.org.

Radosavljevic, A. & Anderson, R. P. (2014). Making better maxent models of species distributions: complexity, overfitting, and evaluation. *Journal of Biogeography*, **41**, 629-643.

Réale, D., McAdam, A. G., Boutin, S. & Berteaux, D. (2003). Genetic and plastic responses of a northern mammal to climate change. *Proceeding of the Royal Society B Biological Sciences*, **270**, 591-596.

Rubidge, E. M., Monahan, W.B., Parra, J.L., Cameron, S.E. & Brashares, J.S. (2011) The role of climate, habitat, and species co-occurrence as drivers of change in small mammal distributions over the past century. *Global Change Biology*, **17**, 696-708.

Santos, M.J., Thorne, J.H. & Moritz, C. (2015). Synchronicity in elevation range shifts among small mammals and vegetation over the last century is stronger for omnivores. *Ecography*, **38**, 556-568.

Schloss, C.A., Nuñez, T.A. & Lawler, J.J. (2012) Dispersal will limit ability of mammals to track climate change in the western Hemisphere. *Proceedings of the National Academy of Sciences of the United States of America*, **109**, 8606–8611.

Serra-Diaz, J.M., Franklin, J., Ninyerols, M., Davis, F.W., Syphard, A.D., Regan, H.M. & Ikegami, M. (2014) Bioclimatic Velocity: the Pace of Species Exposure to Climate Change. *Diversity and Distributions*, **20**, 169-180.

Sexton, J.P., McIntyre, P.J., Angert, A.L. & Rice, K.J. (2009) Evolution and Ecology of Species Range Limits. *Annual Review of Ecology, Evolution, and Systematics*, **40**, 415–436.

Taylor, K.E., Stouffer, R.J. & Meehi, G.A. (2012) An overview of CMIP5 and the experiment design. *American Meteorological Society*, **93**, 485-498.

Thuiller, W., Lafourcade, B., Engler, R. & Araújo, M.B. 2009. BIOMOD-A platform for ensemble forecasting of species distributions. *Ecography*, **32**, 369-373.

Thomas, C.D., Cameron, A., Green, R.E., Bakkenes, M., Beaumont, L.J., Collingham, Y.C., Erasmus, B.F.N., Ferreira de Siqueira, M., Grainger, A., Hannah, L., Hughes, L., Huntley, B., van Jaarsveld, A.S., Midgley, G.F., Miles, L., Ortega-Huerta, M.A., Peterson, A.T., Phillips, O.L. & Williams, S.E. (2004) Extinction risk from climate change. *Nature*, **427**, 145-148.

Tingley, M. W., Monahan, W.B., Beissinger, S.R. & Moritz, C. (2009) Birds track their Grinnellian niche through a century of climate change. *Proceedings of the National Academy of Sciences of the United States of America*, **106**, 19637–19643.

Vallaares, F., Matesanz, S., Guilhaumon, F., Araújo, M. B., Balaguer, L., Benito-Garzón, M., Cornwell, W., Gianoli, E., van Kleunen, M., Naya, D. E., Nicotra, A. B., Poorter, H. & Zavala, M. A. (2014) The effects of phenotypic plasticity and local adaptations on forecasts of species range shifts under climate change. *Ecology Letters*, **17**, 1351-1364.

VanDerWal J., Murphy, H.T., Kutt, A.S., Perkins, G.C., Bateman, B.L., Perry, J.J. & Reside, A.E. (2013) Focus on poleward shifts in species' distribution underestimates the fingerprint of climate change. *Nature Climate Change*, **3**, 239-243

Walther, G., Post, E., Convey, P., Menzel, A., Parmesan, C., Beebee, T.J.C., Fromentin, J., Hoegh-Guldberg, O. & Bairlein, F. (2002) Ecological responses to recent climate change. *Nature*, **416**, 389–395.

Whitmee, S. & Orme, C.D.L. (2013) Predicting dispersal distance in mammals: a trait-based approach. *The Journal of Animal Ecology*, **82**, 211–21.

Williams, J.W., Grimm, E.C., Blois, J.L., Charles, D.F., Davis, E.B., Goring, S.J., Graham, R.W., Smith, A.J., Anderson, M., Arroyo-Cabrales, J., Ashworth, A.C., Betancourt, J.L., Bills, B.W., Booth, R.K., Buckland, P.I., Curry, B.B., Giesecke, T., Jackson, S.T., Latorre, C., Nichols, J., Purdum, T., Roth, R.E., Stryker, M., & Takahara, H. (2018) The Neotoma Paleoecology Database, a multiproxy, international, community-curated data resource. *Quaternary Research*, **89**, 156–177.

Wisz, M. S., Hijmans, R. J., Li, J., Peterson, A. T., Graham, C. H. & Guisan, A. (2008) Effects of sample size on the performance of species distribution models. *Diversity and Distributions*, **14**, 763-773.

Wisz, M. S., Pottier, J., Kissling, W. D., Pellissier, L., Lenoir, J., et al. (2013) The role of biotic interactions in shaping distributions and realised assemblages of species: implications for species distribution modelling. *Biological Reviews*, **88**, 15–30.

Wood, S.N. (2011) Fast stable restricted maximum likelihood and marginal likelihood estimation of semiparametric generalized linear models. *Journal of the Royal Statistical Society* (B), **73**, 3-36

2.8 Tables

Table 2.1: The percentage of species estimated to shift in a specific direction for each time period, both in the past and the future. Southward and Northward percentages reflect the overall percentage of species estimated to shift in that general direction: Southward shifts are the sum of South (S), Southeast (SE), and Southwest (SW) shifts and Northward shifts are the sum of North (N), Northeast (NE), and Northwest (NW) shifts.

Time Period	**NW**	**N**	**NE**	**E**	**SE**	**S**	**SW**	**W**	**Southward**	**Northward**
2050 – 2090 CE RCP 8.5	27.8	40.1	9.8	8.1	9.0	0.8	0.8	3.2	**10.6**	**77.7**
2050 – 2090 CE RCP 4.5	33.6	34.4	10.6	9.0	5.7	2.4	0.8	3.2	**8.9**	**78.6**
1950 – 2050 CE RCP 8.5	22.1	40.1	18.0	13.11	4.0	1.6	0	0.8	**5.6**	**80.2**
1950 – 2050 CE RCP 4.5	22.1	36.8	18.0	14.7	6.5	0.8	0	0.8	**7.3**	**76.9**
6 ka BP-1950	18.8	20.4	19.6	13.1	10.6	4.9	7.3	4.9	**22.8**	**58.8**
10.5-6 ka BP	18.8	15.5	10.6	24.5	16.3	2.4	4.0	7.3	**22.7**	**44.9**
12-10.5 ka BP	31.1	36.0	12.2	13.9	3.2	0	0.8	2.4	**4**	**79.3**
14.5-12 ka BP	33.6	12.2	7.3	29.5	8.1	1.6	3.2	4.0	**12.9**	**53.1**
17-14.5 ka BP	68.0	22.1	4.9	1.6	0	0.8	0	2.4	**0.8**	**95.0**

Table 2.2: Summary statistics for the shift rates (km/yr) of species in all time comparisons and the number of species predicted to be limited and not limited by dispersal ability during each time period.

Time Comparison	**Average**	**Maximum**	**Minimum**	**Median**	**Limited**	**Not Limited**
2050 - 2090 CE RCP 4.5	3.25	20.68	0.11	2.53	7	30
2050 - 2090 CE RCP 8.5	7.86	37.23	0.30	6.18	12	25
1950 - 2050 CE RCP 4.5	2.89	11.03	0.22	2.49	7	30
1950 - 2050 CE RCP 8.5	3.35	14.97	0.11	2.76	7	30
6-0 ka BP	0.01	0.08	0.00	0.01	0	37
10.5-6 ka BP	0.05	0.51	0.00	0.03	0	37
12-10.5 ka BP	0.17	0.74	0.00	0.13	0	37
14.5-12 ka BP	0.19	1.70	0.00	0.12	0	37
17-14.5 ka BP	0.20	1.53	0.02	0.16	0	37

Table 2.3: The significance of each variable in determining the extent of range shifts for each time comparison. *(P ≤ 0.05), ** (P < 0.01), *** (P < 0.001), - (non-significant but included in the best model), NA (not included in the final model). MDD = maximum dispersal distance, Precip. Velocity = precipitation velocity, Temp. Velocity = temperature velocity, and Akaike Weight = the probability that the given model is the best model out of the set of generated models for the given time period (Wagnemakers and Farrell 2004).

Variable	17 – 14.5 (ka BP)	14.5 – 12 (ka BP)	12 – 10.5 (ka BP)	10.5 – 6 (ka BP)	6 – 0 (ka BP)	1950 – 2050 CE (RCP 4.5)	1950 – 2050 CE (RCP 8.5)	2050 – 2090 (RCP 4.5)	2050 – 2090 (RCP 8.5)
Body Mass (g)	-	***	-	NA	-	**	*	*	**
MDD (km)	*	NA	NA	-	-	NA	-	*	*
Precip. Velocity (km/yr)	*	-	-	-	-	NA	NA	**	***
Temp. Velocity (km/yr)	NA	-	-	-	NA	-	NA	-	-
Deviance Explained	42%	25.3%	41.3%	27.2%	27.6 %	22.5%	25.7%	45.5%	43.7%
Akaike Weight	0.30	0.16	0.22	0.15	0.24	0.24	0.20	0.74	0.81

2.9 Figures

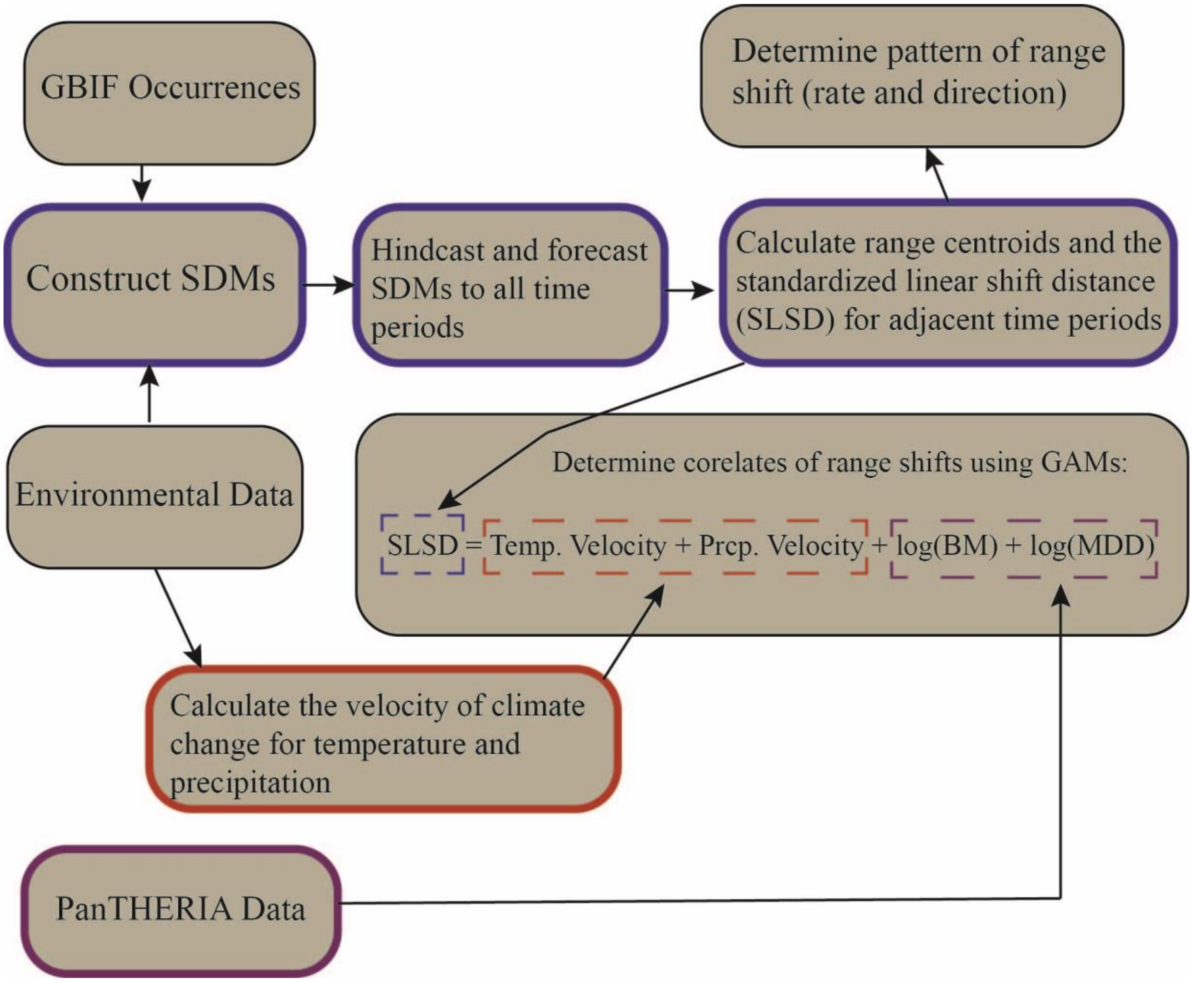

Figure 2.1: Workflow diagram depicting the steps used in this study. The species distribution modelling steps are outlined in blue, the climate velocity step is outlined in red, and the trait data are outlined in purple. SDMs: Species distribution models; GAMs: Generalized additive models; Temp: Temperature; Prcp: Precipitation; BM: Body mass; MDD: Maximum dispersal distance; GBIF: Global Biodiversity Information Facility.

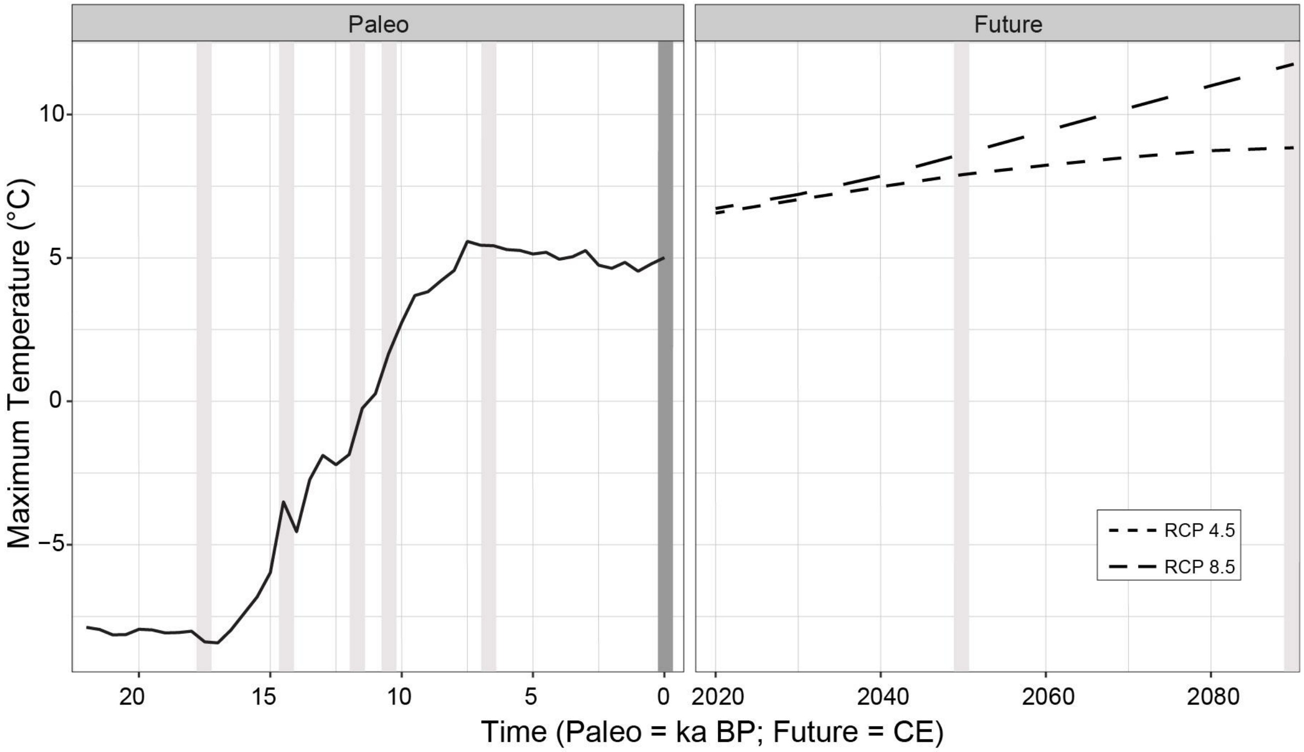

Figure 2.2: Annual average maximum temperature for North America from the Last Glacial Maximum (21 ka BP) to the year 2090 CE, based on the downscaled CCSM3 simulations (notice the break in the scale between 0 BP (equivalent to 1950 CE) and 2020 CE; Lorenz et al., 2016). The dark grey vertical bar represents the contemporary period in which the species distribution models were constructed and validated. The contemporary models were then hindcasted and forecasted to 7 time periods represented by the light grey vertical bars: 17 ka BP, 14.5 ka BP, 12 ka BP, 10.5 ka BP, 6 ka BP, 2050 CE, and 2090 CE.

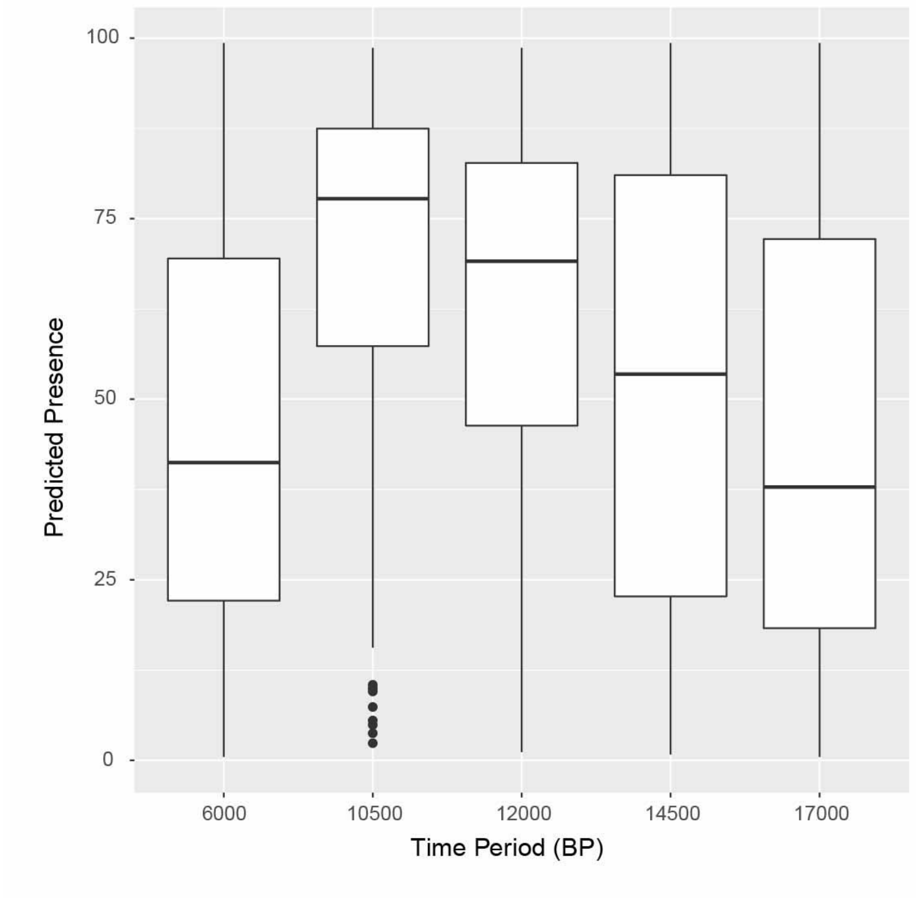

Figure 2.3: Boxplot of the average predicted probability of presence and the upper and lower quantiles for models validated with fossil data in each of the past time periods examined in this study.

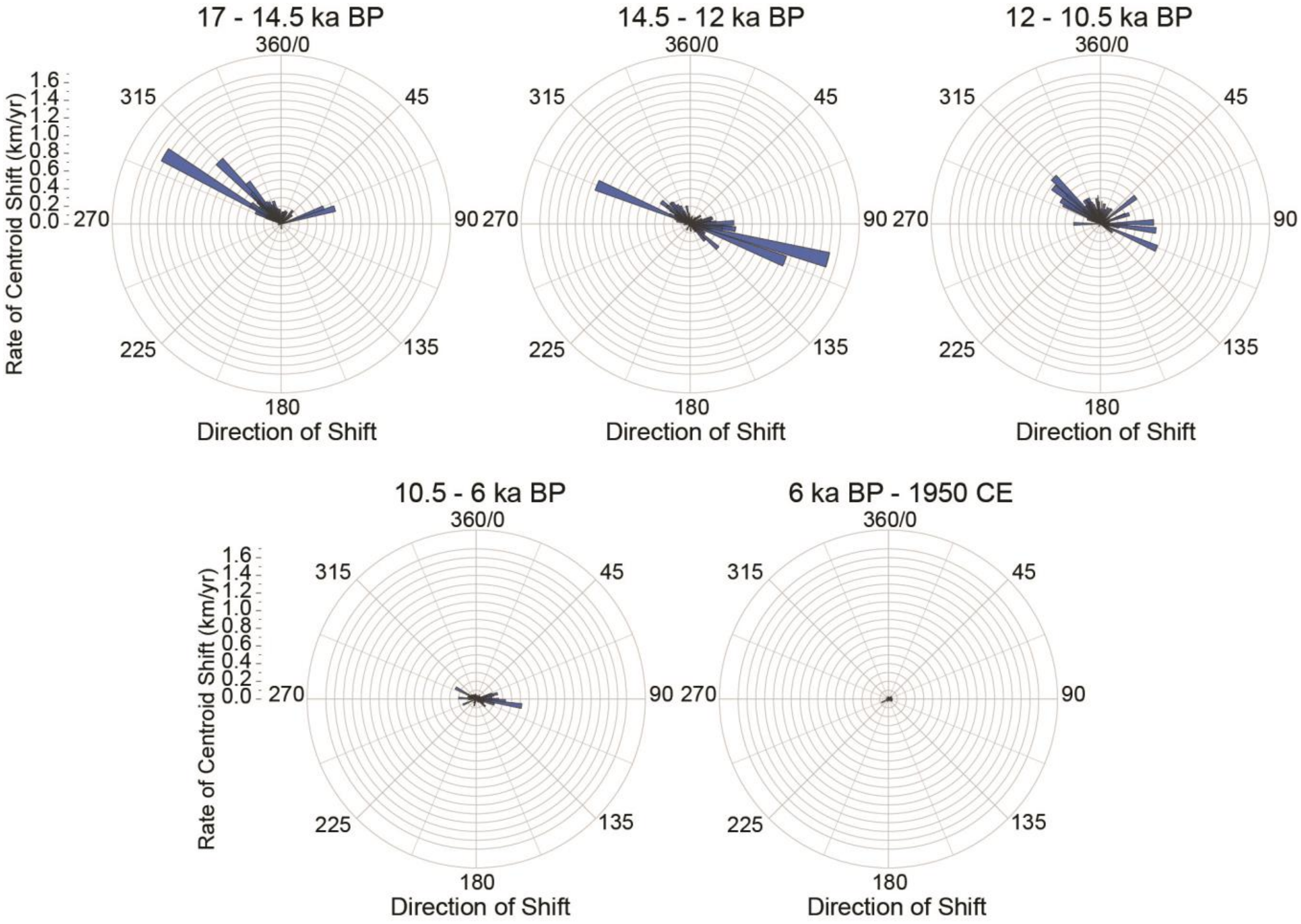

Figure 2.4: Rose diagrams representing the estimated shift direction (indicated by the direction of bars) and the rate of shift (indicated by the length of bars) for 122 mammal species (individual bars) across North America for five time intervals since the end of the Last Glacial Maximum. Rate of centroid shift is at the same scale in all graphs. Shift direction corresponds to 360/0 = North, 90 = East, 180 = South, 270 = West.

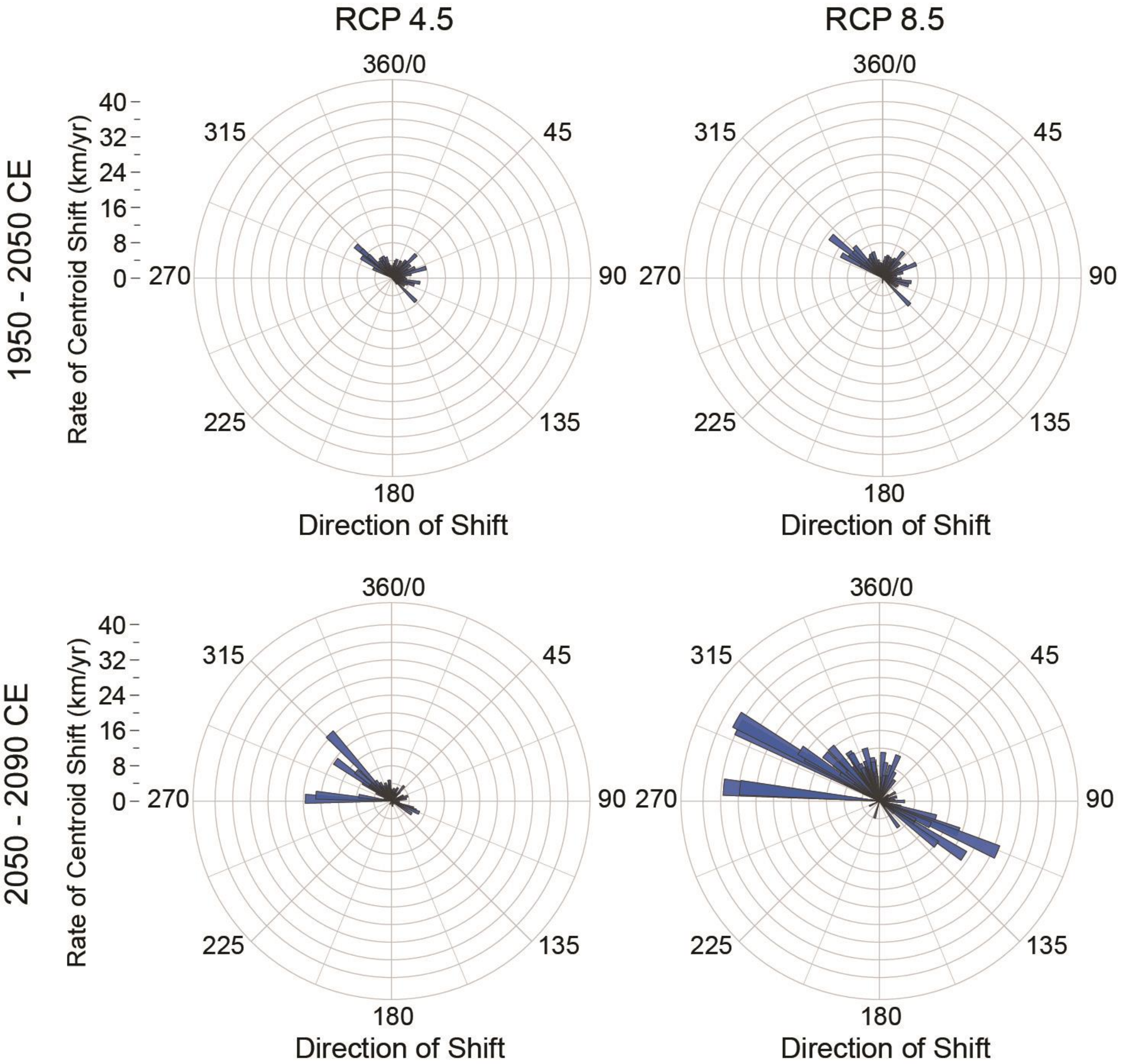

Figure 2.5: Rose diagrams representing the estimated shift direction (indicated by the direction of bars) and the rate of shift (indicated by the length of bars) for 122 mammal species (individual bars) across North America for two future time intervals (rows) under two Representative Concentration Pathways (RCPs; columns). Shift direction corresponds to 360/0 = North, 90 = East, 180 = South, 270 = West.

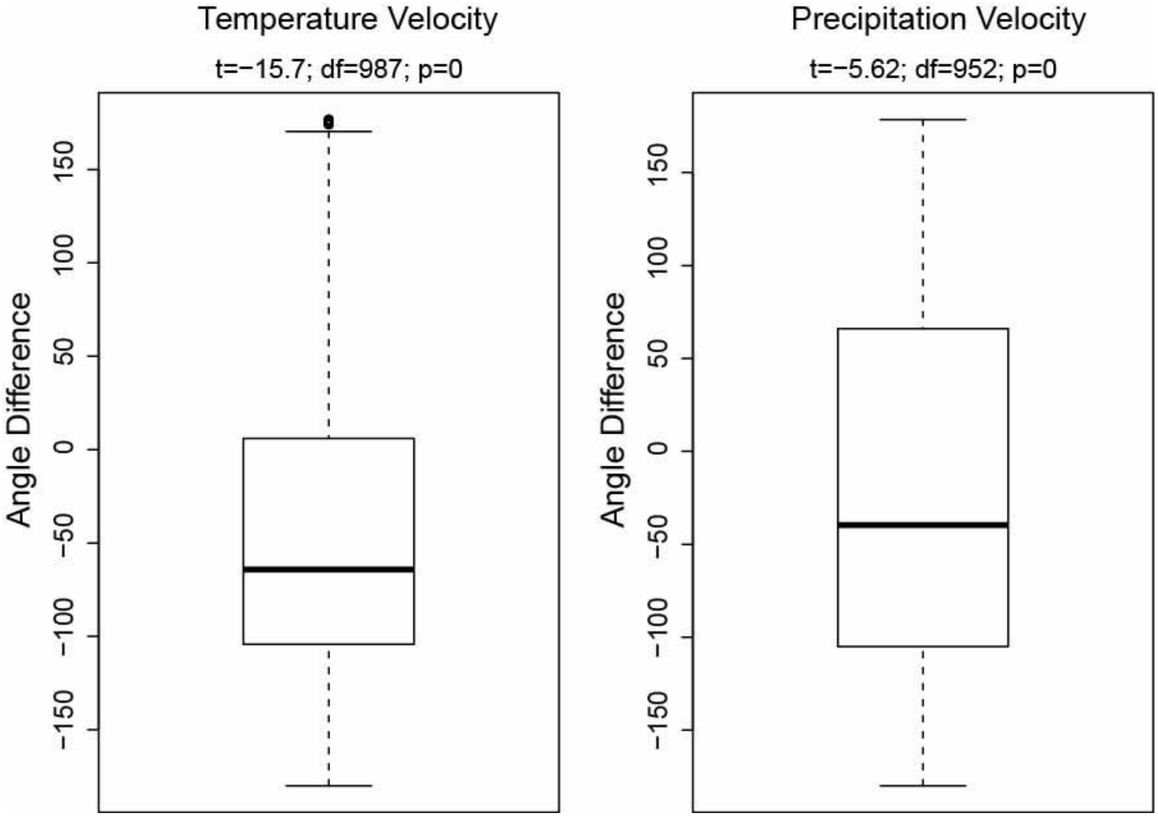

Figure 2.6: The bearing difference between the direction of estimated species range shift and the direction of the climate velocities (left: maximum yearly average temperature velocity; right: yearly average precipitation velocity). Positive values of the bearing difference indicate that the estimated species range shift was clockwise from the direction of climate velocity and negative values indicate that the estimated species range shift was counterclockwise from the direction of climate velocity.

2.10 Appendix

Table 2.10.1: Species examined in this study and the number of filtered occurrences for each species and the associated Boyce index values for each of the ensemble models constructed in this study.

Species	**Number of Occurrences**	**Boyce Index**
Ammospermophilus leucurus	273	0.971
Antilocapra americana	241	0.944
Aplodontia rufa	94	0.913
Baiomys taylori	269	0.980
Bassariscus astutus	270	0.982
Blarina brevicauda	892	0.982
Brachylagus idahoensis	52	0.943
Canis latrans	1426	0.969
Canis lupus	768	0.997
Castor canadensis	733	0.980
Cervus elaphus	218	0.978
Chaetodipus fallax	53	0.835
Chaetodipus nelsoni	126	0.874
Chaetodipus penicillatus	250	0.962
Cryptotis parva	442	0.976
Cynomys gunnisoni	87	0.976
Cynomys leucurus	77	0.863
Cynomys ludovicianus	269	0.977
Dasypus novemcinctus	404	0.988
Didelphis virginiana	895	0.989
Dipodomys agilis	68	0.938
Dipodomys merriami	531	0.954
Dipodomys microps	137	0.881
Dipodomys ordii	775	0.929
Dipodomys panamintinus	49	0.941
Dipodomys spectabilis	149	0.843
Glaucomys sabrinus	490	0.976
Gulo gulo	425	0.980
Lepus americanus	608	0.965
Lontra canadensis	532	0.990
Lynx canadensis	349	0.976
Lynx rufus	972	0.974
Marmota flaviventris	265	0.980
Marmota monax	480	0.975

Species	**Number of Occurrences**	**Boyce Index**
Martes americana	499	0.981
Martes pennanti	228	0.979
Mephitis mephitis	875	0.991
Microdipodops megacephalus	91	0.960
Microtus californicus	148	0.972
Microtus montanus	398	0.983
Microtus ochrogaster	430	0.987
Microtus oregoni	99	0.881
Microtus pennsylvanicus	1369	0.989
Microtus richardsoni	98	0.989
Mustela erminea	740	0.982
Mustela frenata	867	0.968
Mustela nivalis	212	0.956
Myodes californicus	34	0.843
Myodes gapperi	604	0.992
Neotoma albigula	488	0.976
Neotoma cinerea	506	0.993
Neotoma lepida	316	0.971
Neotoma micropus	282	0.966
Neurotrichus gibbsii	123	0.945
Ochotona princeps	250	0.990
Odocoileushemionus	639	0.991
Odocoileus virginianus	964	0.988
Ondatra zibethicus	840	0.983
Onychomys leucogaster	666	0.947
Onychomys torridus	308	0.974
Oreamnos americanus	82	0.977
Pecari tajacu	219	0.965
Perognathus flavus	467	0.972
Perognathus inornatus	34	0.866
Perognathus longimembris	182	0.987
Perognathus merriami	129	0.891
Perognathus parvus	267	0.994
Peromyscus boylii	496	0.982
Peromyscus californicus	71	0.891
Peromyscus crinitus	262	0.950
Peromyscus keeni	188	0.967
Peromyscus leucopus	1559	0.994
Peromyscus maniculatus	2890	0.998
Peromyscus pectoralis	192	0.821

Species	**Number of Occurrences**	**Boyce Index**
Peromyscus truei	439	0.967
Procyon lotor	1192	0.985
Puma concolor	398	0.978
Rangifer tarandus	163	0.963
Reithrodontomys fulvescens	496	0.970
Reithrodontomys megalotis	1045	0.955
Reithrodontomys montanus	277	0.967
Scalopus aquaticus	445	0.985
Scapanus orarius	93	0.931
Sciurus aberti	105	0.934
Sciurus carolinensis	683	0.960
Sciurus griseus	135	0.981
Sigmodon ochrognathus	36	0.794
Sorex arcticus	95	0.938
Sorex cinereus	1229	0.984
Sorex monticolus	737	0.978
Sorex palustris	411	0.994
Sorex vagrans	370	0.985
Spermophilus beecheyi	144	0.934
Spermophilus spilosoma	202	0.932
Spermophilus tereticaudus	83	0.882
Spermophilus tridecemlineatus	390	0.979
Spermophilus variegatus	246	0.968
Spilogale putorius	388	0.992
Sylvilagus audubonii	692	0.981
Sylvilagus bachmani	126	0.927
Sylvilagus floridanus	1097	0.993
Tamias amoenus	365	0.992
Tamias dorsalis	170	0.887
Tamias minimus	664	0.973
Tamias quadrivittatus	118	0.952
Tamias senex	57	0.844
Tamias speciosus	37	0.864
Tamias townsendii	102	0.940
Tamias umbrinus	118	0.946
Tamiasciurus douglasii	198	0.989
Tamiasciurus hudsonicus	1257	0.998
Taxidea taxus	597	0.970
Thomomys bottae	629	0.936
Thomomys mazama	47	0.733

Species	**Number of Occurrences**	**Boyce Index**
Thomomys monticola	38	0.881
Ursus americanus	805	0.987
Ursus arctos	407	0.991
Vulpes macrotis	136	0.945
Vulpes velox	89	0.941
Vulpes vulpes	848	0.994
Zapus hudsonius	748	0.997
Zapus princeps	375	0.978

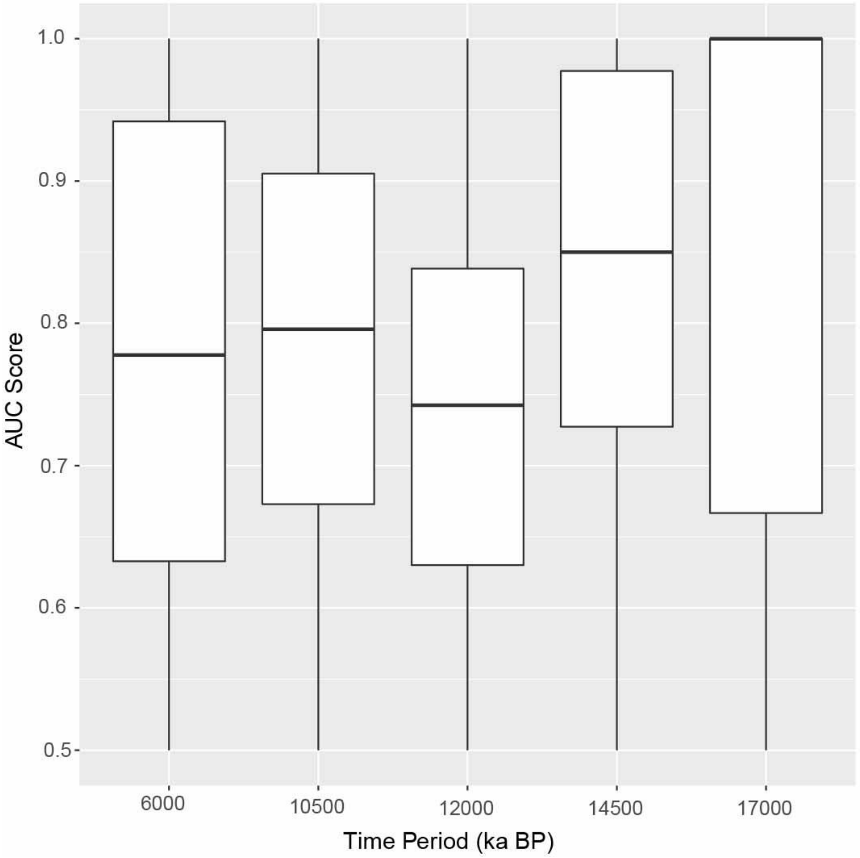

Figure 2.10.2: Box plots of the AUC scores for the fossil validation of hindcasted models in each of the past time periods. Total range of AUC scores is indicated by the thin vertical lines, whereas the boxes represent the upper and lower quantile, and the thicker horizontal line within the box indicates the average AUC score.

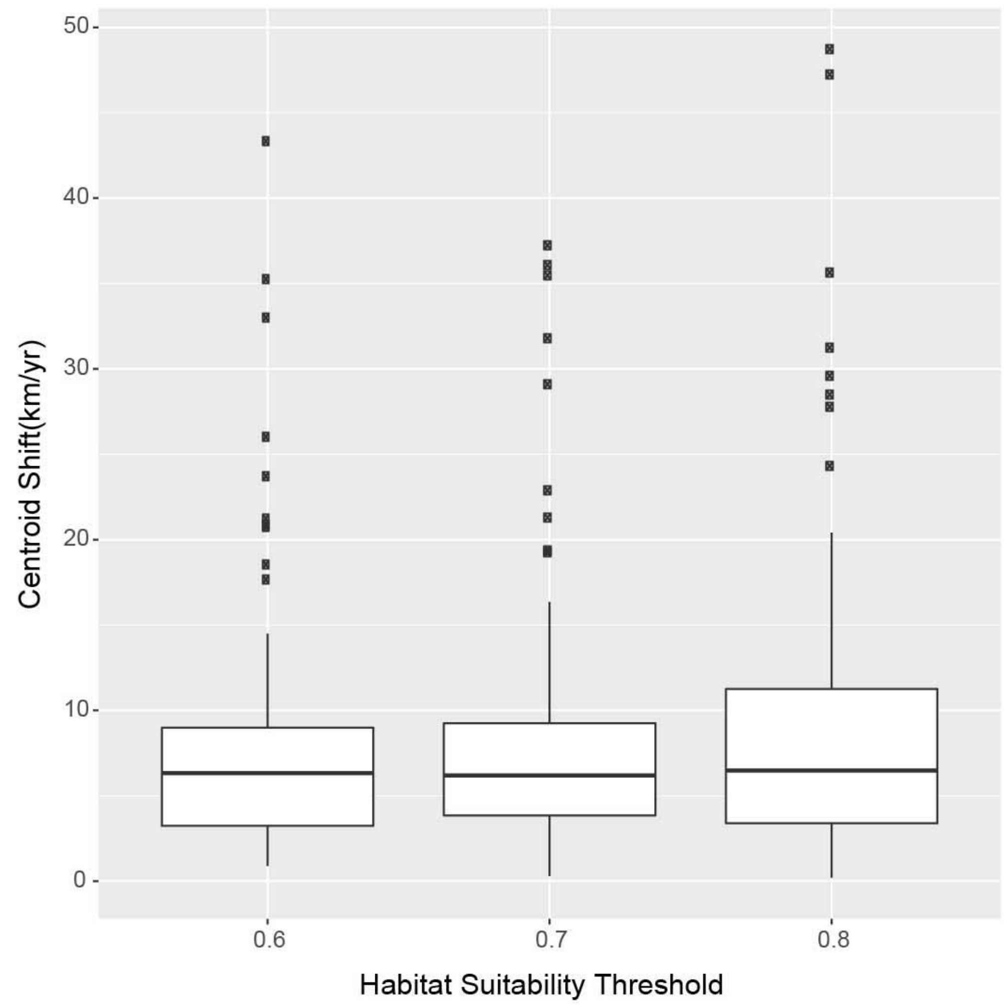

Figure 2.10.3: Boxplots of centroid shifts using three habitat suitability threshold values during the 2050 – 2090 CE in the RCP 8.5 scenario. Boxplot interpretation as indicated in the caption for appendix Fig. 2.10.2.

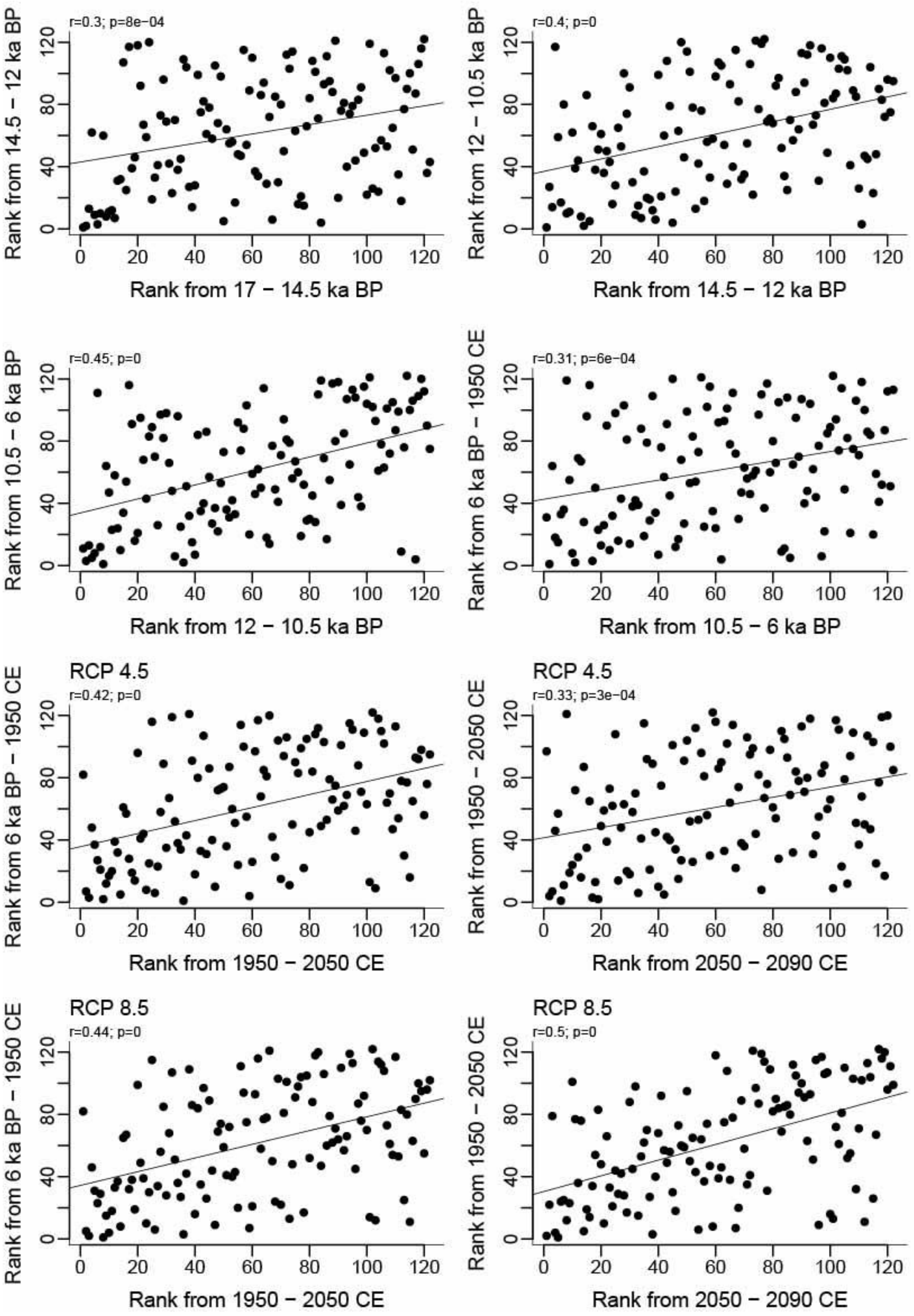

Figure 2.10.4: Correlation between rank of species range shifts across time periods.

Table 2.10.5: Models generated for each time period and their associated AIC, Delta AIC (from the best model), and Akaike Weight values. SLSD = Standardized Linear Shift Distance.

Model	**Time Period**	**AIC**	**Delta AIC**	**Akaike Weight**
~shift_areas(log(Body_mass), bs = "cr") + s(log(Max_disp), bs = "cr") + s(CV_prcp, bs = "cr")	17 - 14.5 kya	-4175.27	0.00	0.31
~shift_areas(log(Body_mass), bs = "cr") + s(log(Max_disp), bs = "cr") + s(CV_temp, bs = "cr")	17 - 14.5 kya	-4175.27	0.00	0.31
~shift_areas(log(Body_mass), bs = "cr") + s(log(Max_disp), bs = "cr") + s(CV_prcp, bs = "cr") + s(CV_temp, bs = "cr")	17 - 14.5 kya	-4175.27	0.00	0.31
~shift_areas(log(Max_disp), bs = "cr") + s(CV_temp, bs = "cr")	17 - 14.5 kya	-4169.93	5.35	0.02
~shift_areas(log(Max_disp), bs = "cr") + s(CV_prcp, bs = "cr")	17 - 14.5 kya	-4169.93	5.35	0.02
~shift_areas(log(Max_disp), bs = "cr") + s(CV_prcp, bs = "cr") + s(CV_temp, bs = "cr")	17 - 14.5 kya	-4169.93	5.35	0.02
~shift_areas(log(Body_mass), bs = "cr") + s(CV_prcp, bs = "cr") + s(CV_temp, bs = "cr")	17 - 14.5 kya	-4166.98	8.30	0.00
~shift_areas(log(Body_mass), bs = "cr") + s(CV_temp, bs = "cr")	17 - 14.5 kya	-4166.98	8.30	0.00
~shift_areas(log(Body_mass), bs = "cr") + s(CV_prcp, bs = "cr")	17 - 14.5 kya	-4166.98	8.30	0.00
~shift_areas(log(Body_mass), bs = "cr") + s(log(Max_disp), bs = "cr")	17 - 14.5 kya	-4165.38	9.89	0.00
~shift_areas(CV_prcp, bs = "cr")	17 - 14.5 kya	-4164.00	11.28	0.00
~shift_areas(CV_temp, bs = "cr")	17 - 14.5 kya	-4164.00	11.28	0.00
~shift_areas(CV_prcp, bs = "cr") + s(CV_temp, bs = "cr")	17 - 14.5 kya	-4164.00	11.28	0.00
~shift_areas(log(Body_mass), bs = "cr")	17 - 14.5 kya	-4154.85	20.43	0.00
~shift_areas(log(Max_disp), bs = "cr")	17 - 14.5 kya	-4154.21	21.07	0.00
~shift_area1	17 - 14.5 kya	-4143.47	31.80	0.00
~shift_areas(log(Body_mass), bs = "cr") + s(CV_prcp, bs = "cr") + s(CV_temp, bs = "cr")	14.5 - 12 kya	-4677.95	0.00	0.17
~shift_areas(log(Body_mass), bs = "cr") + s(CV_temp, bs = "cr")	14.5 - 12 kya	-4677.95	0.00	0.17
~shift_areas(log(Body_mass), bs = "cr") + s(CV_prcp, bs = "cr")	14.5 - 12 kya	-4677.95	0.00	0.17
~shift_areas(log(Body_mass), bs = "cr") + s(log(Max_disp), bs = "cr") + s(CV_prcp, bs = "cr")	14.5 - 12 kya	-4677.72	0.23	0.15

~shift_areas(log(Body_mass), bs = "cr") + s(log(Max_disp), bs = "cr") + s(CV_temp, bs = "cr")	14.5 - 12 kya	-4677.72	0.23	0.15
Model	**Time Period**	**AIC**	**Delta AIC**	**Akaike Weight**
~shift_areas(log(Body_mass), bs = "cr") + s(log(Max_disp), bs = "cr") + s(CV_prcp, bs = "cr") + s(CV_temp, bs = "cr")	14.5 - 12 kya	-4677.72	0.23	0.15
~shift_areas(log(Body_mass), bs = "cr")	14.5 - 12 kya	-4673.67	4.28	0.02
~shift_areas(log(Body_mass), bs = "cr") + s(log(Max_disp), bs = "cr")	14.5 - 12 kya	-4672.14	5.81	0.01
~shift_areas(log(Max_disp), bs = "cr")	14.5 - 12 kya	-4670.03	7.92	0.00
~shift_areas(log(Max_disp), bs = "cr") + s(CV_temp, bs = "cr")	14.5 - 12 kya	-4668.27	9.68	0.00
~shift_areas(log(Max_disp), bs = "cr") + s(CV_prcp, bs = "cr")	14.5 - 12 kya	-4668.27	9.68	0.00
~shift_areas(log(Max_disp), bs = "cr") + s(CV_prcp, bs = "cr") + s(CV_temp, bs = "cr")	14.5 - 12 kya	-4668.27	9.68	0.00
~shift_area1	14.5 - 12 kya	-4662.60	15.35	0.00
~shift_areas(CV_prcp, bs = "cr")	14.5 - 12 kya	-4660.67	17.28	0.00
~shift_areas(CV_temp, bs = "cr")	14.5 - 12 kya	-4660.67	17.28	0.00
~shift_areas(CV_prcp, bs = "cr") + s(CV_temp, bs = "cr")	14.5 - 12 kya	-4660.67	17.28	0.00
~shift_areas(log(Body_mass), bs = "cr") + s(CV_prcp, bs = "cr") + s(CV_temp, bs = "cr")	12 - 10.5 kya	-4845.59	0.00	0.23
~shift_areas(log(Body_mass), bs = "cr") + s(CV_temp, bs = "cr")	12 - 10.5 kya	-4845.59	0.00	0.23
~shift_areas(log(Body_mass), bs = "cr") + s(CV_prcp, bs = "cr")	12 - 10.5 kya	-4845.59	0.00	0.23
~shift_areas(log(Body_mass), bs = "cr") + s(log(Max_disp), bs = "cr") + s(CV_prcp, bs = "cr")	12 - 10.5 kya	-4843.58	2.01	0.08
~shift_areas(log(Body_mass), bs = "cr") + s(log(Max_disp), bs = "cr") + s(CV_temp, bs = "cr")	12 - 10.5 kya	-4843.58	2.01	0.08
~shift_areas(log(Body_mass), bs = "cr") + s(log(Max_disp), bs = "cr") + s(CV_prcp, bs = "cr") + s(CV_temp, bs = "cr")	12 - 10.5 kya	-4843.58	2.01	0.08
~shift_areas(log(Max_disp), bs = "cr") + s(CV_prcp, bs = "cr") + s(CV_temp, bs = "cr")	12 - 10.5 kya	-4840.61	4.98	0.02
~shift_areas(log(Max_disp), bs = "cr") + s(CV_temp, bs = "cr")	12 - 10.5 kya	-4840.61	4.98	0.02
~shift_areas(log(Max_disp), bs = "cr") + s(CV_prcp, bs = "cr")	12 - 10.5 kya	-4840.61	4.98	0.02
~shift_areas(CV_prcp, bs = "cr") + s(CV_temp, bs = "cr")	12 - 10.5 kya	-4837.18	8.41	0.00
~shift_areas(CV_prcp, bs = "cr")	12 - 10.5 kya	-4837.18	8.41	0.00

~shift_areas(CV_temp, bs = "cr")	12 - 10.5 kya	-4837.18	8.41	0.00
~shift_areas(log(Body_mass), bs = "cr") + s(log(Max_disp), bs = "cr")	12 - 10.5 kya	-4827.60	17.99	0.00
Model	**Time Period**	**AIC**	**Delta AIC**	**Akaike Weight**
~shift_areas(log(Body_mass), bs = "cr")	12 - 10.5 kya	-4826.12	19.47	0.00
~shift_areas(log(Max_disp), bs = "cr")	12 - 10.5 kya	-4813.52	32.08	0.00
~shift_area1	12 - 10.5 kya	-4800.01	45.58	0.00
~shift_areas(log(Max_disp), bs = "cr") + s(CV_prcp, bs = "cr") + s(CV_temp, bs = "cr")	10.5 - 6 kya	-4986.91	0.00	0.16
~shift_areas(log(Max_disp), bs = "cr") + s(CV_temp, bs = "cr")	10.5 - 6 kya	-4986.91	0.00	0.16
~shift_areas(log(Max_disp), bs = "cr") + s(CV_prcp, bs = "cr")	10.5 - 6 kya	-4986.91	0.00	0.16
~shift_areas(CV_prcp, bs = "cr") + s(CV_temp, bs = "cr")	10.5 - 6 kya	-4985.32	1.59	0.07
~shift_areas(CV_prcp, bs = "cr")	10.5 - 6 kya	-4985.32	1.59	0.07
~shift_areas(CV_temp, bs = "cr")	10.5 - 6 kya	-4985.32	1.59	0.07
~shift_areas(log(Body_mass), bs = "cr") + s(log(Max_disp), bs = "cr") + s(CV_prcp, bs = "cr")	10.5 - 6 kya	-4985.24	1.67	0.07
~shift_areas(log(Body_mass), bs = "cr") + s(log(Max_disp), bs = "cr") + s(CV_temp, bs = "cr")	10.5 - 6 kya	-4985.24	1.67	0.07
~shift_areas(log(Body_mass), bs = "cr") + s(log(Max_disp), bs = "cr") + s(CV_prcp, bs = "cr") + s(CV_temp, bs = "cr")	10.5 - 6 kya	-4985.24	1.67	0.07
~shift_areas(log(Body_mass), bs = "cr") + s(CV_prcp, bs = "cr") + s(CV_temp, bs = "cr")	10.5 - 6 kya	-4984.08	2.82	0.04
~shift_areas(log(Body_mass), bs = "cr") + s(CV_temp, bs = "cr")	10.5 - 6 kya	-4984.08	2.82	0.04
~shift_areas(log(Body_mass), bs = "cr") + s(CV_prcp, bs = "cr")	10.5 - 6 kya	-4984.08	2.82	0.04
~shift_areas(log(Max_disp), bs = "cr")	10.5 - 6 kya	-4970.55	16.36	0.00
~shift_areas(log(Body_mass), bs = "cr") + s(log(Max_disp), bs = "cr")	10.5 - 6 kya	-4969.37	17.54	0.00
~shift_area1	10.5 - 6 kya	-4954.07	32.84	0.00
~shift_areas(log(Body_mass), bs = "cr")	10.5 - 6 kya	-4954.06	32.85	0.00
~shift_areas(log(Body_mass), bs = "cr") + s(log(Max_disp), bs = "cr") + s(CV_prcp, bs = "cr")	6 - 0 kya	-5234.93	0.00	0.24
~shift_areas(log(Body_mass), bs = "cr") + s(log(Max_disp), bs = "cr") + s(CV_temp, bs = "cr")	6 - 0 kya	-5234.93	0.00	0.24

~shift_areas(log(Body_mass), bs = "cr") + s(log(Max_disp), bs = "cr") + s(CV_prcp, bs = "cr") + s(CV_temp, bs = "cr")	6 - 0 kya	-5234.93	0.00	0.24
~shift_areas(log(Body_mass), bs = "cr") + s(log(Max_disp), bs = "cr")	6 - 0 kya	-5231.79	3.14	0.05
Model	**Time Period**	**AIC**	**Delta AIC**	**Akaike Weight**
~shift_areas(log(Body_mass), bs = "cr") + s(CV_temp, bs = "cr")	6 - 0 kya	-5231.44	3.49	0.04
~shift_areas(log(Body_mass), bs = "cr") + s(CV_prcp, bs = "cr")	6 - 0 kya	-5231.44	3.49	0.04
~shift_areas(log(Body_mass), bs = "cr") + s(CV_prcp, bs = "cr") + s(CV_temp, bs = "cr")	6 - 0 kya	-5231.44	3.49	0.04
~shift_areas(log(Body_mass), bs = "cr")	6 - 0 kya	-5231.39	3.54	0.04
~shift_areas(log(Max_disp), bs = "cr")	6 - 0 kya	-5229.95	4.98	0.02
~shift_areas(log(Max_disp), bs = "cr") + s(CV_temp, bs = "cr")	6 - 0 kya	-5228.60	6.33	0.01
~shift_areas(log(Max_disp), bs = "cr") + s(CV_prcp, bs = "cr")	6 - 0 kya	-5228.60	6.33	0.01
~shift_areas(log(Max_disp), bs = "cr") + s(CV_prcp, bs = "cr") + s(CV_temp, bs = "cr")	6 - 0 kya	-5228.60	6.33	0.01
~shift_area1	6 - 0 kya	-5224.67	10.27	0.00
~shift_areas(CV_prcp, bs = "cr") + s(CV_temp, bs = "cr")	6 - 0 kya	-5223.09	11.84	0.00
~shift_areas(CV_prcp, bs = "cr")	6 - 0 kya	-5223.09	11.84	0.00
~shift_areas(CV_temp, bs = "cr")	6 - 0 kya	-5223.09	11.84	0.00
~shift_areas(log(Body_mass), bs = "cr") + s(CV_temp, bs = "cr")	0 - 2050 RCP 4.5	-4999.37	0.00	0.25
~shift_areas(log(Body_mass), bs = "cr") + s(CV_prcp, bs = "cr") + s(CV_temp, bs = "cr")	0 - 2050 RCP 4.5	-4999.29	0.08	0.24
~shift_areas(log(Body_mass), bs = "cr")	0 - 2050 RCP 4.5	-4997.71	1.65	0.11
~shift_areas(log(Body_mass), bs = "cr") + s(CV_prcp, bs = "cr")	0 - 2050 RCP 4.5	-4997.62	1.75	0.10
~shift_areas(log(Body_mass), bs = "cr") + s(log(Max_disp), bs = "cr") + s(CV_temp, bs = "cr")	0 - 2050 RCP 4.5	-4997.43	1.94	0.09
~shift_areas(log(Body_mass), bs = "cr") + s(log(Max_disp), bs = "cr") + s(CV_prcp, bs = "cr") + s(CV_temp, bs = "cr")	0 - 2050 RCP 4.5	-4997.41	1.96	0.09
~shift_areas(log(Body_mass), bs = "cr") + s(log(Max_disp), bs = "cr") + s(CV_prcp, bs = "cr")	0 - 2050 RCP 4.5	-4996.27	3.10	0.05
~shift_areas(log(Body_mass), bs = "cr") + s(log(Max_disp), bs = "cr")	0 - 2050 RCP 4.5	-4995.85	3.51	0.04
~shift_areas(log(Max_disp), bs = "cr") + s(CV_prcp, bs = "cr")	0 - 2050 RCP 4.5	-4991.89	7.47	0.01

~shift_areas(log(Max_disp), bs = "cr") + s(CV_temp, bs = "cr")	0 - 2050 RCP 4.5	-4991.24	8.13	0.00
~shift_areas(log(Max_disp), bs = "cr") + s(CV_prcp, bs = "cr") + s(CV_temp, bs = "cr")	0 - 2050 RCP 4.5	-4990.07	9.30	0.00
~shift_areas(log(Max_disp), bs = "cr")	0 - 2050 RCP 4.5	-4990.01	9.36	0.00
~shift_areas(CV_prcp, bs = "cr") + s(CV_temp, bs = "cr")	0 - 2050 RCP 4.5	-4987.45	11.91	0.00
Model	**Time Period**	**AIC**	**Delta AIC**	**Akaike Weight**
~shift_areas(CV_prcp, bs = "cr")	0 - 2050 RCP 4.5	-4987.44	11.92	0.00
~shift_areas(CV_temp, bs = "cr")	0 - 2050 RCP 4.5	-4986.79	12.57	0.00
~shift_area1	0 - 2050 RCP 4.5	-4982.64	16.73	0.00
~shift_areas(log(Body_mass), bs = "cr") + s(log(Max_disp), bs = "cr")	0 - 2050 RCP 8.5	-4938.01	0.00	0.21
~shift_areas(log(Body_mass), bs = "cr") + s(CV_prcp, bs = "cr")	0 - 2050 RCP 8.5	-4937.83	0.18	0.19
~shift_areas(log(Body_mass), bs = "cr") + s(log(Max_disp), bs = "cr") + s(CV_prcp, bs = "cr")	0 - 2050 RCP 8.5	-4937.61	0.40	0.17
~shift_areas(log(Body_mass), bs = "cr") + s(log(Max_disp), bs = "cr") + s(CV_temp, bs = "cr")	0 - 2050 RCP 8.5	-4937.21	0.80	0.14
~shift_areas(log(Body_mass), bs = "cr") + s(CV_prcp, bs = "cr") + s(CV_temp, bs = "cr")	0 - 2050 RCP 8.5	-4936.71	1.30	0.11
~shift_areas(log(Body_mass), bs = "cr")	0 - 2050 RCP 8.5	-4935.70	2.31	0.07
~shift_areas(log(Body_mass), bs = "cr") + s(log(Max_disp), bs = "cr") + s(CV_prcp, bs = "cr") + s(CV_temp, bs = "cr")	0 - 2050 RCP 8.5	-4935.16	2.85	0.05
~shift_areas(log(Body_mass), bs = "cr") + s(CV_temp, bs = "cr")	0 - 2050 RCP 8.5	-4934.57	3.44	0.04
~shift_areas(log(Max_disp), bs = "cr") + s(CV_prcp, bs = "cr")	0 - 2050 RCP 8.5	-4931.70	6.31	0.01
~shift_areas(log(Max_disp), bs = "cr")	0 - 2050 RCP 8.5	-4931.41	6.60	0.01
~shift_areas(log(Max_disp), bs = "cr") + s(CV_temp, bs = "cr")	0 - 2050 RCP 8.5	-4931.32	6.69	0.01
~shift_areas(CV_prcp, bs = "cr")	0 - 2050 RCP 8.5	-4927.59	10.42	0.00
~shift_areas(log(Max_disp), bs = "cr") + s(CV_prcp, bs = "cr") + s(CV_temp, bs = "cr")	0 - 2050 RCP 8.5	-4927.52	10.49	0.00
~shift_areas(CV_prcp, bs = "cr") + s(CV_temp, bs = "cr")	0 - 2050 RCP 8.5	-4926.53	11.48	0.00
~shift_areas(CV_temp, bs = "cr")	0 - 2050 RCP 8.5	-4926.29	11.72	0.00
~shift_area1	0 - 2050 RCP 8.5	-4923.87	14.15	0.00

~shift_areas(log(Body_mass), bs = "cr") + s(log(Max_disp), bs = "cr") + s(CV_prcp, bs = "cr") + s(CV_temp, bs = "cr")	2050 - 2090 RCP 4.5	-5094.13	0.00	0.74
~shift_areas(log(Max_disp), bs = "cr") + s(CV_prcp, bs = "cr") + s(CV_temp, bs = "cr")	2050 - 2090 RCP 4.5	-5091.00	3.13	0.16
~shift_areas(CV_prcp, bs = "cr") + s(CV_temp, bs = "cr")	2050 - 2090 RCP 4.5	-5088.37	5.76	0.04
~shift_areas(log(Body_mass), bs = "cr") + s(CV_prcp, bs = "cr") + s(CV_temp, bs = "cr")	2050 - 2090 RCP 4.5	-5087.93	6.20	0.03
Model	**Time Period**	**AIC**	**Delta AIC**	**Akaike Weight**
~shift_areas(log(Body_mass), bs = "cr") + s(log(Max_disp), bs = "cr") + s(CV_prcp, bs = "cr")	2050 - 2090 RCP 4.5	-5086.31	7.83	0.01
~shift_areas(log(Body_mass), bs = "cr") + s(log(Max_disp), bs = "cr") + s(CV_temp, bs = "cr")	2050 - 2090 RCP 4.5	-5083.27	10.87	0.00
~shift_areas(log(Max_disp), bs = "cr") + s(CV_prcp, bs = "cr")	2050 - 2090 RCP 4.5	-5083.03	11.10	0.00
~shift_areas(log(Body_mass), bs = "cr") + s(CV_prcp, bs = "cr")	2050 - 2090 RCP 4.5	-5082.17	11.96	0.00
~shift_areas(log(Body_mass), bs = "cr") + s(CV_temp, bs = "cr")	2050 - 2090 RCP 4.5	-5081.18	12.96	0.00
~shift_areas(log(Body_mass), bs = "cr") + s(log(Max_disp), bs = "cr")	2050 - 2090 RCP 4.5	-5079.70	14.44	0.00
~shift_areas(CV_prcp, bs = "cr")	2050 - 2090 RCP 4.5	-5078.30	15.83	0.00
~shift_areas(log(Max_disp), bs = "cr") + s(CV_temp, bs = "cr")	2050 - 2090 RCP 4.5	-5076.61	17.53	0.00
~shift_areas(log(Body_mass), bs = "cr")	2050 - 2090 RCP 4.5	-5072.79	21.35	0.00
~shift_areas(CV_temp, bs = "cr")	2050 - 2090 RCP 4.5	-5069.83	24.31	0.00
~shift_areas(log(Max_disp), bs = "cr")	2050 - 2090 RCP 4.5	-5067.12	27.01	0.00
~shift_area1	2050 - 2090 RCP 4.5	-5049.02	45.12	0.00
~shift_areas(log(Body_mass), bs = "cr") + s(log(Max_disp), bs = "cr") + s(CV_prcp, bs = "cr") + s(CV_temp, bs = "cr")	2050 - 2090 RCP 8.5	-4798.95	0.00	0.82

~shift_areas(log(Body_mass), bs = "cr") + s(log(Max_disp), bs = "cr") + s(CV_prcp, bs = "cr")	2050 - 2090 RCP 8.5	-4795.73	3.21	0.16
~shift_areas(log(Body_mass), bs = "cr") + s(CV_prcp, bs = "cr") + s(CV_temp, bs = "cr")	2050 - 2090 RCP 8.5	-4790.92	8.02	0.01
~shift_areas(log(Body_mass), bs = "cr") + s(CV_prcp, bs = "cr")	2050 - 2090 RCP 8.5	-4786.75	12.20	0.00
~shift_areas(log(Max_disp), bs = "cr") + s(CV_prcp, bs = "cr") + s(CV_temp, bs = "cr")	2050 - 2090 RCP 8.5	-4785.50	13.45	0.00
Model	**Time Period**	**AIC**	**Delta AIC**	**Akaike Weight**
~shift_areas(CV_prcp, bs = "cr") + s(CV_temp, bs = "cr")	2050 - 2090 RCP 8.5	-4783.59	15.35	0.00
~shift_areas(log(Max_disp), bs = "cr") + s(CV_prcp, bs = "cr")	2050 - 2090 RCP 8.5	-4781.30	17.64	0.00
~shift_areas(CV_prcp, bs = "cr")	2050 - 2090 RCP 8.5	-4777.66	21.28	0.00
~shift_areas(log(Body_mass), bs = "cr") + s(log(Max_disp), bs = "cr")	2050 - 2090 RCP 8.5	-4769.69	29.25	0.00
~shift_areas(log(Max_disp), bs = "cr") + s(CV_temp, bs = "cr")	2050 - 2090 RCP 8.5	-4768.75	30.20	0.00
~shift_areas(log(Max_disp), bs = "cr")	2050 - 2090 RCP 8.5	-4768.58	30.37	0.00
~shift_areas(log(Body_mass), bs = "cr") + s(log(Max_disp), bs = "cr") + s(CV_temp, bs = "cr")	2050 - 2090 RCP 8.5	-4766.90	32.04	0.00
~shift_areas(log(Body_mass), bs = "cr")	2050 - 2090 RCP 8.5	-4763.56	35.39	0.00
~shift_areas(log(Body_mass), bs = "cr") + s(CV_temp, bs = "cr")	2050 - 2090 RCP 8.5	-4763.02	35.93	0.00
~shift_area1	2050 - 2090 RCP 8.5	-4761.48	37.47	0.00
~shift_areas(CV_temp, bs = "cr")	2050 - 2090 RCP 8.5	-4760.71	38.24	0.00

3 Processes driving small mammal community composition over the previous 18,000 years.

3.1 Abstract

The importance of neutral and non-neutral processes on community composition is often debated. The relative importance of different processes can vary depending on the scale of sampling, species pool size, and the nature of climate or habitat change experienced by a community. However, predicting which processes are important under specific scenarios is difficult, making it challenging to determine how species will assemble into communities as they respond to future climate change. Here, we assess the importance of climate and stochastic processes for facilitating the assembly of small mammals at Samwell Cave in northern California over the previous 18,000 years. We generated climate-based predictions of community composition at fourteen past time periods and also estimated potential community composition based on the species pool, which served as a neutral hypothesis. The neutral and non-neutral predictions were then compared to the empirically-observed fossil communities found at Samwell Cave in each of the time periods. Results suggest that community composition at Samwell Cave is primarily shaped by climate, but mismatches between predictions and observations suggest that climate is not the only factor determining community composition. We then explored whether mismatches could be explained by similarity in species traits, indicating potential competition among species. Climate predictions did significantly better at predicting species composition than did stochastic predictions. Our results suggest that climate-based community predictions do well at predicting past community composition, which will be important as we predict community change in the future.

3.2 Introduction

Simulations of future climate change predict that the Earth’s global mean surface temperature could increase by as much as 4.8°C by the year 2100 (IPCC 2014). If we are to better understand and predict how species will respond to climate change, then understanding the global patterns of biodiversity, the processes responsible for those patterns, and the role of climate in particular is essential (Chase 2007; Lavergne et al. 2010; Pio et al. 2014; Walther et al. 2002). The ecological mechanisms that lead to the distribution of global biodiversity ultimately play out within local communities; thus, an understanding of the processes that govern the properties and diversity of local communities is required.

Community composition is hypothesized to be determined primarily through two different mechanisms. The first is non-random, deterministic mechanisms such as environmental filtering and interactions with other species (i.e., competition; Chase and

Myers 2011; Jackson and Overpeck 2000; Schoener 1983). The second mechanism is random or stochastic processes such as ecological drift, random extinction or extirpation events, and chance colonizations (Hubble 2001). The relative importance of each mechanism in determining community composition is debated (Connor and Simberloff 1979; Diamond 1975; Hubble 2001; Keddy 1992), and all mechanisms likely work in unison to determine community assembly patterns (Vellend 2010).

Deterministic mechanisms are highly dependent upon the functional traits and physiological characteristics of a species, which determine its ecological fit to local environmental conditions, the potential interactions it may have with other species, and its ability to persist within a community (Keddy 1990, 1992; Lebrija-Trejos et al. 2010). When environmental filtering is the primary deterministic mechanism structuring community composition, the community is expected to consist of ecologically similar species. This occurs because species with similar traits tend to have similar physiological tolerances and thus similar environmental niches (Chase 2007; Diamond 1975; MacAuthur and Levines 1964; Mayfield and Levine 2010). On the other hand, even if the local environment is within the range of a species environmental niche, the species may not occur in that local environment due to competitive exclusion (Diamond 1975; Grime 1973), which may occur when two species, often congeners, have similar traits and physiological characteristics. Overlap in traits and resource use means the two species have similar ecological requirements, which may lead to resource competition between them, with one species eventually outcompeting the other and excluding it from the community (Diamond 1975; Fox 1987). Therefore, if community assembly has been shaped by intraspecific competition, then the traits of the species within the community will exhibit patterns of trait over-dispersion (Moulton and Pimm 1987; Weiher and Keddy 1995). In all likelihood, both deterministic processes – environmental filtering and interactions such as competition – are operating simultaneously during community assembly (Ayarza et al. 2011; Ellwood et al. 2009; Kelt et al. 1995; Rodríguez et al. 2006).

Alternatively, community assembly may also be influenced by stochastic processes (Connor and Simberloff 1979; Hubble 2001), which are independent of species traits. In this hypothesis, all species have an equal chance of assembling into a community, so communities located in areas with similar environmental conditions can have different community compositions simply through the random trajectory of colonizations and extirpations that occur in each location (Hubble 2001). The existence of multiple stable states within communities that have assembled under largely stochastic processes can lead to higher community dissimilarity between communities than expected based on environmental differences between locations, and stochastically assembled communities should contain species that are more dissimilar in their climatic niches and functional traits than expected by environment or trait filtering, respectively (Chase 2003; Sutherland 1974).

The different community assembly processes are complementary and act in unison, and it has been difficult to predict when any of the suggested mechanisms are important in facilitating community assembly. This is in part because the dominant mechanism may vary depending upon the spatial scale of the study of interest and the intensity of the environmental filter (Cavender-Bares et al. 2006; Chase 2007; Gomez et al. 2010). As the scale (regional vs. local) of the study changes so does the species pool, as well as the magnitude of environmental and climatic heterogeneity observed in the study area, influencing the strength of the environmental filters (Chase 2007; Chase and Myers 2011; Lessard et al. 2012; Meyer et al. 2011). Environmental filtering is known to structure communities at regional scales where there is a significant amount of habitat heterogeneity (Gomez et al. 2010). However, at local scales with less habitat heterogeneity, competitive exclusion or stochastic processes may dominate the assembly process (Brown 1989; Kelt et al. 1995).

Climate and habitats are continually changing through time and the species assembled into a local community can be exposed to both rapidly changing and relatively stable climates. Given these environmental changes, the mechanisms important in determining community composition will likely vary at a single location (local scale) through time analogous to how communities differ with changing environments across the landscape. There is little knowledge and research, however, on how the importance of deterministic and stochastic mechanisms will variably affect the assembly of communities through time. Therefore, we examined the role and relative importance of deterministic and stochastic mechanisms in structuring communities at a single fossil locality over the past 18,000 years. We compared the ability of different deterministic and stochastic processes to accurately predict local communities.

In this study, we focused on the late Quaternary, during which the Earth has experienced significant climate change events such as rapid cooling (Younger Dryas) and warming episodes (Bølling-Allerød), as well as periods of relative climatic stability (Dansgaard et al. 1993; Liu et al. 2009). Because the late Quaternary encompasses periods of both rapid climate change and climate stability, it provides a unique time period to examine the processes important for community assembly under varying climate scenarios, where the strength of the environmental filter varies even as the spatial scale of the study site remains the same. Specifically, we examined the community assembly processes important in a small mammal community found at Samwell Cave in northern California over the past 18,000 years. First, we determined if the small mammal communities observed at different time periods in Samwell Cave assembled as a function of climatic filtering by comparing climate-based community hypotheses generated from species distribution models with observed fossil communities. Second, we examined the outliers – species that were not present in the fossil community even though they were predicted to be present for a particular time period – to determine if competition was a potential explanation for the exclusion of the species from the community. Finally, we compared stochastically-assembled communities with observed communities and determined which mechanism, deterministic or stochastic, better predicts community composition across all time periods.

3.3 Methods

3.3.1 Study system

The study system consists of the small mammal assemblage excavated from the Samwell Cave Popcorn Dome (SCPD) fossil deposit, located in Shasta County, Northern California (N 40.920, W -122.239). This deposit extends from contemporary times back to end of the Last Glacial Maximum (LGM), approximately 18,000 years ago (Blois et al. 2010). There are 14 different strata within the deposit, each representing on average 1,285 years of time. Because SCPD is a cave deposit derived from woodrat midden material, we focused on small mammals (i.e., mammals from Orders Rodentia and Soricomorpha) that are well-represented in the SCPD fossil record. Other work has shown that cave deposits capture a highly representative sample of the surrounding small mammal community (Hadly 1999; Terry 2010). Overall, each "community" in this study represents the empirical or predicted taxa list for a single stratum or time slice at Samwell Cave.

3.3.2 Regional species pool

We first determined the regional species pool for Samwell Cave. Small mammal species were included in the regional species pool if their contemporary range overlapped Samwell Cave. Because species ranges have shifted through time, we also considered species with contemporary ranges that occurred in the region around Samwell Cave (which included small mammals generally located in northern CA, NV and OR). In total, the regional species pool contained 35 small mammal species (Appendix Table 3.10.1).

3.3.3 Community composition inferences

To determine the relative importance of different community assembly processes, we compared the empirically observed community with predicted communities based on two contrasting assumptions: that climate is the only factor determining community composition or that stochastic processes determine community composition. To do this, three community lists were generated for each stratum in SCPD: empirically-observed communities, climate-predicted communities, and stochastically-predicted communities.

Empirically-observed communities: The small mammal taxon lists for each stratum of SCPD (Table 3.1) were originally generated by Blois et al. (2010) and represent the empirically-observed community list for a single time period. SCPD specimens were originally identified to the genus level (*Microtus*, *Neotoma*, *Peromyscus*, *Sorex*, and *Tamias*) in most cases and species level when possible (Blois et al. 2010).

Climate-predicted communities: Predicted communities for all time periods were generated using species distribution models (SDMs). Models were constructed, validated, and hindcasted following the methods of Williams and Blois (2018). Briefly, we constructed SDMs for all 35 species in the regional species pool using presence-only data from the contemporary period, downloaded from the Global Biodiversity Information Facility (GBIF; www.GBIF.org). The GBIF data were cleaned and manually inspected for discrepancies, and the species occurrences were spatially thinned based on the cell resolution of the underlying climate layers. This prevented any pseudoreplication in the model building process.

Species distribution models were constructed using climate variables downscaled to 0.5° x 0.5° grid cells (~50 x 50 km) (Lorenz et al. 2016), which were originally simulated with the Community Climate System Model version 3 (CCSM3) transient simulation (Liu et al. 2009; Liu et al. 2012). The downscaled simulations represent the average North American climate at every 500 years from 21,000 years ago to present (i.e., the variables are 200-year averages centered on the 500-year time slices for most times, though the contemporary simulations represent the average climate from 1850 to 1990 CE). Out of a possible 54 climate variables, we used six uncorrelated and biologically relevant variables: maximum precipitation of the wettest quarter, mean yearly potential evapotranspiration, maximum temperature of the warmest quarter, mean yearly water deficit index, mean yearly actual evapotranspiration, and minimum precipitation of the driest quarter. All climate layers contained paleoshorelines and have been clipped to represent the presence of ice sheets during each time period.

All models were initially constructed in the contemporary time period and evaluated using the geographically structured k-fold cross-validation approach outlined in Williams and Blois (2018). Five models were constructed for each species using different model algorithms (maxent, artificial neural networks, generalized linear models, multiple adaptive regression splines, and boosted regression trees) and the results from each algorithm underwent the geographically structured k-fold evaluation process.

An ensemble distribution model was generated for each of the 35 species using predictions from each of the algorithms and their associated averaged AUC values from the evaluation process (Araújo & New, 2007), providing a probability of presence distribution that is a function of the five underlying statistical models. By generating the SDMs through the ensemble process, the process is not relying on a single algorithm for its predictions and more robust predictions can be made for each species by weighting the useful information from each individual forecast into a single consensus model (Araújo & New 2007). Ensemble predictions for the contemporary distributions were evaluated using the Boyce index (Hirzel et al. 2006), calculated using the R package ‘ecospat’ (v. 2.2.0; Broennimann et al. 2016) with a moving window of 0.1 of the habitat suitability range to determine the habitat suitability bins.

Contemporary ensemble models were hindcasted to times that best matched the midpoint age of the individual strata in SCPD. Since the CCSM3 paleoclimate simulation only contains climate layers for 200-year intervals spaced 500 years apart, if the midpoint age of a sediment layer did not fall within one of the intervals, the closest 500-year layer was used (Fig. 3.1).

We determined if a species was predicted to be present, based on its climatic niche, at a particular time period by establishing the species-specific probability of presence threshold as the lowest predicted probability once the lowest 30% of the probability scores were discarded (Pearson et al. 2007). If the predicted probability of presence at Samwell Cave for a species was higher than the established threshold, the species was predicted to have been present at Samwell Cave during the associated time period. The climate-predicted community list was thus all species predicted present at Samwell Cave in a given time period. However, for taxa that were not able to be identified to the species level in the fossil record, the genus was predicted to be present during a time period if at least one species in the genus was predicted to be present based on the SDM or the stochastic predictions. The final community list represents a snapshot of community composition if climate filtering was the driving factor in community assembly (i.e., if the contemporary climatic tolerances of species completely determine which species assemble into a community).

All species distribution models and model statistics were constructed using the program BIOMOD2 (Thuiller et al. 2009) unless otherwise stated.

Stochastically-predicted communities: We generated random predictions of community composition for each time period by randomly sampling taxa from our regional species pool without replacement using R (v. 3.4.3; R Development Core Team, 2017). The number of taxa sampled was equivalent to the number of taxa in the empirically-observed community for that time period from the fossil deposit. We repeated the sampling process 1000 times for each time period.

Dissimilarity calculations: We used Sørenson's index to determine how closely the climate- or stochastically-predicted communities compared with the empirically-observed community composition for each time period. For the stochastically-predicted communities, we calculated the average dissimilarity across the 1000 simulations. The average stochastically-predicted dissimilarities were then compared to the climate-predicted dissimilarities to determine which method better predicted the empirical community composition at Samwell Cave. Our assumption is that the method that creates the closest match (i.e., the lowest dissimilarity) approximates the most relevant community assembly process for Samwell Cave, though we recognize that both processes likely are acting simultaneously. We statistically compared the climate-based versus stochastic-based dissimilarities using an analysis of variance statistical test.

3.3.4 The significance of competition in community assembly

Neither of the processes mentioned above, climate or stochastic assembly, is likely to perfectly predict community composition. This can be the result of several factors that would differently affect one or more of our empirical or predicted communities: 1) species interactions such as competition may hinder climate-predicted species from integrating into a community; 2) geographic and dispersal barriers may prevent climate-predicted or stochastically-predicted species from reaching a community; 3) taphonomy issues may bias estimation of the empirically-observed communities; or 4) model error may bias the climate-predicted communities (Thuiller 2004; Zhang et al. 2015). Here, we focus on determining if competition (factor #1) may explain mismatches between the climate-predicted and empirically-observed community composition, using a trait-based approach. We specifically focus on the scenario where SDMs predict a species to be present at Samwell Cave during a given time period, but that species is not observed in the fossil assemblage.

The trait-based approach is based on the assumption that species with similar traits will be more likely to compete with one another for resources if occupying the same local environment (Fargione et al. 2004; Moulton and Pimm 1987). Our trait analysis examined each community throughout the SCPD fossil deposit, focusing on the taxa predicted to be present in a community based on their climatic niches, but empirically determined to be absent (“incorrectly-predicted” taxa). For this subset of taxa, we determined if there is evidence from their traits to suggest that they were competitively excluded from Samwell Cave in the past due to competition.

First, for each empirical community (i.e., time period), we determined the overall community trait space. Traits examined in this analysis were body mass (g), foraging habits (fossorial, semi-fossorial, and not fossorial), foraging height (arboreal, scansorial, and terrestrial), activity time (nocturnal, diurnal, crepuscular, and cathermal), and the use of potential food sources. Trait data were downloaded from PanTHERIA (Jones et. al. 2009), and missing trait values were filled in by referencing the literature (Appendix Table 3.10.2). Some fossil specimens were identified to the genus and not the species level; in these instances, we calculated the most common (modal) trait value among all members of each genus included in the species pool (Table 3.2). All taxa analyzed in this study are extant and because of this we used modern trait values, with the assumption that these traits have remained consistent through time (Miller et al. 2014). The community trait space was generated using the trait values for all taxa observed in a single community at Samwell Cave (grey circles; Fig. 3.2.A). Next, for each taxon observed in the community, we calculated the minimum Euclidean distance between it and all other taxa in the assemblage, and a density plot of the minimum Euclidean distances among all taxa was generated for each community (Fig. 3.2.A). This represents the empirically-observed minimum trait spacing between all taxa in a community (Fig. 3.2.B). Finally, we determined the minimum Euclidean distance between each incorrectly-predicted and all empirically observed taxa in a community (red circle, Fig. 3.2.A). We then compared the minimum distances of the incorrectly-predicted taxa to the minimum Euclidean distance value that represented the lower 5% percent of the density distribution of the empirically-observed community (Fig. 3.2.B). This minimum value was generated using the R function *quantile* on each of the empirical communities. If competitive exclusion was a primary factor in community assembly at Samwell Cave over the previous 18,000 years, then the minimum Euclidean distance of most excluded taxa is expected to be smaller than the minimum distances of the taxa observed in the empirical community into which they are trying to assemble, suggesting that they are ecologically similar to taxa that were already present in the community.

3.4 Results

3.4.1 Community composition through time

Predicted community composition varied through time; climate-predicted communities contained an average of 15 taxa per time period, higher than the average of 11.2 taxa in the observed communities. Species distribution models used to generate the climate-predicted communities were accurate, but the accuracy varied across taxa. The average Boyce index value for our ensemble SDMs was 0.90 (± 0.12; Appendix Table 3.10.1) with a minimum value of 0.54 (*Sorex pacificus*) and a maximum value of 1.00 (*Peromyscus maniculatus*). Several taxa were predicted by the SDMs to be present at Samwell Cave during all past time periods (*Microtus*, *Peromyscus*, *Neotoma*, *Sorex*, *Tamias*, *Tamiasciurus douglasii*, *Sciurus griseus*, *Spermophilus lateralis*, *Glacomys sabrinus*, and *Zapus trinotatus*), three taxa were predicted to be present in only the cooler time periods that occurred at the end of the LGM (*Aplodontia rufa*, *Arborimus albipes*, and *Myodes californicus*), one taxon (*Scapanus latimanus*) was predicted to be present in all time periods except for 17,500 ka BP, and one taxon (*Thomomys bottae*) was predicted to be present in all time periods except 17,500 and 16,500 ka BP. The remaining taxa were predicted to be present at Samwell Cave intermittently (Table 3.1).

The climate-based communities matched the empirically-observed communities better than did the stochastically-generated communities (Fig. 3.3). Dissimilarity between climate-based community predictions and the empirically-observed community lists was low: across all time periods, there was an average dissimilarity of 0.21 (± 0.08; min = 0.11, 6,000 ka BP; max = 0.42, 10,000 ka BP). In contrast, the stochastically-generated community predictions and the observed community lists had an average dissimilarity of 0.611 (± 0.06; min = 0.54, 6,000 ka BP; max = 0.74, 10,000 ka BP). Climate-based dissimilarities were significantly lower than stochastically-based dissimilarities ($f = 211.8$, $df = 26$, $p < 0.0001$).

3.4.2 Potential for competitive exclusion

Comparisons between the climate-predicted and the empirically-observed fossil community assemblages at Samwell Cave revealed 65 instances where our models predicted a taxon to be present at Samwell Cave during a particular time period but the taxon was not observed in the fossil record (Appendix Table 3.10.3). Taxa that were incorrectly predicted across all 14 time periods were *Zapus trinotatus* (14/65); *Neurotrichus gibbsii* (9/65); *Glaucomys sabrinus* (9/65); *Reithrodontomys megalotis* (8/65); *Sciurus griseus* (5/65); *Sorex* (4/65); *Myodes californicus* (4/65); *Spermophilus lateralis* (4/65); *Tamias* (4/65); *Scapanus lateralis* (1/65); *Aplodontia rufa* (1/65); *Tamiasciurus douglasii* (1/65); *Thomomys bottae* (1/65). Species distribution models predicted the presence of *Z. trinotatus* in all time periods and *N. gibbsii* was predicted to be present in 5 of the 14 examined time periods, but neither taxa were present at any time period throughout fossil deposit (Table 3.1).

Twenty of the 65 instances where taxa were incorrectly predicted to be present may have been the result of competitive exclusion from the community in the examined time period. In these instances, the minimum trait distance of the incorrectly predicted taxon fell in the lower 5% of the distribution for the empirical communities' trait space (Appendix Table 3.10.3). *Neurotrichus gibbsii* (8/20) and *R. megalotis* (6/20) made up 70% of the 20 possible instances of competitive exclusion. The remaining instances of potential competitive exclusion included *Z. trinotatus* (3/20), *Sorex* (2/20), and *Tamias* (1/20; Appendix Table 3.10.3).

Results for our trait analysis show that in all instances where *N. gibbsii* had the potential to have been competitively excluded from the Samwell Cave community, the taxon to which it was most similar in trait space was *Sorex*. However, in the single instance where *N. gibbsii* was predicted to be present but absent and *Sorex* was also absent, and *N. gibbsii* was more similar to *R. megalotis*. *Reithrodontomys megalotis* was generally most functionally similar to *Sorex* and when *Sorex* was not empirically observed to be present, *R. megalotis* was most similar to *Peromyscus* in trait space. *Zapus trinotatus* was also predicted to have been competitively excluded from Samwell Cave and was ecologically similar to *Peromyscus*, *Tamias*, and *Scapanus lateralis*. Finally, in the two instances that *Sorex* was significantly more similar to another taxon in trait space, it was more similar to *Peromyscus* and *R. megalotis*.

3.5 Discussion

3.5.1 Climate vs random assembly

Communities are hypothesized to assemble as a function of environmental and habitat filtering, species interactions, and/or stochastic mechanisms (Hille Ris Lambers et al. 2012; Hubble 2001; Keddy 1992). Our analyses demonstrate that the fossil small mammal communities at Samwell Cave over the late Quaternary were consistently structured by climate: the observed species composition is similar to what would be expected if the communities assembled only as a function of climate filtering (Sørenson dissimilarities ranged between 0.11 - 0.42 through time; Fig. 3.3). We found little support for stochastic mechanisms leading to community assembly, a result that varies from others, as stochastic mechanisms are found to drive community composition mostly at local scales (Shipley et al. 2012; Weiher et al. 2011). In all time periods examined, the dissimilarities between the stochastically-predicted community hypotheses and the fossil community were significantly higher than the dissimilarity between the climate-predicted community hypotheses and the observed fossil community. This suggests that the community at Samwell Cave was assembled largely based on deterministic mechanisms (Cornwall and Ackerly 2009; Gómez et al. 2010; Lebrija-Trejos et al. 2010). However, we recognize that our approach examines the importance of environmental filtering and stochastic assembly individually rather than simultaneously. As acknowledged previously, both mechanisms likely work in unison. Our results, therefore, indicate which process is important under a scenario where one mechanism is likely to strongly determine community composition over the other. A more integrative analysis would examine the mechanisms in tandem by analyzing the residuals of the climate-based models for signals of stochastic assembly patterns. We plan to incorporate such analyses in future work to determine if both processes are in fact working in unison to determine community composition.

Even though climate appears to be the dominant mechanism determining community assembly, the match between the climate-predicted and empirically-observed communities was not perfect, however, and the magnitude of the mismatch was higher in the past (Fig. 3.3). This result could be linked to the effect of projecting SDMs to novel climates. For example, Maguire et al. (2016) found that SDMs decrease in accuracy when projected to areas with a climate that differs from the climate in which the SDMs were constructed. This is indicted in our results as the dissimilarity between the climate-based community predictions and the empirical fossil community increases, on average, as the models are projected farther back in time to periods that were much cooler than today (Liu et al. 2009). The presence or absence of a taxon in any given community in the region around Samwell Cave is largely based on physiological tolerances or habitat and therefore driven by climate (or climate as a surrogate for habitat). However, if the model used to predict the presence of the species does not include the complete range of climate tolerances in which the species can persist, the species potential distribution in the past may be underestimated (Thuiller et al. 2004). In addition, the climate simulations themselves may be less accurate further back in time (Harrison et al. 2015), which could influence resulting species range hypotheses. Both of these potential mechanisms may lead to incorrect predictions of species presence in a community.

3.5.2 Trait filtering

The increased mismatch in the past, however, may also arise because other mechanisms besides climate are driving community assembly patterns at the end of the Last Glacial Maximum, such as competition, dispersal limitation, and geographic barriers (Kelt et al. 1995). Competition between mammal species can restructure species distributions and occupancy in a community as species respond to competitive interactions. Hallett et al. (1983) determined that *Peromyscus maniculatus* distribution in a wet grassland was primarily structured based on competitive interactions with *Microtus pennsylvanicus*, *Zapus hudsonius*, and *Spermophilus tridecemlineatus*, resulting in *P. maniculatus* occupying areas where the other three species were not found. Abramsky et al. (1979) provided similar results when they analyzed competitive ineractions of small mammals on a shortgrass prairie ecosystem. They determined that *Microtus ochrogaster* directly altered the distribution and abundance of *Peromyscus maniculatus* through competitive interactions. Although climate appears to be a large factor in determining the taxa present in a community at any given time and some mismatches may result from modeling error, our results suggest that competitive exclusion may have inhibited some taxa from becoming integrated into the local community at Samwell Cave. Two species, *Neurotrichus gibbsii* and *Zapus trinotatus*, appear to have been potentially excluded from Samwell Cave as both species were predicted to be present in all time periods but never appeared in the fossil record (Table 3.1). Results from our trait similarity analysis suggest that *Sorex* may have competitively excluded *N. gibbsii* from Samwell Cave, while *Peromyscus* may have excluded *Z. trinotatus* at the end of the LGM. Both *Sorex* and *Permyscus* were present at Samwell Cave 17,500 yr BP, while *N. gibbsii* and *Z. trinotatus* were predicted to be present but were absent. The presence of *Sorex* and *Peromyscus* at Samwell Cave before *N. gibbsii* and *Z. trinotatus* may have prevented the integration of *N. gibbsii* and *Z. trinotatus* into the community, especially since *Sorex* and *Peromyscus* are almost always present in the SCPD fossil deposit (Table 1). However, our results suggest *Peromyscus* to be the dominant competitior, while previous research has shown that *Peromyscus* is generally the non-dominant competitor (Abramsky et al. 1979; Hallett et al. 1983). This discrepancy may be due to the fact that *Peromyscus* is identified to the genus level at SCPD; more refined taxonomic identifications may reveal hidden importance of competitive interactions for this group.

The competitive exclusion of *N. gibbsii* by *Sorex* is biologically plausible, as both taxa are primarily crepuscular and consume similar resources such as seeds, plant material, and invertebrates (Table 3.2). *Sorex* can also make use of other resources such as fungi, which *N. gibbsii* is not known to use, thus allowing *Sorex* access to resources not associated with *N. gibbsii* (Carraway 1975; Beneski and Stinson 1987; Carraway and Verts 1991; George 1989; Gillihan and Foresman 2004; Pattie 1973; Table 3.2). However, during the one instance when *Sorex* was not present in the fossil record (12,500 yr BP), *N. gibbsii* was predicted present but absent. Since *N. gibbsii* still didn’t assemble into the community in the absence of its most functionally similar species, competition may not be the main reason for its absence from the fossil record at Samwell Cave; instead, other factors such as dispersal limitation or geographic barriers may better explain its absence.

Zapus trinotatus and *Peromyscus* also share similar resource overlap, with both taxa consuming seeds, fruits, fungi, plant material, and invertebrates. Their activity times can vary slightly as *Z. trinotatus* is mainly nocturnal with crepuscular tendencies, while *Peromyscus* is nocturnal (Gannon 1988; Kalcounis-Rueppell and Spoon 2009; Sullivan 1995; Table 3.2). Because both taxa are primarily nocturnal, they likely would have been active at the same time and competed for the same resources, with *Peromyscus* likely outcompeting *Z. trinotatus*. However, further insight is limited because it is unknown which species of *Peromyscus* was present at Samwell Cave at this time.

Other taxa suggested to have been competitively excluded were likely absent from the fossil record due to taphonomic processes. For example, some taxa, such as *R. megalotis*, *Sorex*, and *Tamias,* were only found in the fossil record during some time periods at Samwell Cave. Their absence in the fossil deposit during intermittent time periods is likely an artifact of taphonomy and rarity (Behrensmeyer et al. 1979; Behrenmeyer and Boaz 1980). Bones of small mammals are more prone to destruction by carnivores, scavengers, and weathering processes as their surface area is increased through fragmentation from trampling (Behrensmeyer et al. 1979; Behrensmeyer and Boaz 1980). Because of these factors small mammal remains tend to preserve significantly less well than those of larger mammals, resulting in taxa potentially not being represented in the fossil record even though they existed on the landscape. Other research also suggests that the increase in the surface-to-volume ratio of small mammal bones allows them to be more susceptible to acidic dissolution than those of large mammals and they are therefore found in the fossil record less often (Retallack 1988). Therefore, the instances where *Sorex*, *R. megalotis*, and *Tamias* appear to have been competitively excluded from SCPD are likely artifacts of rarity and the fossilization process. A similarly small mammal, *Peromyscus* sp., was present in all levels of the deposit and was the most common taxon found in the deposit, but it is also very common on the landscape (Blois et al. 2010).

3.5.3 Other factors

Size of species pool: The scale at which a community is defined has a dramatic influence on the mechanisms that facilitate community assembly processes (Cavender-Bares et al. 2006, Gomez et al. 2010, Lessard et al. 2012). Here, we apply a conservative definition of the species source pool, where we define the source as the species that are observed in the SCPD fossil deposit and any small mammal whose range was located in the broad region around the cave (northern California, Oregon, and Nevada). This definition represents a relatively local source pool compared to the number of small mammal species that would have been included, for example, if we had included all species in the western United States. Different delineations of the source pool would potentially alter the results (Cavender-Bares et al. 2006, Lessard et al. 2012). For example, we would expect the strength of climate filtering to increase as the definition of the source pool changed from our locally defined pool to one that included all small mammal species in California and its surrounding states, the result of increased habitat heterogeneity encompassed by broader spatial extents. We also expect the accuracy of our stochastic predictions to decrease with a larger species pool, simply because the addition of more species will make it less likely for the stochastic models to sample the 15 or so species empirically observed in the SCPD fossil deposit. Overall, broadening the source pool would serve to widen the gap between climatically vs. stochastically-inferred communities and thus reinforce our finding that climate predicts community composition relatively well. Further, the increased species pool size would likely allow for a greater detection of competition throughout the SCPD fossil deposit, since the larger species pool would include more species that potentially were competitively excluded in the past. Finally, the fact that we aggregated many of the species in our analyses to the genus level to match the taxonomic resolution of the fossil record is not likely to alter our fundamental conclusions substantially, though it may underestimate the importance of competition in some cases.

Priority effects: We did not consider priority effects when we constructed our climate and stochastic predictions: our results assume that all species have an equal probability of being integrated into the community at Samwell Cave regardless of the order that species assemble into the community. Some studies have shown that the order (i.e., site history) in which species integrate into communities has no effect on the final compostion of communities (Chase 2007; Sommer 1991; Tilman et al. 1986), while other studies suggest that site history does indeed matter and that communities with similar environmental conditions can comprise multiple compositional states, which are dependent upon which species initially integrate into the community (Drake 1991; Law 1999; Samuels and Drake 1997). Including priority effects into our analyses could cause our inferences of the important community assembly mechanisms to differ. For example, if priority effects were strong, the importance of competition might also be initially very high as newly arriving species would be excluded or included based on the presence of the first few species that integrate into the community (Drake 1991, Law 1999). However, the fossil record at SCPD is not long enough to capture the initial community assembly process to test for priority effects. Replicated fossil deposits that preserved other records from the same region and time would be a useful addition to test for priority effects.

3.6 Conclusions

Results from this study suggest that communities present at Samwell Cave have assembled largely due to climate filtering, with competitive exclusion serving as a secondary potential mechanism that fine tunes the community composition. Two taxa, *N. gibbsii* and *Z. trinotatus*, show potential evidence of competitive exclusion, by *Sorex* and *Peromyscus*, respectively. Our study also shows that SDMs have the ability to be used to predict community composition relatively confidently in this system and that SDMs predict community composition better than stochastic sampling methods. However, caution must be used when projecting models into differing climates, which can lead to increased model error and incorrect community predictions (Maguire et al. 2016). One potential method of combating the issues associated with projecting models into climates that differ from those in which the models were constructed is to use pooled species distribution models (Nogués-Bravo, 2009). Pooled SDMs provide a more complete estimation of the niche and the models can then be used to more accurately estimate changes in community composition as the result of future climate change.

This study, one of the first to estimate mechanisms of community assembly through time at a local scale, could be strengthened by extending the methods used here to multiple sites. Increasing the number of replicated sites, while using the same analyses, would help further disentangle the importance of the different mechanisms that determine community composition. For example, replication would indicate if there are priority effects influencing community composition, and if the observed patterns in this study are idiosyncratic or instead representative of strong climatic influence on community assembly, with additional but low influence of competition.

3.7 References

Abramsky, Z., Dyer, M.I., & Harrison, P.D. (1979) Competition among small mammals in experimentally perturbed areas of the shortgras prairie. *Ecology*, **60**, 530–536.

Araújo, M.B. & New, M. (2007) Ensemble forecasting of species distributions. *Trends in Ecology and Evolution*, **22**, 42–47.

Ayarza, J.M. & Erijman, L. (2011) Balance of Neutral and Deterministic Components in the Dynamics of Activated Sludge Floc Assembly. *Microbial Ecology*, **61**, 486–495.

Behrensmeyer, A.K. & Boaz, D. (1987) Late Pleistocene geology and paleontology of Amboseli National Park, Kenya. *Paleoecology of Africa* (ed. by J. Coetzee and E.M. van Zinderen Bakker), pp. 135–188.

Behrensmeyer, A.K., Western, D., & Boaz, D. (1979) New Perspectives in Vertebrate Paleoecology from a Recent Bone Assemblage. *Paleobiology*, **5**, 12–21.

Beneski, J.T. & Stinson, D.W. (1987) Sorex palustris. *Mammalian Species*, 1.

Blois, J.L., McGuire, J.L., & Hadly, E.A. (2010) Small mammal diversity loss in response to late-Pleistocene climatic change. *Nature*, **465**, 771–4.

Broennimann, O., Treier, U.A., Müller-Schärer, H., Thuiller, W., Peterson, A.T., & Guisan, A. (2007) Evidence of climatic niche shift during biological invasion. *Ecology Letters*, **10**, 701–709.

Broennimann, O., Valeria, D.C., Petitpierre, B., Breiner, F., D’Amen, M., Randin, Christophe, Engler, R., Hordijk, W., Pottier, J., Di Febbraro, M., Pellissier, L., Pio, D., Dubuis, A., Scherrer, D., Maiorano, L., Psomas, A., Ndiribe, C., Salamin, N., Zimmermann, N., & Guisan, A. (2016) Package ‘ ecospat ’ v2.2.0

Brown, J.S. (1989) Desert rodent community structure: a test of four mechanism of coexistence. *Ecological Monographs*, **59,** 1-20

Carraway, L.N. & Verts, B.J. (1991) Neurotrichus gibbsii. *Mammalian Species*, **387**, 1-7.

Cavender-Bares, J., Keen, A., & Miles, B. (2006) Phylogenetic structure of Floridian plant communities depends on taxonomic and spatial scale. *Ecology*, **87**, S109-S122

Chase, J.M. (2003) Community assembly: when should history matter? *Oecologia*, **136**, 489–98.

Chase, J.M. (2007) Drought mediates the importance of stochastic community assembly. *Proceedings of the National Academy of Sciences of the United States of America*, **104**, 17430–4.

Chase, J.M. & Myers, J.A. (2011) Disentangling the importance of ecological niches from stochastic processes across scales. *Philosophical transactions of the Royal Society of London. Series B, Biological sciences*, **366**, 2351–63.

Connor, E.F. & Simberloff, D. (1979) The assembly of species communities: chance or competition? *Ecology* **60**, 1132-1140.

Cornwell, W.K. & Ackerly, D.D. (2009) Community assembly and shifts in plant trait distributions across an environmental gradient in coastal California. *Ecological Monographs*, **79**, 109–126.

Dansgaard, W., Johnsen, S.J., Clausen, H.B., Dahl-Jensen, D., Gundestrup, N.S., Hammer, C.U., Hvidberg, C.S., Steffensen, J.P., Sveinbjörnsdottir, A.E., Jouzel, J., & Bond, G. (1993) Evidence for general instability of past climate from a 250-kyr ice-core record. *Nature*, **364**, 218–220.

Diamond, J.M. (1975) Assembly of Species Communities. *Ecology and Evolution of Communities* (ed. by J.M. Diamond and M.L. Cody), pp. 342–344. Harvard University Press, Boston.

Drake, J.A. (1991) Community-Assembly Mechanics and the Structure of an Experimental Species Ensemble. *The American Naturalist*, **137**, 1–26.

Ellwood, M.D.F., Manica, A., & Foster, W.A. (2009) Stochastic and deterministic processes jointly structure tropical arthropod communities. *Ecology letters*, **12**, 277–84.

Fargione, J., Brown, C.S., & Tilman, D. (2004) Community assembly and invasion: An experimental test of neutral versus niche processes. *Proceedings of the National Academy of Sciences*, **101**, 8916–8920.

Fernández, M. & Hamilton, H. (2015) Ecological Niche Transferability Using Invasive Species as a Case Study. *PLOS ONE*, **10**, e0119891.

Fox, B.J. (1987) Species assembly and the evolution of community structure. *Evolutionary Ecology*, 1, 201-213.

Gannon, W.L. (1988) Zapus trinotatus. *Mammalian Species*, **315**, 1-5.

George, S.B. (1989) Sorex trowbridgii. *Mammalian Species*, **337**, 1-5.

Gillihan, S.W. & Foresman, K.R. (2004) Sorex vagrans. *Mammalian Species*, **744**, 1–5.

Gómez, J.P., Bravo, G. a., Brumfield, R.T., Tello, J.G., & Cadena, C.D. (2010) A phylogenetic approach to disentangling the role of competition and habitat filtering in community assembly of Neotropical forest birds. *Journal of Animal Ecology*, **79**, 1181–1192.

Grime, J.P. (1973) Competitive Exclusion in Herbaceous Vegetation. *Nature*, **242**, 344-347.

Hadly, E.A. (1999) Fidelity of terrestrial vertebrate fossils to a modern ecosystem. *Palaeogrography, Palaeoclimatology, Palaeoecology*, **149**, 389–409.

Hallett, J.G., O'Connell, M.A., & Honeycutt, R.L. (1983) Competition and habitat selection: test of a theory using small mammals. *OIKOS*, **40**, 175–181.

Harrison S.P., Bartlein P.J., Izumi K., Li G., Annan J., Hargreaves J., Braconnot P., & Kageyama M. (2015) Evaluation of CMIP5 palaeo-simulations to improve climate projections. *Nature Climate Change*, **5**, 735–743.

Hille Ris Lambers, J., Adler, P.B., Harpole, W.S., Levine, J.M., & Mayfield, M.M. (2012) Rethinking Community Assembly through the Lens of Coexistence Theory. *Annual Review of Ecology, Evolution, and Systematics*, **43**, 227–248.

Hirzel, A.H., Le Lay, G., Helfer, V., Randin, C., & Guisan, A. (2006) Evaluating the ability of habitat suitability models to predict species presences. *Ecological Modelling*, **199**, 142–152.

Hubbell, S.P. (2001) *The unified neutral theory of biodiversity and biogoegraphy.* Princeton University Press, Princeton.

IPCC, (2014) Climate change 2014: synthesis report. Contribution of Working Groups I, II, and III to the Fifth Assessment Report of the Intergovernmental Panel on Climate Change [Core Writing Team, Pachauri, R.K. & Meyer, L.A. (eds.)]. IPCC, Geneva, Switzerland, 151 pp.

Jackson, S.T. & Overpeck, J.T. (2000) Responses of plant populations and communities to environmental changes of the late Quaternary. *Paleobiology*, **26**, 194-220.

Jones, K.E., Bielby, J., Cardillo, M., et al. (2009) PanTHERIA: a species-level database of life history, ecology, and geography of extant and recently extinct mammals. *Ecology*, **90**, 2648.

Kalcounis-Rueppell, M.C. & Spoon, T.R. (2009) Peromyscus boylii (Rodentia: Cricetidae). *Mammalian Species*, **838**, 1–14.

Keddy, P.A. (1990) Competitive Hierarchies and Centrifugal Organization in Plant Communities. *Perspectives on plant competition* (ed. by J. Grace and D. Tilman), pp. 265–290. Academic Press, New York.

Keddy, P.A. (1992) Assembly and response rules: two goals for predictive community ecology. *Journal of Vegetation Science,* **3**, 157–164.

Kelt, D. a, Brown, J.H., Heske, E.J., Marquet, P. a, Morton, S.R., Reid, J.R.W., Rogovin, K. a, & Shenbrot, G. (1996) Community structure of desert small mammals: comparisons across four continents. *Ecology,* **77**, 746-761.

Lavergne, S., Mouquet, N., Thuiller, W., & Ronce, O. (2010) Biodiversity and Climate Change: Integrating Evolutionary and Ecological Responses of Species and Communities. *Annual Review of Ecology, Evolution, and Systematics*, **41**, 321–350.

Law, R. (1999) Theoretical aspects of community assembly. *Advance in ecological theory: principles and applications* pp. 141–171. Blackwell, Oxford.

Lebrija-Trejos, E., Pérez-García, E.A., Meave, J.A., Bongers, F., & Poorter, L. (2010) Functional traits and environmental filtering drive community assembly in a species-rich tropical system. *Ecology*, **91**, 386–398.

Lessard, J.-P., Borregaard, M.K., Fordyce, J.A., Rahbek, C., Weiser, M.D., Dunn, R.R., & Sanders, N.J. (2012) Strong influence of regional species pools on continent-wide structuring of local communities. *Proceedings. Biological sciences / The Royal Society*, **279**, 266–74.

Liu, Z., Otto-Bliesner, B.L., He, F., Brady, E.C., Tomas, R., Clark, P.U., Carlson, A.E., Lynch-Stieglitz, J., Curry, W., Brook, E., Erickson, D., Jacob, R., Kutzbach, J., & Cheng, J. (2009) Transient simulation of last deglaciation with a new mechanism for Bolling-Allerod warming. *Science,* **325**, 310–4.

Liu, Z., Carlson, A.E., He, F., Brady, E.C., Otto-Bliesner, B.L., Briegleb, B.P., Wehrenberg, M., Clark, P.U., Wu, S., Cheng, J., Zhang, J., Noone, D., & Zhu, J. (2012) Younger Dryas cooling and the Greenland climate response to CO2. *Proceedings of the National Academy of Sciences of the United States of America,* **109**, 11101–4.

Lorenz, D.J., Nieto-Lugilde, D., Blois, J.L., Fitzpatrick, M.C., & Williams, J.W. (2016) Downscaled and debiased climate simulations for North America from 21,000 years ago to 2100AD. *Scientific Data*, **3**, 160048.

Losos, J.B., Leal, M., Glor, R.E., de Queiroz, K., Hertz, P.E., Rodríguez Schettino, L., Chamizo Lara, A., Jackman, T.R., & Larson, A. (2003) Niche lability in the evolution of a Caribbean lizard community. *Nature*, **424**, 542–545.

Macarthur, R. & Levins, R. (1964) Competition, habitat selection, and character displacement in a patchy environment. *Proceedings of the National Academy of Sciences of the United States of America*, **51**, 1207–10.

Maguire, K.C., Nieto-Lugilde, D., Blois, J.L., Fitzpatrick, M.C., Williams, J.W., Ferrier, S., & Lorenz, D.J. (2016) Controlled comparison of species- and community-level models across novel climates and communities. *Proceedings of the Royal Society B: Biological Sciences*, **283**, 20152817.

Martinez-Meyer, E., Townsend Peterson, A., & Hargrove, W.W. (2004) Ecological niches as stable distributional constraints on mammal species, with implications for Pleistocene extinctions and climate change projections for biodiversity. *Global Ecology and Biogeography*, **13**, 305–314.

Mayfield, M.M. & Levine, J.M. (2010) Opposing effects of competitive exclusion on the phylogenetic structure of communities. *Ecology Letters*, **13**, 1085–1093.

Miller, J.H., Behrensmeyer, A.K., Du, A., Lyons, S.K., Patterson, D., Tóth, A., Villaseñor, A., Kanga, E., & Reed, D. (2014) Ecological fidelity of functional traits based on species presence-absence in a modern mammalian bone assemblage (Amboseli, Kenya). *Paleobiology*, **40**, 560–583.

Moulton, M.P. & Pimm, S.L. (1987) Morphological assortment in introduced Hawaiian passerines. *Evolutionary Ecology*, **1**, 113–124.

Nogués-Bravo, D. (2009) Predicting the past distribution of species climatic niches. *Global Ecology and Biogeography*, **18**, 521–531.

Pearson, R.G., Raxworthy, C.J., Nakamura, M., & Townsend Peterson, A. (2007) Predicting species distributions from small numbers of occurrence records: a test case using cryptic geckos in Madagascar. *Journal of Biogeography*, **34**, 102–117.

Pio, D. V., Engler, R., Linder, H.P., Monadjem, A., Cotterill, F.P.D., Taylor, P.J., Schoeman, M.C., Price, B.W., Villet, M.H., Eick, G., Salamin, N., & Guisan, A. (2014) Climate change effects on animal and plant phylogenetic diversity in southern Africa. *Global Change Biology*, **20**, 1538–1549.

Retallack, G.J. (1988) Down-to-Earth Approaches to Vertebrate Paleontology. *PALAIOs*, **3**, 335–344.

R Development Core Team (2017). R: A language and environment for statistical computing. R Foundation for Statistical Computing, Vienna, Austria. Available from http://www.R-project.org.

Rodríguez, J., Hortal, J., & Nieto, M. (2006) An evaluation of the influence of environment and biogeography on community structure: The case of Holarctic mammals. *Journal of Biogeography*, **33**, 291–303.

Samuels, C.L. & Drake, J.A. (1997) Divergent perspectives on community convergence. *Trends in Ecology and Evolution*, **12**, 427–432.

Schoener, T.W. (1983) Field Experiments on Interspecific Competition. *The American Naturalist*, **122**, 240–285.

Shipley, B., Paine, C.E.T., & Baraloto, C. (2012) Quantifying the importance of local niche-based and stochastic processes to tropical tree community assembly. *Ecology*, **93**, 760–769.

Sommer, U. (1991) Convergent succession of phytoplankton in microcosms with different inoculum species composition. *Oecologia*, **87**, 171–179.

Sullivan, J. (1995) *Peromyscus maniculatus*. In: Fire effects information system, [Online]. U.S. Department of Agriculture, Forest Service, Rocky Mountains Research Station, Fire Sciences Laboratory. Available: http://www.fs.fed.us/database/feis.

Sutherland, J.P. (1974) Multiple stable points in natural communities. *The American Naturalist*, **108**, 859-873

Terry, R.C. (2010) On raptors and rodents: testing the ecological fidelity and spatiotemporal resolution of cave death assemblages. *Paleobiology*, **36**, 137–160.

Thuiller, W. (2004) Patterns and uncertainties of species' range shifts under climate change. *Global Change Biology*, **10**, 2020–2027.

Thuiller, W., Lafourcade, B., Engler, R., & Araujo, M.B. (2009) BIOMOD - A platform for ensemble forecasting of species distributions. *Ecography*, **32**, 369–373.

Tilman, D., Kiesling, R., Sterner, R., Kilham, S., & Johnson, F.A. (1986) Green, bluegreen, and diatom algae: Tazonomic differences in competitive ability for phosphorus, silicon and nitrogen. *Arch Hydrobiol*, **106**, 473–485.

Vellend, M. (2010) Conceptual Synthesis in Community Ecology. *The Quarterly Review of Biology*, **85**, 183–206.

Walther, G.-R., Post, E., Convey, P., Menzel, A., Parmesan, C., Beebee, T.J.C., Fromentin, J.-M., Hoegh-Guldberg, O., & Bairlein, F. (2002) Ecological responses to recent climate change. *Nature*, **416**, 389–95.

Weiher, E. & Keddy, P.A. (1995) Assembly Rules, Null Models, and Trait Dispersion: New Questions from Old Patterns. *Oikos*, **74**, 159.

Weiher, E., Freund, D., Bunton, T., Stefanski, A., Lee, T., & Bentivenga, S. (2011) Advances, challenges and a developing synthesis of ecological community assembly theory. *Philosophical Transactions of the Royal Society B: Biological Sciences*, **366**, 2403–2413.

Williams, J.E. & Blois, J.L. (2018) Range shifts in response to past and future climate change: Can climate velocities and species' dispersal capabilities explain variation in mammalian range shifts? *Journal of Biogeography*, **45**, 2175–2189.

Zhang, L., Liu, S., Sun, P., Wang, T., Wang, G., Zhang, X., & Wang, L. (2015) Consensus forecasting of species distributions: the effects of niche model performance and niche properties. *PloS one*, **10**, e0120056.

3.8 Tables

Table 3.1. Taxon presences through time for the climate and empirically-observed community predictions for Samwell Cave. The left value indicates the taxa that were present (1) or absent (0) for the climate predictions and the right value indicates the presences and absences for the empirically-observed taxa from the SCPD fossil deposit. Total taxonomic richness is also indicated for each time period.

	A. rufa	*Microtus*	*Neotoma*	*N gibbsii*	*Peromyscus*	*R. megalotis*	*Sorex*	*S. beecheyi*	*Tamias*	*T. douglasii*	*T. bottae*	*S. latimanus*	*A. albipes*	*S. griseus*	*S. lateralis*	*G. sabrinus*	*M californicus*	*Z. trinotatus*	Taxonomic Richness
1 Kyr BP	0 / 0	1 / 1	1 / 1	1 / 0	1 / 1	1 / 0	1 / 1	1 / 1	1 / 1	1 / 1	1 / 1	1 / 1	0 / 0	1 / 0	1 / 0	1 / 0	0 / 0	1 / 0	15 / 9
3 Kyr BP	0 / 0	1 / 1	1 / 1	1 / 0	1 / 1	1 / 1	1 / 1	1 / 1	1 / 0	1 / 1	1 / 1	1 / 1	0 / 1	1 / 1	1 / 1	1 / 0	0 / 0	1 / 0	15 / 12
4.5 Kyr BP	0 / 0	1 / 1	1 / 1	1 / 0	1 / 1	1 / 1	1 / 1	1 / 1	1 / 0	1 / 1	1 / 1	1 / 1	0 / 0	1 / 1	1 / 0	1 / 0	0 / 0	1 / 0	15 / 10
6 Kyr BP	0 / 0	1 / 1	1 / 1	1 / 0	1 / 1	0 / 1	1 / 1	1 / 1	1 / 1	1 / 1	1 / 1	1 / 1	0 / 0	1 / 1	1 / 1	1 / 1	0 / 0	1 / 0	14 / 13
7 Kyr BP	0 / 0	1 / 1	1 / 1	0 / 0	1 / 1	1 / 0	1 / 1	1 / 1	1 / 1	1 / 1	1 / 1	1 / 1	0 / 0	1 / 1	1 / 0	1 / 1	0 / 0	1 / 0	14 / 11
8 Kyr BP	0 / 0	1 / 1	1 / 1	0 / 0	1 / 1	1 / 0	1 / 0	1 / 1	1 / 0	1 / 1	1 / 1	1 / 1	0 / 0	1 / 1	1 / 1	1 / 0	0 / 0	1 / 0	14 / 9
9 Kyr BP	0 / 0	1 / 1	1 / 1	0 / 0	1 / 1	1 / 0	1 / 1	1 / 1	1 / 0	1 / 1	1 / 1	1 / 1	0 / 1	1 / 1	1 / 1	1 / 1	0 / 1	1 / 0	14 / 13
10 Kyr BP	0 / 0	1 / 1	1 / 1	0 / 0	1 / 1	1 / 0	1 / 0	1 / 1	1 / 1	1 / 0	1 / 1	1 / 0	0 / 1	1 / 0	1 / 0	1 / 0	0 / 0	1 / 0	14 / 7
11.5 Kyr BP	0 / 0	1 / 1	1 / 1	0 / 0	1 / 1	1 / 1	1 / 1	1 / 1	1 / 1	1 / 1	1 / 1	1 / 1	0 / 1	1 / 1	1 / 1	1 / 0	0 / 0	1 / 0	14 / 13
12.5 Kyr BP	0 / 0	1 / 1	1 / 1	1 / 0	1 / 1	1 / 0	1 / 0	1 / 1	1 / 1	1 / 1	1 / 1	1 / 1	0 / 1	1 / 0	1 / 1	1 / 0	0 / 0	1 / 0	15 / 10
14 Kyr BP	1 / 1	1 / 1	1 / 1	1 / 0	1 / 1	1 / 0	1 / 1	1 / 1	1 / 1	1 / 1	1 / 0	1 / 1	0 / 1	1 / 1	1 / 1	1 / 1	1 / 0	1 / 0	17 / 13
15 Kyr BP	1 / 0	1 / 1	1 / 1	1 / 0	1 / 1	1 / 1	1 / 1	1 / 1	1 / 1	1 / 1	1 / 1	1 / 1	0 / 1	1 / 0	1 / 1	1 / 0	1 / 0	1 / 0	17 / 12
16.5 Kyr BP	1 / 1	1 / 1	1 / 1	1 / 0	1 / 1	1 / 1	1 / 0	1 / 1	1 / 1	1 / 1	0 / 0	1 / 1	0 / 1	1 / 1	1 / 1	1 / 0	1 / 0	1 / 0	16 / 12
17.5 Kyr BP	1 / 1	1 / 1	1 / 1	1 / 0	1 / 1	1 / 0	1 / 1	1 / 1	1 / 1	1 / 1	0 / 1	0 / 1	1 / 1	1 / 0	1 / 1	1 / 1	1 / 0	1 / 0	16 / 13

Table 3.2: Trait data and resource use for each taxon examined in the study. Keys for traits are as follows: activity time (1 = nocturnal, 2 = diurnal, 3 = crepuscular, 4 = cathermal), foraging habits (1 = not fossorial, 2 = semi-fossorial, 3 = terrestrial), and foraging height (1= arboreal, 2 = scansorial, 3 = terrestrial). For the food resources (seeds, fruits, fungi, plant material, invertebrates, vertebrates, and fish), whether a taxon consumed (1) or did not consume (0) the food resources is indicated. References for trait data other than the PanTHERIA database are found in Appendix table 3.10.2.

Taxa	**Body Mass (g)**	**Activity Time**	**Foraging Habits**	**Foraging Height**	**Seeds**	**Fruits**	**Fungi**	**Plant Material**	**Invertebrates**	**Vertebrates**	**Fish**
Aplodontia rufa	806.21	1	3	2	1	0	0	1	0	0	0
Arborimus albipes	23	1	3	1	0	0	0	1	0	0	0
Glaucomys sabrinus	137.53	1	1	2	1	1	0	1	1	1	0
Microtus spp	41.26	1	2	3	1	0	0	1	0	0	0
Myodes californicus	18.3	1	3	3	1	0	1	1	0	0	0
Neotoma spp	249.57	1	1	3	1	1	0	1	0	0	0
Neurotrichus gibbsii	9.56	3	2	2	1	0	0	1	1	0	0
Peromyscus spp	23.62	1	1	3	1	1	1	1	1	1	0
Reithrodontomys megalotis	10.72	1	2	3	1	0	0	1	1	0	0
Scapanus latimanus	62.46	3	3	3	0	0	0	0	1	0	0
Sciurus griseus	703.85	4	1	1	1	0	1	1	1	0	0
Sorex spp	10.8	3	1	3	1	0	1	1	1	0	0
Spermophilus beecheyi	597.82	2	3	3	1	1	1	1	1	1	0
Spermophilus lateralis	175.1	2	2	3	1	0	1	1	1	1	0
Tamias spp	71.65	2	1	2	1	1	1	1	1	1	0
Tamiasciurus douglasii	225	2	1	1	1	0	1	1	1	1	0
Thomomys bottae	98.92	3	2	3	1	1	0	1	0	0	0
Thomomys mazama	93.07	3	2	3	1	0	0	1	0	0	0
Zapus trinotatus	27.45	3	1	3	1	1	1	1	1	0	1

3.9 Figures

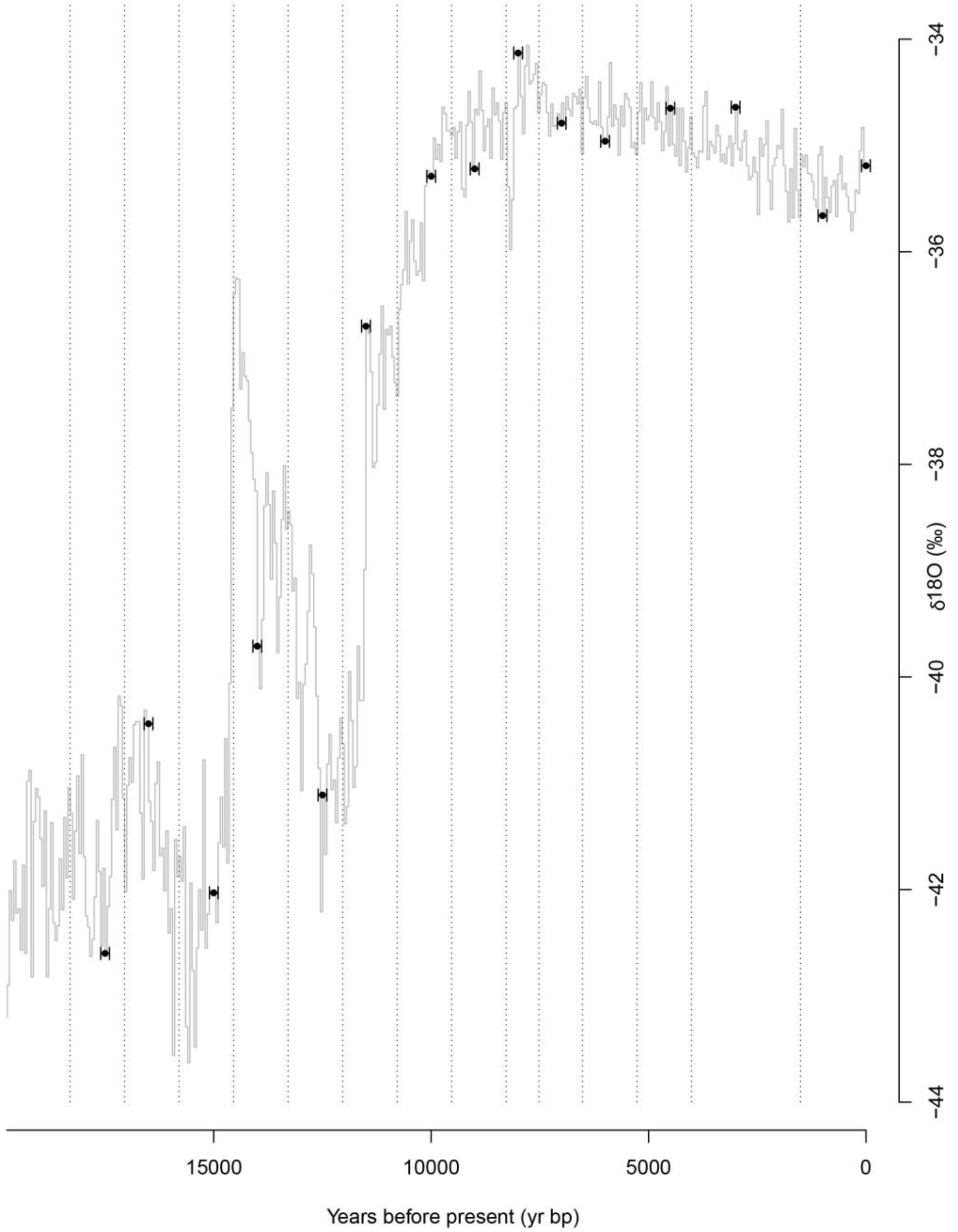

Figure 3.1: The relationship between the strata in the Samwell Cave Popcorn Dome (SCPD) fossil deposit and temperature through time. The temperature proxy (solid grey line) is based on δ^{18}O from the North Greenland Ice Core Project ice-core record (North Greenland Ice Core Project memers 2004). Vertical dashed lines indicate the boundaries between strata within SCPD. Points represent the time to which species distribution models were hindcast in order to generate climate predictions for taxa in each community throughout the SCPD fossil deposit. The 200 year climate average is depicted by the horizontal lines associated with the points.

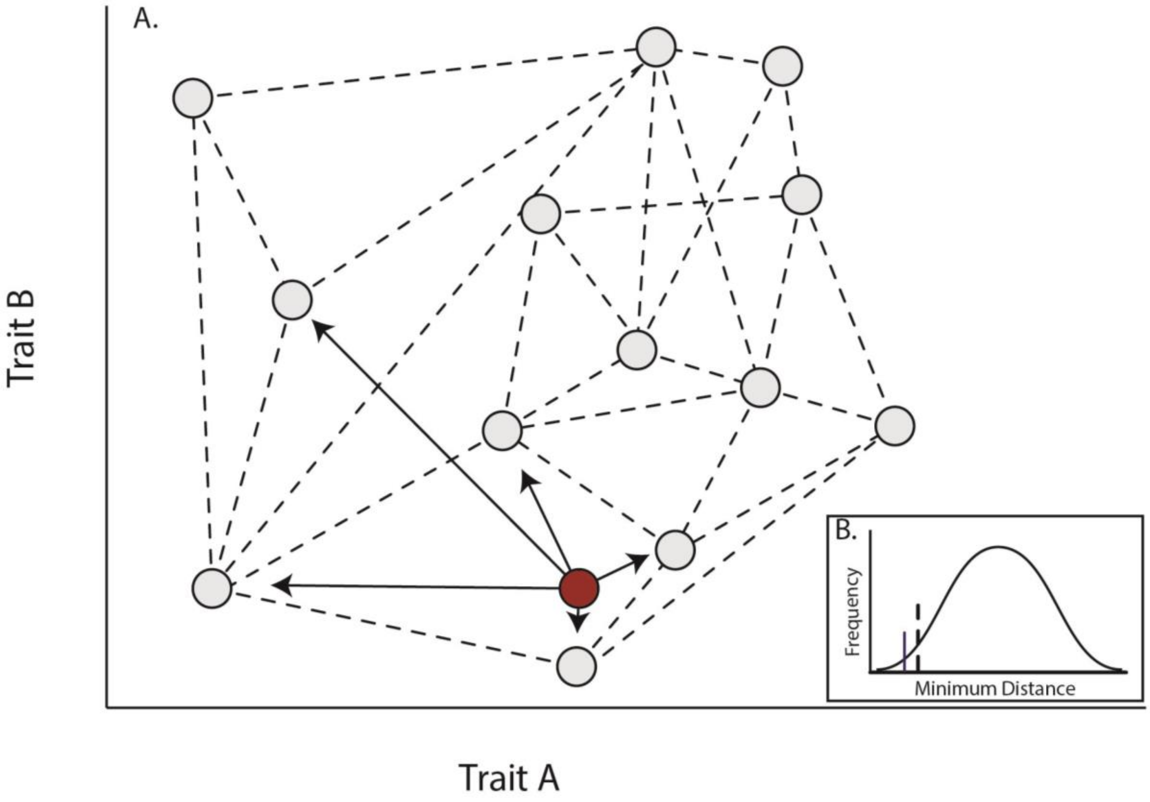

Figure 3.2: Hypothetical community trait analysis examining the ecological similarity of taxa using two traits (trait A and trait B). For each taxon observed within a single community at Samwell Cave (grey circles), the ecological distance based on traits was calculated to all other taxa within the community (dashed lines; for simplicity, not all pairwise associations were drawn in the figure). All pairwise distances among empirically-observed taxa were used to determine the distribution of ecological distances for the community. Then, the ecological distances of a taxon that was predicted to be present in the community based on its climactic tolerances but was not observed in the fossil record for the time period was determined (red circle; ecological distances for this taxon are represented by the black arrows). B) If the minimum observed distance (solid vertical line) of the mismatched taxon is smaller than the lower 0.05 threshold of the empirical community distribution (dashed vertical line), then the taxon may have been competitively excluded from the community during the examined time period.

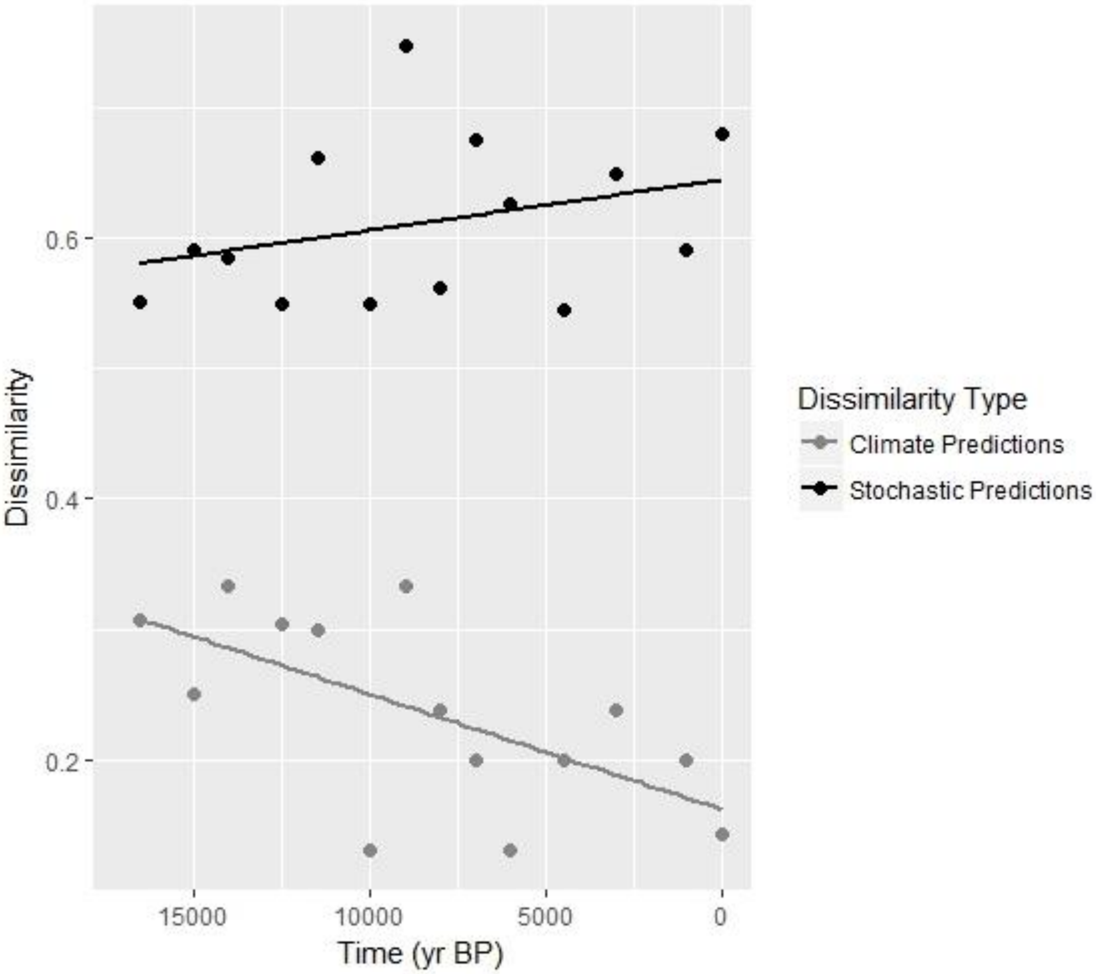

Figure 3.3: The fit of climate predictions and stochastic predictions to the empirically observed community composition. The scatterplot depicts the Sørenson's dissimilarity between empirical communities and the climatically predicted (gray) and stochastically predicted (black) communities from the Last Glacial Maximum to the present day.

3.10 Appendix

Table 3.10.1: List of the species examined in this study, which represents the regional species pool. Also listed are the Boyce index values for the ensemble model constructed for each species using contemporary occurrence data and the CCSM3 paleoclimate simulation.

Species	**Boyce index**
Aplodontia rufa	0.92
Arborimus albipes	0.56
Glaucomys sabrinus	0.96
Microtus californicus	0.98
Microtus longicaudus	0.90
Microtus ochrogaster	0.99
Microtus oregoni	0.96
Myodes californicus	0.90
Neotoma cinerea	1.00
Neotoma fuscipes	0.97
Neurotrichus gibbsii	0.97
Peromyscus boylii	0.98
Peromyscus maniculatus	1.00
Peromyscus truei	0.99
Reithrodontomys megalotis	0.98
Scapanus latimanus	0.97
Sciurus aberti	0.97
Sciurus griseus	0.97
Sorex bendirii	0.98
Sorex pacificus	0.55
Sorex palustris	0.99
Sorex trowbridgii	0.89
Sorex vagrans	0.99
Spermophilus beecheyi	0.99
Spermophilus lateralis	0.95
Tamias amoenus	1.00
Tamias senex	0.80
Tamias siskiyou	0.91
Tamias sonomae	0.58
Tamias speciosus	0.69
Tamias townsendii	0.98
Tamiasciurus douglasii	0.99
Thomomys bottae	0.98

Thomomys mazama	0.82
Zapus trinotatus	0.72

Table 3.10.2: A list of all the species included in the trait analysis, before the trait values were consolidated to account for the fact that some taxa in the fossil record were not identified to the species level. Trait data were taken from the PanTHERIA database (Jones et al. 2009) and values that were not present in PanTHERIA were generated from the references listed in the table.

Species	**Body Mass (g)**	**Activity Time**	**Foraging Habits**	**Foraging Height**	**Seeds**	**Fruits**	**Fungi**	**Plant Material**	**Invertebrates**	**Vertebrates**	**Fish**	**Reference**
Aplodontia rufa	806.2	1	3	2	1	0	0	1	0	0	0	Carraway, L.N. and B.J. Verts. 1993. Aplodontia rufa. Mammalian Species 431: 1-10.
Arborimus albipes	23	1	3	1	0	0	0	1	0	0	0	Verts, B.J. and L.N. Carraway. 1995. Phenacomys albipes. Mammalian Species 494:1-5
Glaucomys sabrinus	137.5	1	1	2	1	1	0	1	1	1	0	Wells-Gosling, N. and Heaney L.R. 1984. Glaucomys sabrinus. Mammalian Species 229:1-8.
Microtus californicus	57.4	4	2	3	1	0	0	1	0	0	0	Cudworth, N.L. and J.L. Koprowski. 2010. Microtus californicus (Rodentia: Cricetidae). Mammlian Species 868:230-243
Microtus longicaudus	44.8	1	3	3	1	1	1	1	0	0	0	Smolen, M.J. and B.L. Keller. 1987. Microtus longicaudus. Mammalian Species 271:1-7
Microtus ochrogaster	42.5	1	3	3	1	0	0	1	1	1	0	Stalling, D.T. 1990. Mammalian Species 355:1-9
Microtus oregoni	20.3	3	2	3	0	0	1	1	0	0	0	Carraway, L.N. and B.J. Verts. 1985. Mammalian Species 233:1-6; IUCN data base
Myodes californicus	18.3	1	3	3	1	0	1	1	0	0	0	Alexander, L.F. and B.J. Verts. 1992. Clethrionomys californicus. Mammalian Species 406:1-6
Neotoma cinereal	285.8	1	1	3	1	1	0	1	0	0	0	Smith, F.A. 1997. Neotoma cinerea. Mammalian Species 564:1-8
Neotoma fuscipes	213.2	1	1	3	0	0	0	1	0	0	0	Carraway, L.N. and B.J. Verts. 1991. Mammalian Species 386:1-10
Neurotrichus gibbsii	9.5	3	2	2	1	0	0	1	1	0	0	Carraway,L.N. and B.J. Verts. 1991. Neurotrichus gibbsii. Mammalian Species 387:1-7

Species	Body Mass (g)	Activity Time	Foraging Habits	Foraging Height	Seeds	Fruits	Fungi	Plant Material	Invertebrates	Vertebrates	Fish	Reference
Peromyscus boylii	23.9	1	2	3	1	1	1	1	1	1	0	Kalcounis-Rueppell, M.C. and T.R. Spoon. 2009. Peromyscus boylii (Rodentia: Cricetidae). Mammalian Species 838:1-14
Peromyscus maniculatus	19.9	1	1	3	1	1	1	1	1	0	0	Sullivan, J. 1995. Peromyscus maniculats. In: Fire effects information system, [Online]. U.S. Department of Agriculture, Forest Service, Rocky Mountains Research Station, Fire Sciences Laboratory. Available: http://www.fs.fed.us/database/feis/
Peromyscus truei	27	1	1	2	1	1	0	1	1	1	0	Hoffmeister, D.F. Peromyscus truei. Mammalian Species 161:1-5; IUCN database
Reithrodontomys megalotis	10.7	1	2	3	1	0	0	1	1	0	0	Webster, W.D. and Jones J.K. Jr. 1982. Reithrodontomys megalotis. Mammalian Species 167:1-5
Scapanus latimanus	62.4	3	3	3	0	0	0	0	1	0	0	Verts, B.J. and L.N. Carraway. 2001. Scapanus latimanus. Mammalian Species 666:1-7; Harris J. 2000. Broad-footed mole. California Wildlife Habitat Relationships System.
Sciurus aberti	622.9	1	1	1	1	0	1	1	0	1	0	Nash, D.J. and R.N. Seaman. 1977. Sciurus aberti. Mammalian Species 80:1-5
Sciurus griseus	703.8	4	1	1	1	0	1	1	1	0	0	Carraway, L.N. and B.J. Verts. 1994. Sciurus griseus. Mammalian Species 474:1-7
Sorex bendirii	15.7	3	1	3	0	0	0	0	1	0	0	Pattie, D. 1973. Sorex bendirii. Mammalian Species 27:1-2
Sorex pacificus	10.5	3	1	3	1	0	1	1	1	1	0	Carraway, L.N. 1985. Sorex pacificus. Mammalian Species 231:1-5
Sorex palustris	13.5	3	1	3	0	0	1	1	1	1	1	Beneski, J.T. Jr. and D.W. Stinson. 1987. Sorex palustris. Mammalian Species 296 1-6
Sorex trowbridgii	5.02	3	1	3	1	0	1	1	1	0	0	George, S.B. 1989. Sorex trowbridgii. Mammalian Species 337:1-5

Species	Body Mass (g)	Activity Time	Foraging Habits	Foraging Height	Seeds	Fruits	Fungi	Plant Material	Invertebrates	Vertebrates	Fish	Reference
Sorex vagrans	5.9	3	1	3	1	1	1	1	1	0	0	Gillihan, S.W. and K.R. Foresman. 2004. Sorex vagrans. Mammalian Species 744:1-5
Spermophilus beecheyi	597.8	2	3	3	1	1	1	1	1	1	0	Polite, C. and G. Ahlborn. 1990. California Ground Squirrel. California Wildlife Habitat Relationships System.
Spermophilus lateralis	175.1	2	2	3	1	0	1	1	1	1	0	Bartels, M.A. and D.P. Thompson. 1993. Spermophilus lateralis. Mammalian Species 440:1-8
Tamias amoenus	50.6	2	2	2	1	1	1	1	1	1	0	Sutton, D.A. 1992. Tamias amoenus. Mammalian Species 390:1-8
Tamias senex	89.3	2	2	2	1	1	1	1	1	0	0	Gannon, W.L. and R.B. Forbes. 1995. Mammalian Species 502:1-6
Tamias siskiyou	75	2	2	2	1	1	1	1	1	0	0	IUCN data base
Tamias sonomae	75	2	2	2	1	1	1	1	0	0	0	IUCN data base; T.L. Best. 1993. Tamias sonomae. Mammalian Species 444:1-5
Tamias speciosus	60.8	2	2	2	1	1	1	1	1	1	0	IUCN data base; T.L. Best. 1994. Tamias speciosus. Mammalian Species 478:1-9
Tamias townsendii	79.1	2	2	2	1	1	1	1	1	1	0	D.A. Sutton. 1993. Tamias townsendii. Mammlian Species 435:1-6
Tamiasciurus douglasii	225	2	1	1	1	0	1	1	1	1	0	Steele, M.A. 1999. Tamiasciurus douglasii. Mammalian Species 630:1-8
Thomomys bottae	122.7	3	2	3	1	1	0	1	0	0	0	Jones, C.A. and C.N. Baxter. 2004. Mammalian Species 742:1-14
Thomomys Mazama	93.0	3	2	3	1	0	0	1	0	0	0	Berts, B.J. and L.N. Carraway. 2000. Mammalian Species 641:1-7
Zapus trinotatus	27.4	3	1	3	1	1	1	1	1	0	1	Gannon, W.L. 1988. Zapus triotatus. Mammalian Species 315:1-5

Table 3.10.3: List of taxa that were predicted to be present in the SCPD fossil deposit based on their climatic tolerances but were not observed in the fossil record. 'Minimum Community Distance' is the value that represents the lower five percent of the minimum ecological distance distribution for the empirical community. 'Taxon Minimum Distance' is the minimum ecological distance for the predicted present but empirically absent taxon in the community for the associated time period. If the taxon minimum distance is less than the minimum community distance, it is possible that the associated taxon was competitively excluded from the SCPD fossil deposit (indicated in the "Competition" column).

Species	**Minimum Community Distance**	**Taxon Minimum Distance**	**Time Period**	**Competition**
Aplodontia rufa	2.45	208.44	15000 yr BP	No
Glaucomys sabrinus	9.92	38.71	1000 yr BP	No
Glaucomys sabrinus	2.45	37.84	3000 yr BP	No
Glaucomys sabrinus	2.45	38.71	4500 yr BP	No
Glaucomys sabrinus	18.47	37.84	8000 yr BP	No
Glaucomys sabrinus	3.66	38.71	10000 yr BP	No
Glaucomys sabrinus	2.45	37.84	11500 yr BP	No
Glaucomys sabrinus	3.66	37.84	12500 yr BP	No
Glaucomys sabrinus	2.45	37.84	15000 yr BP	No
Glaucomys sabrinus	3.66	37.84	16500 yr BP	No
Myodes californicus	3.66	5.30	14000 yr BP	No
Myodes californicus	2.45	5.30	15000 yr BP	No
Myodes californicus	3.66	5.30	16500 yr BP	No
Myodes californicus	3.66	5.30	17500 yr BP	No
Neurotrichus gibbsii	9.92	2.13	1000 yr BP	**Yes**
Neurotrichus gibbsii	2.45	2.13	3000 yr BP	**Yes**
Neurotrichus gibbsii	2.45	2.13	4500 yr BP	**Yes**
Neurotrichus gibbsii	2.45	2.13	6000 yr BP	**Yes**
Neurotrichus gibbsii	3.66	13.73	12500 yr BP	No
Neurotrichus gibbsii	3.66	2.13	14000 yr BP	**Yes**

Species	**Minimum Community Distance**	**Taxon Minimum Distance**	**Time Period**	**Competition**
Neurotrichus gibbsii	2.45	2.13	15000 yr BP	**Yes**
Neurotrichus gibbsii	3.66	2.52	16500 yr BP	**Yes**
Neurotrichus gibbsii	3.66	2.13	17500 yr BP	**Yes**
Reithrodontomys megalotis	9.92	2.45	1000 yr BP	**Yes**
Reithrodontomys megalotis	9.92	2.45	7000 yr BP	**Yes**
Reithrodontomys megalotis	18.47	13.05	8000 yr BP	**Yes**
Reithrodontomys megalotis	3.66	2.45	9000 yr BP	**Yes**
Reithrodontomys megalotis	3.66	12.56	10000 yr BP	No
Reithrodontomys megalotis	3.66	12.56	12500 yr BP	No
Reithrodontomys megalotis	3.66	2.45	14000 yr BP	**Yes**
Reithrodontomys megalotis	3.66	2.45	17500 yr BP	**Yes**
Sciurus griseus	9.92	106.08	1000 yr BP	No
Sciurus griseus	3.66	106.08	10000 yr BP	No
Sciurus griseus	3.66	106.08	12500 yr BP	No
Sciurus griseus	2.45	106.08	15000 yr BP	No
Sciurus griseus	3.66	102.47	17500 yr BP	No
Spermophilus lateralis	9.92	49.95	1000 yr BP	No
Spermophilus lateralis	2.45	49.95	4500 yr BP	No
Spermophilus lateralis	9.92	37.84	7000 yr BP	No
Spermophilus lateralis	3.66	74.61	10000 yr BP	No
Scapanus latimanus	3.66	9.92	10000 yr BP	No
Sorex spp	18.47	13.05	8000 yr BP	**Yes**
Sorex spp	3.66	12.80	10000 yr BP	No
Sorex spp	3.66	12.80	12500 yr BP	No
Sorex spp	3.66	2.45	16500 yr BP	**Yes**
Thomomys bottae	3.66	27.43	14000 yr BP	No

Species	**Minimum Community Distance**	**Taxon Minimum Distance**	**Time Period**	**Competition**
Tamiasciurus douglasii	3.66	25.05	10000 yr BP	No
Tamias spp	2.45	9.92	3000 yr BP	No
Tamias spp	2.45	9.92	4500 yr BP	No
Tamias spp	18.47	9.92	8000 yr BP	**Yes**
Tamias spp	3.66	9.92	9000 yr BP	No
Zapus trinotatus	9.92	4.20	1000 yr BP	**Yes**
Zapus trinotatus	2.45	4.20	3000 yr BP	No
Zapus trinotatus	2.45	4.20	4500 yr BP	No
Zapus trinotatus	2.45	4.20	6000 yr BP	No
Zapus trinotatus	9.92	4.20	7000 yr BP	**Yes**
Zapus trinotatus	18.47	4.20	8000 yr BP	**Yes**
Zapus trinotatus	3.66	4.20	9000 yr BP	No
Zapus trinotatus	3.66	4.20	10000 yr BP	No
Zapus trinotatus	2.45	4.20	11500 yr BP	No
Zapus trinotatus	3.66	4.20	12500 yr BP	No
Zapus trinotatus	3.66	4.20	14000 yr BP	No
Zapus trinotatus	2.45	4.20	15000 yr BP	No
Zapus trinotatus	3.66	4.20	16500 yr BP	No
Zapus trinotatus	3.66	4.20	17500 yr BP	No

4 Estimates of changes in North American mammalian species richness and community response patterns to future climate change

4.1 Abstract

Determining how biodiversity dynamics will change in response to future climate change is essential to the development of effective conservation management strategies. Increased rates of climate change are expected over the next century as well as the development of local or regional abiotic conditions with no current analog. The development of novel climatic conditions is expected to lead to the development of novel community assemblages since species distributions are largely determined at a broad scale by species' physiological tolerences. Here, we estimate how North American mammal species richness and community composition is expected to change between today, AD 2050, and AD 2070 under two representative concentration pathways. We also estimate the potential emergence of novel communities in the future as well. To exmine these patterns we generated contemporary species distributions for 348 North American mammal species using ensembled and stacked species distribution models to determine how species ranges are expected to change in the future and how those changes will ultimately affect species richness and community composition across North America. Our results indicate that species richness is expected to change significantly across North America in the future. Species richness is expected to decrease in the southeastern U.S., the northeastern U.S., and the southwestern deserts of the U.S. Speces richness is expected to increase in the Rocky Mountains, the Sierra Nevada Mountain, the interior of Canada, southwestern Alaska, and the Canadian Shield. Further, our results indicate that the areas of high change in species ricness are also the areas that show high change in community composition between contemporary and future communities. We predict the appearance of novel communities throughout the interior of Canada and the Canadian Shield.

4.2 Introduction

Climate change affects the distributions of species and communities both directly and indirectly (Barnosky et al. 2003, Blois and Hadly 2009; Blois et al. 2010; Chen et al. 2011; Jackson and Overpeck 2000; Spooner et al. 2018; Williams and Blois 2018). With future global climate change expected to occur at rates not seen since the late Pleistocene (IPCC 2013), understanding how biodiversity changes across space and time as a response to both natural and anthropogenic change is important if conservation strategies are to be effective at mitigating biodiversity loss in the future (Myers et al. 2000; Purvis and Hector 2000). The increased rate of climate change over the next century is expected to lead to the emergence of abiotic conditions that have no historical analog (i.e., novel climates; Radeloff et al. 2015; Williams and Jackson 2007), especially in tropical and subtropical areas (Williams et al. 2007). Because climate is one of the main factors that determine species distributions, due to the constraints of species physiological tolerences, the increase in novel climatic conditions has the potential to lead to the development of highly novel communities. No-analog communities consist of assemblages and species associations that have not been observed before (i.e., the communities have high novelty; Radeloff et al. 2015). Previous evidence shows that biological communities become more novel as abiotic conditions increase in novelty (Finsinger et al. 2017, Fitzpatrick et al. 2018, Maguire et al. 2016, Williams et al. 2007), thereby suggesting that communities as well as climate exist on a continuum of novelty (Radeloff et al. 2015). However, while community novelty is correlated to climatic novelty, communities that are located in areas experiencing a high degree of climatic change are not necessarily the communities that will be the most novel in the future (Radeloff et al. 2015; Williams and Jackson 2007).

Theory regarding the formation of novel communities is based on a large body of evidence showing that species generally respond to climate change in an individualistic manner (Graham et al. 1996; Lyons 2003; Webb 1987), with species either adapting to climate change *in situ*, shifting their distributions to track their preferred climatic niche, or becoming extinct or locally extirpated if they are not able to adapt (Mortiz and Agudo 2013). Generally, species exhibit multidirectional range shifts in response to climate change due to idiosyncratic responses (Lyons 2003, Williams and Blois 2018; VanDerWal et al. 2013). Overall, regardless of which particular climate change response is exhibited by a species, the aggregate of individualistic changes in multiple species across both space and time has the potential to result in changes to local community structure and species interactions (Graham et al. 1988, Williams and Jackson 2007; Williams et al. 2007). This reshuffling of species and communities can lead to the development of highly novel communities and species interactions (Williams and Jackson 2007). Further, even if the reshuffling of species does not lead to highly novel communities, the community composition may change enough to indicate large structural shifts such as observed in community structure differences between biomes, effectively leading to an introduction of new evolutionary histories in a specific locality.

Assessing of the development of highly novel communities in reponse to future climate change is important if management agencies are to effectively manage species and communities in the future: highly novel communities may be difficult to plan for or manage because of their novelty. However, generating accurate predictions of species responses to novel climates is difficult because model transferability decreases as the climates into which models are predicted become more novel (Fitzpatrick and Hargrove 2009; Maguire et al. 2016; Owens et al. 2013). Nonetheless, quantifying the expected extent of novel communities provides a starting point for the development of management strategies.

In determining the novelty of a community, the first question must be: what is the ecological significance of different levels of community novelty? Novelty is necessarily calculated relative to some set of baseline data (Radeloff et al. 2015). Further, community novelty exists as a continuum from low to high novelty, and so the interpretation of the ecological significance of different levels of novelty must be calibrated from baseline, historical data (Radeloff et al. 2015). For example, methods have been developed in the fossil pollen community to determine the threshold at which highly novel communities can be considered "no-analog", ie, without any analog in the past (Williams and Jackson 2007, Radeloff et al. 2015), based on the minimum dissimilarity observed between future and past communities. However, research in the vertebrate community has not yet established such thresholds to interpret meaningful novelty in vertebrate communities. A recent revision to the Wallace zoogeographic realms and regions (Holt et al. 2013) provides a way to assess different levels of novelty in mammalian communities: we can assess average novelty of contemporary communities within zoogeographic regions as compared to between regions, and use this information to interpret the novelty we expect for the future to understand whether regions will experience community change analogous to a shift from one zoogeographic region to another.

Here we estimate the response of North American mammalian communities to future climate change (for AD 2050 and 2070) using stacked species distribution models (SDMs) under two representation concentration pathways (RCPs) (RCP 4.5 and RCP 8.5). We specifically determine: 1) What areas are expected to exhibit the largest change in community composition in terms of both richness and dissimilarity? 2) Which areas are expected to develop into highly novel communities in the future? 3) Do the areas of high richness change correlate with high community novelty? As part of these questions we also explore a fourth question: 4) What amount of novelty is meaningful for mammalian communities? By estimating the potential shifts in species richness and community novelty we can begin to devlop management strategies that account for changes in community composition and potential zoogeographic shifts that may result from species individualistic responses to climate change.

4.3 Methods

4.3.1 Occurrence Data

To determine how mammalian communities are expected to respond to future climate change, contemporary occurrence data for North and Central American mammals were downloaded from the online database, Global Biodiversity Information Facility (www.GBIF.org). While our study is focused on species and community responses in North America, we included occurrence data from Central American species as well because we wanted to capture most of the species that could potentially shift into North America in the future. Due to known data quality issues in GBIF data sets (Beck et al. 2014), downloaded occurrences were cleaned, examined, and compared to their known modern ranges from the NaturServe database (Patterson et al. 2007) to check for any potential errors in their spatial accuracy. Occurrences whose basis of record was labeled as either "unknown" or "fossil record" were removed from the data set. The occurrences were spatially thinned to match the climate raster resolution, and to prevent spatial autocorrelation and pseudoreplication during the model building process (Guisan and Zimmerman 2000). Only species with greater than 20 occurrences remaining after the data cleaning step were used during the model construction process, to prevent issues from modeling species with small sample sizes (Wisz et al. 2013). In total, our final data set contained occurrence data from 348 mammalian species (Appendix Table 4.10.1).

4.3.2 Climate Data

Species distribution models were constructed using climate simulations from WorldClim version 1.4 (Hijmans et al. 2005; worldclim.org). The contemporary climate variables are interpolations of global weather data using averages from 1960 – 1990. Future climate simulations are downscaled global climate models (GCMs) taken from the IPCC AR5 future climate projections (Hijmans et al. 2005). Four of the 19 avilable bioclimatic variables were chosen to construct the SDMs and were selected based on the results of a correlation analysis, allowing us to determine and use the least correlated climate variables. The selected bioclimatic variables were annual mean temperature, annual precipitation, precipitation seasonality, and precipitation of the driest quarter. Species distribution models were constructed using climate data from contemporary climatic conditions and were forecasted into two different future periods, AD 2050 (AD 2041-2060 climate averages) and AD 2070 (AD 2061 – 2080 climate averages), under two representative concentration pathways (RCP 4.5 & RCP 8.5). Five global climate models were used to generate future distributions (ACCESS0-1, BCC-CSM1-1, CNRM-CM5, INMCM4, and MIROC5) and were chosen using a model selection guidline developed by Sanderson et al. (2015) to incorporate the five least similar GCMs available in the WorldClim data set.

4.3.3 Constructing species distribution models

Species distribution models were constructed for all species using the R package “BIOMOD2” (v. 3.3-7; Thuiller et al. 2009). Contemporary models were built following methods from Williams and Blois (2018). Five models were constructed for each species, one for each of five algorithms (generalized linear model, MAXENT, artificial neural network, boosted regression tree, and multivariate adaptive regression splines). The selected algorithms represent a range of approaches for modelling species distributions and were among the best performing algorithms in an analysis by Elith et al. (2006). Individual species occurrences were geographically partitioned into four quadrants; SDMs were constructed iteratively using occurrences from three quadrants and were evaluated with occurrences from the unused fourth quadrant (Radosavljevic and Anderson 2014). This process was repeated for all possible iterations, resulting in four different models per species per algorithm. The area under the receiver operating characteristic curve (AUC) was obtained for all algorithms in each of the four iterations and was used to prouduce an average AUC value for each algorithm per species. The

AUC values were then used to generate a weighted ensemble distribution model for each species during the contemporary time period (Araújo & New 2007). Because the Boyce index provides a model evaluation metric that is simiar to AUC but more appropriate for presence only data (Hirzel et al. 2006), ensemble models were evaluated using the Boyce index. The Boyce index was calculated using the R package "ecospat" (v. 2.2.0; Broennimann et al. 2016; Appendix table 4.10.1), with a moving window of 0.1 of the habitat suability range to determine the necessary habitat suitability bins. The Boyce index ranges between -1 and 1, with values near zero representing models that are simiar to random distributions, positive values indicating that model performance is consistent with the data set used to generate the models, and negative values indicating that models are poor estimates of species distributions.

4.3.4 Future projections

Contemporary ensemble models were projected to two future time periods (AD 2050 and 2070) given two different RCP scenarios (RCP 4.5 and RCP 8.5), for each of the 5 GCMs. This resulted in five individual models per combination of time period and RCP. The five distribution models were then averaged together to produce a single ensemble projection for each species in the associated time period and RCP. Projecting responses to different RCPs enables us to determine if communities will be expected to respond differently to future climate change based on different emissions scenarios and using multiple GCMs allows us to combine estimated responses from multiple different climate predictions.

4.3.5 Estimates of species richness and community dissimilarity

Converting SDMs to presence/absence data: All species ensemble models were converted to binary presence/absence distributions by generating species specific thresholds. These thresholds were determined by examining the contemporary species occurrences and their associated habitat suitability scores from the contemporary ensemble models. We then used the 30th percentile habitat suitability score as the threshold value for a species. Any gridcell that had a habitat suitablility score greater than or equal to the species-specific threshold value was converted to a presence (Pearson et al. 2007). Gridcells with habitat suitability scores lower than the threshold were converted to an absence. Once the species distributions were converted to binary distributions, we stacked all individual binary distributions together in a single time period, for all time periods (contemporary, AD 2050 and AD 2070) and RCPs, to provide estimates of community composition for each grid cell.

Species richness estimates: We summed the number of species present in each grid cell for each time and RCP combo to determine species richness across North America through time. To estimate changes in species richness, the difference between estimated future and contemporary species richness was calculated. We also calculated species richness change from 2050 to 2070 under both RCP scenarios.

Estimates of community dissimilarity: We determined changes in community similarity across time periods and RCPs using the Sorensen index of dissimilarity, which is appropriate for binary data and is not as succeptible to differences in sample size if those differences are assumed to be real and not an artifact of sample size (Wolda 1981). Specifically, we examined changes between the contemporary time period – AD 2050 (RCP 4.5 and 8.5), the contemporary time period – AD 2070 (RCP 4.5 and 8.5) and between AD 2050 – AD 2070 for each RCP.

4.3.6 Estimating community novelty

To determine a baseline for interpreting high versus low community dissimilarity, we relied on community dissimilarity among sites across North Amarica during the contemporary time period (Radeloff et al. 2015). The dissimilarity baseline was generated by separating North America into six zooregions, following the updated mammalian zooregions from Holt et al. (2013). We then randomly selected two communities (ie, gridcells) across North America and calculated Sørenson's dissimilarity between the two communities using the R function "*vegdist*" in the *vegan* package (Oksanen et al. 2017), tracking the zooregion of each gridcell in the pair. We repeated this process 100,000 times. This process generated two distributions of dissimilarity values, one that quantified the range of dissimilarity of two communities within the same zoogeographic region (within region dissimilarity) and one that quantified the dissimilarity of two communities from different zoogeographic regions (between region dissimilarity). Because the zoogeographic regions were determined by a combination of species ranges as well as ancestral relationships and the evolutionary history of species, communities drawn from the same zoogeographic region should be more similar than communities from different zoogeographic regions (Holt et al. 2013). Therefore, by determining the dissimilarity distribution of both within and between region communities, we can determine a novelty threshold that is based on historical, baseline data, which can be used to gauge the ecological and evolutionary significance of changes in novelty in the future. After determining an appropriate dissimilarity threshold to represent highly novel communities (0.8, see results below), we converted all dissimilarity maps into maps of potential novel communities by labeling any community with a dissimilarity of 0.8 or higher relative to baseline as novel.

4.4 Results

4.4.1 Accuracy of species distribution models

Species distribution models generated in the contemporary time period represented current mammal distributions with acceptable accuracy. The average Boyce index value for contemporary SDMs was 0.88 (± 0.15) and ranged from -0.27 for Habromys lepturus (Zempoaltepec deer mouse) to 0.999 for Ursus americanus (American black bear; Appendix Table 4.10.1).

4.4.2 Estimated patterns of changes in species richness

Based on forecasted SDMs, mammal species richness in North America is expected to change substantially in the future, for all combinations of time and RCP (Fig. 4.1). On average, North American mammal communities will increase in species richness, but the amount of change will vary depending on the the time period and RCP examined. Average estimated change in species richness for each time period is 8.2 (AD 2050 RCP 4.5), 10.8 (AD 2050 RCP 8.5), 11.7 (AD 2070 RCP 4.5), and 21.0 species (AD 2070 RCP 8.5; Table 4.1). The average increase in species richness is also significantly different between RCP for a given time period, with the RCP 8.5 expected to experience a much higher change in species richness compared to RCP 4.5 (AD 2050: t = -147.43, df = 932620, p = 0; AD 2070: t = -380.5, df = 894200, p = 0). The maximum increase in species richness across North America for each time period and RCP scenario is 42 (AD 2050 RCP 4.5), 48 (AD 2050 RCP 8.5), 50 (AD 2070 RCP 4.5), and 62 (AD 2070 RCP 8.5; Table 4.1). However, even though we estimate that species richness will increase on average, there are communities in all time periods and RCPs that are expected to lose species. The estimated maximum loss of species from a community (with average estimates of species loss in parenthesis) is 21 (3.5), 22 (4.0), 21 (4.2), and 24 (5.3) species for AD 2050 RCP 4.5, AD 2050 RCP 8.5, AD 2070 RCP 4.5 and AD 2070 RCP 8.5, respectively (Table 4.1).

A majority of the contiguous United States is expected to experience decline in species richness regardless of the time period and RCP (Fig. 4.1). However, high elevation areas such as the Rocky Mountains and the Sierra Nevada Mountains, the northern Great Plains, the interior regions of Canada, and the Canadian Shield between 50° and 60° North are expected to increase in species richness. The magnitude of increase in richness and the areal extent that experiences that increase is dependent upon the future time period and RCP (Fig. 4.1). The year AD 2070 under RCP 8.5 exhibits the largest increase in species richness and is expected to conatin the largest area of richness increase compared to any other time period and RCP examined in this study (Fig. 4.1). The cumulative increase in species richness from now until AD 2070 is expected to result in a larger overall area of richness increase than in AD 2050 and RCP 8.5 is predicted to have a larger area of richness increase than RCP 4.5 in both time periods.

4.4.3 Estimated changes in community dissimilarity

Average community dissimilarities between contemporary communities and future communities across North America are predicted to be 0.50 (AD 2050 RCP 4.5), 0.55 (AD 2050 RCP 8.5), 0.56 (AD 2070 RCP 4.5), and 0.66 (AD 2070 RCP 8.5; Table

4.1). Areas of high and low dissimilarity overlap with areas of high and low species richness change, respectively (e.g., compare Figs. 4.1 and 4.2). Because of this overlap, dissimilarity is significantly correlated with species richness change for all times and RCPs (AD 2050 RCP 4.5: $p = 0$, $r = 0.41$; AD 2050 RCP 8.5: $p = 0$, $r = 0.44$; AD 2070 RCP 4.5: $p = 0$, $r = 0.41$; AD 2070 RCP 8.5: $p = 0$, $r = 0.47$; Fig. 4.3). Therefore, we estimate that communities in the Rocky Mountains, Canada, southwestern Alaska, and the Arctic are expected to become more dissimilar compared to the contemporary time period as we move into the future and species respond to changing climates.

4.4.4 Estimating areas of community novelty

Two communities located in different zoogeographic regions within North and Central America are, on average, highly dissimilar (Fig. 4.4); while there is a large range of between-region dissimilarities, the average between-region dissimilarity is 1, the maximum possible. This means that, on average, communities from different zoogeographic regions have completely different species compositions. In contrast, the within-region dissimilarity values are generally much less than 1 (Fig. 4.4). In terms of setting an appropriate novelty threshold, all within-region community dissimilarity analyses contained an average dissimilarity below 0.8 except for region 3, which consists of Canada, Alaska, and the Arctic (Fig. 4.5). Thus, a dissimilarity value of 0.8 by and large reflects the amount of dissimilarity that would correspond to a shift into a new zoogeographic region for contemporary mammals across North and Central America. The major exception to this pattern is zoogeographic region 3, which had an estimated community dissimilarity average of 1.0, the same value as the average between-region dissimilarity. Thus, communities within region 3 are as different from one another as two communities located in different zoogeographic regions (Fig. 4.4).

With a dissimilarity threshold established that indicates potential novel communities, our conversion of community dissimilarity to community novelty show that the Arctic, southern Alaska, interior Canada, and the Canadian Shield are areas in North America that are likely to become novel in the future. These areas, excluding the Rocky Mountains and northern Great Plains, are the same areas that are expected to have a large increase in species richness in the future (Fig. 4.1). Community novelty also increases in area between AD 2050 and AD 2070. The area of estimated novel communities in North America is estimated to be the largest at AD 2070 RCP 8.5 and appears to be drastically larger than the area estimated from the AD 2070 RCP 4.5, as over half of Canada is estimated to contain novel communities during this time period.

4.5 Discussion

Species respond to climate change in an individualistic manner and given this, communities rarely respond as a single unit (Graham et al. 1996; Lyons 2003; Webb 1987). Here, we estimated how independent species responses to future climate change may affect patterns of species richness and community composition across North America. Overall, our results show that mammalian species richness and community composition are expected to undergo significant changes as individual species respond to anthropogenic climate change, and as a result, significant part of northern North America will harbor highly novel mammalian communities in the future.

4.5.1 Changes in mammalian species richness across North America

On average, species richness is expected to increase across North America as species shift their ranges due to climate change (Table 4.1; Fig. 4.1). However, not all regions are expected to experience increases in species richness: only the higher elevational, mountainous areas of the Rocky and Sierra Nevada Mountains, the cooler regions of the interior of Canada, and the southwestern portion of Alaska show an increase in species richness. The estimated species richness increase in these areas suggests that species will mainly be migrating upward in elevation or northward to track their preferred climatic niche. While species have individual and multidirectional responses to climate change (Lyons 2003; VanDerWal et al. 2013, Williams and Blois 2018), the suggested poleward and elevational migration corresponds with previous estimates of species shift patterns in North America, as on average species have shifted or are expected to shift their ranges northward as a response to climate change (Chen et al. 2011; Davis and Shaw 2001; Parmesan and Yohe 2003). Large regions of North America, however, are expected to see decreases in species richness with anthropogenic climate change. Areas where species richness is predicted to decrease or remain constant are the southeastern United States, the Great Basin region, portions of Mexico, and the deserts of southwestern United States (Fig. 4.1). Our results also estimate that in RCP 8.5, which is the scenario with the largest estimate of global temperature change (Meinshausen et al. 2011), species richness increases will be significantly higher on average than in RCP 4.5 and consequently species richness increases will be larger in the mountainous and northern portions of North America.

Currie (2001) and Lawler (2009) report similar patterns in mammal species turnover and species richness. However, Currie (2001) estimated that their cumulative species richness changes would likely take upwards of a millennium and that short-term richness changes would likely be negative (i.e., loss in species richness). Results from Currie (2001) are based on modeling contemporary species richness against contemporary climate using multiple regression analyses. This approach varies from the approaches of Lawler (2009) and the current manuscript, which both used species distribution models to estimate future species richness. A notable difference between our results and Currie (2001) is that our changes in species richness are expected to occur over a time period of decades instead of millennia (though species richness may continue to accumulate beyond the time periods in this study as well), if species are tracking climate change synchronously. This is an important distinction, because for species richness to increase as a response to climate change (vs. other mechanisms such as non-native species introductions), species will need to be able to spatially track shifts in their preferred climatic niche (La Sorte and Jetz 2012; Pinsky et al. 2013; Tingley et al. 2009). Therefore, species ranges must be able to shift the necessary distances to track their preferred abiotic conditions, which implies that species range shift rates must be faster for our estimates when compared to the necessary rates needed for species under the estimates of Currie (2001). Our estimates assume, however, that there are no lags in species responses to climate change and that species have unlimited dispersal capibilities. Both of these factors are known to be issues: species have shown lags in their responses to climate change and species can also be hindered by geographic barriers (La Sorte and Jetz 2012; Schloss et al. 2012). Therefore, our estimates of changes in speices richness are likely on the high end of what will be seen in the near future and these limitations should be accounted for in any management strategies related to our results.

4.5.2 Patterns of community change

The cumulative responses of individual species to climate change alter and affect community composition across the landscape as species migrate into and out of particular locations. Our results estimate that mammalian communities across North America are going to experience significant species turnover (average dissimilarity of 0.50 – 0.66; Table 4.1; Fig. 4.2). The highest expected dissimilarity occurs between contemporary communities and communities at AD 2070 RCP 8.5. Like the pattern seen at AD 2070, the expected dissimilarity in AD 2050 is highest with RCP 8.5 when compared to RCP 4.5 (Table 4.1; Fig. 4.2). While future dissimilarity and changes in species richness are moderately correlated (Fig. 4.3), not all areas of increased richness are expected to have high dissimilarity between contemporary and future communities. In all time periods and both RCPs, the areas estimated to experience high dissimilarities (approximately 0.60 and higher) are the Great Plains region, Canada, and the Arctic Circle (Fig. 4.3). The only scenario that estimates large dissimilarity increases in the Rocky Mountains (an area of estimated increased species richness) is AD 2070 RCP 8.5. This scenario (AD 2070 RCP 8.5) also estimates that most of Canada, the Arctic, and Greenland will experience increased turnover in community composition (Fig 4.2). The increases in community turnover will most likely lead to new species interactions, community reorganizations, changes in ecosystem structure, changes in community evolutionary histories, modification of ecological networks, and shifts into novel communities (Bellard et al. 2012; Walther 2010, Walther et al. 2002). The change of species composition in communities not only affects interactions among mammals, but it also influences herbivore-vegetation interactions. Recent work has shown that changes in mammalian community composition can lead to herbivory release or suppression via herbivory on vegetation communities, resulting in substantial changes in vegetation composition and the formation of novel plant communities (Gill et al. 2009). These types of community composition changes can lead to drastic and important changes in ecosystem structure and function (e.g., Williams et al. 2004).

4.5.3 Development of novel communities

The cumulative response of individual species to climate change can lead to changes in community composition that are unlike any observed previously (Williams and Jackson 2007). The development of novel communities puts scientists and conservation managers in a unique position to determine the best management practices for these types of systems. Novel communities can serve as unique ecosytems to better understand and study how new species interactions, ecosystem functions, and ecosystem services arise from community compositions not observed before. However, novel communities also challenge conservation practitioners because current management strategies are often based on preserving the current structure of a community or an ecosystem, and current management strategies (i.e., National Parks) are not completely successful in accommodating climate change (Burns et al. 2003).

To determine if novel communities may develop in response to future climate change, some baseline of community data for comparison to future communities is needed (Radeloff et al. 2015). However, community novelty exists as a continuum and a dissimilarity framework has to be established to determine when a community becomes so compositionally different when compared to the baseline data that it represents some significantly new and unique combination of species (e.g., "no-analog; Radeloff et al. 2015). While a framework for detecting novelty exists for fossil pollen communities through time (e.g., Jackson and Williams 2004), there is no such framework established for detecting novelty in terrestrial vertebrate communities. Previous approaches examining community novelty estimated the minimum community dissimilarity across the landscape by comparing one community (i.e., a single grid cell) to all other communities in the baseline data set. A community is determined to be novel if the minimum dissimilarity is greater than a dissimilarity threshold established by the researcher. Our approach differs from the previously described framework in that we calculate dissimilarity only within the same location through time and our dissimilarity metric is based on presence-absence data rather than relative abundance data like that used in pollen-based work (Fitzpatrick et al. 2018; Mahony et al. 2017; Mahony et al. 2018; Williams et al. 2007). Our results examining community dissimilarity both within and between zoogeographic regions for the contemporary time period (Holt et al. 2013) thus serve as initial first estimates of dissimilarity thresholds needed to quantify when communites become different enough to be classified as novel mammal communities (Fig. 4.4). Given that our analyses are aimed at understanding dissimilarity across zoogeographic regions that delineate important transitions between communities composed of species with similar ranges as well as evolutionary histories, similar levels of community dissimilarity expected for the future are both ecologically and evolutionarily meaningful. However, because we are not quantifying the minimum dissimilarity of our communities to that of all communities in our baseline data, we may not be directly estimating novel communities in the future. In other words, because we are examining within-region dissimilarities only, we are only predicting how different future communities will be with respect to their baseline regional community. Thus, in some cases we may be detecting shifts of zoogeographic regions across the landscape in the future rather than reshuffling of species in an individualistic fashion. Future work will identify the differences between the two methods of determining mammalian climate novelty.

Our results also indicate that one of the six updated zoogeographic regions established by Holt et al. (2013) (our region 3, Fig. 4.4 and Fig. 4.5, which contains the northwestern part of the US, Canada, Alaska, and the Arctic) may need to be re-examined as a unique zoogeographic region. Average within dissimilarities for region 3 show that communities from this region are completely different compositionally (i.e., average dissimilarity value of 1.0), while all other regions have an average within-region dissimilarity that ranges between 0.6 and 0.7 (Fig. 4.4). The high within-region dissimilarity in region 3 echoes other concerns of the use of zoogeographic regions to delineate the world into similar faunistic and floristic communities (Kreft and Jetz 2013) and at the very least, region 3 should be reconsidered as a single unique zoogeographic region. Overall, given the uncertainty in some of the zoogeographic regions, other methods of determinining levels of substantial novelty in mammalian communities should be explored.We suggest using a method that examines communities at a finer scale than zoogeographic regions, with more similar climatic and environmental conditions, such as ecoregions, which typically contain communities with similar compositions throughout the region. These ecoregions serve to represent divisions between distinct biological communities with community composition expected to be more similar within an ecoregion than between ecoregions (Smith et al. 2018). Conducting the same community novelty analysis as the one used in the study, but with ecoregions (i.e. from Dinerstein et al. 2017) instead of zoogeographic regions may provide added insight if one scheme performs better than another.

Results from our community novelty analysis indicate that regardless of the time period and RCP, large portions of interior Canada, the Arctic, and southwest Alaska are expected to transition into novel communities as species migrate poleward in response to future climate change (Fig. 4.5). However, the RCP does influence how large of a geographic region the novel communities are expected to cover as the area of novelty increase as the projected amount of climate warming increase from RCP 4.5 to RCP 8.5. While these areas are located in zoogeographic region 3, which inherently has an average within-region dissimilarity value that is above our novelty threshold, our results still represent the likely development of novel communities. This is because the threshold within-region dissimilarity value is generated from spatial dissimilarities for each zoogeographic region and are generally highly consistent among all other regions. Thus, this threshold represents a meaningful transition from one evolutionarily cohesive set of species to another, while the high within-region dissimilarity for region 3 is likely a reflection of an artificial grouping of ecologically and evolutionarily distinct species. The spatial dissimilarity serves a baseline of expected community dissimilarities for North America as a whole. Further, the community dissimilarity values used to delimit regions with highly novel future communities are temporal dissimilarities, which compare the change in species composition of single community (i.e., gridcell) through time. This makes the temporal dissimilarity an independent measurement of community turnover with respect to the measurement of the spatial dissimilarity of a region.

It is important to note that the development of these novel communities (as well as our estimates of richness) relies on the assumption that we are correctly capturing species environmental niches and that their environmental niches are stable through time (Thuiller 2004; Zhang et al. 2015). Further, our models may be estimating species and community changes into novel climates, which increase model error and thus directly affects our results (Fitzpatrick and Hargrove 2009; Maguire et al. 2016; Owens et al. 2013). Finally, our analyses are based on individualistic SDMs, whereas other work has suggested that community-level models (CLMs) or mechanistic models are not as succeptible to the issue of model transferability into novel climates and may be more appropriate to determine species responses to future climate change (Nieto-Lugilde et al. 2018; Williams et al. 2013). Community-level models are an "assemble-and-predict-together" modeling strategy that simultaneously models co-occurring species and environmental variables by determining the shared requirements of species and any other processes driving co-occurrence patterns, including biotic interactions, without discarding information on species level responses to the environment (Nieto-Lugilde et al., 2018). However, they are computationally expensive and not suitable for modeling such a large region as North America. Future work will involve trying to circumvent the computational issues of CLMs and then developing CLMs using the same species data set to determine how robust our results are to varying methods. We also plan to include a second climate model for estimating contemporary niches, to examine how robust our projections are to differences in climate models. Finally, we will examine actual differences in species lists of communities through time, to determine how different or similar functional diversity and evolutionary histories will be in areas that are expected to undergo drastic community compostion changes.

4.6 Conclusions

We estimated the response of mammalian species and communities to future climate change and determined changes in the patterns of species richness, community composition, and areas of potential novel communities. While estimates of future mammalian species richness have been established previously (Curry 2001; Lawler 2009), this is the first paper that delineates the potential location and magnitude of future highly novel communities for mammals across North America. It is important to note that our methods estimate community novelty as a function of only climate and our study does not estimate areas of novel communities due to land use changes, extinction events, and invasive species, all of which can alter community composition. Even though we only include estimates that are based on climate, our results can serve as initial measures for guiding management planning strategies. For example, our results show that species richness will likely increase in the Rocky Mountains, Sierra Nevada mountains, and large portions of Canada, making them ideal areas of management focus if the management goal is to conserve regions that will be hotspots of future richness. However, this region is also where the highest novelty communities will potentially be located, which may make management decisions more complex since there may not be any current analogs for species composition in these regions. To facilitate species movements and formation of novel communities with climate change, managers can focus efforts on restoring and maintaining habitat continuity. For example, constructing habitat corridors or protecting important parcels of land that serve as links between where species are located now and where they are predicted to be in the future would facilitate climate-driven range shifts.

Similarly, if managers want to mitigate or forestall species losses, then it is imperative to maintain habitat connectivity between regions estimated to undergo species loss into regions with species increases. It is highly unlikely that we will be able to manage communties in a way that prevents alterations of present day communities in response to climate change, but ensuring that species are able to respond as naturally as possible to climate change is an important first response for conservation managers.

4.7 References

Araújo, M.B. & New, M. (2007) Ensemble forecasting of species distributions. *Trends in Ecology and Evolution*, **22**, 42–47.

Barnosky, A.D., Hadly, E.A., & Bell, C.J. (2003) Mammalian Response to Global Warming on Varied Temporal Scales. *Journal of Mammalogy*, **84**, 354–368.

Beck, J., Böller, M., Erhardt, A., & Schwanghart, W. (2014) Spatial bias in the GBIF database and its effect on modeling species' geographic distributions. *Ecological Informatics*, **19**, 10–15.

Bellard, C., Bertelsmeier, C., Leadley, P., Thuiller, W., & Courchamp, F. (2012) Impacts of climate change on the future of biodiversity. *Ecology Letters*, **15**, 365–377.

Blois, J.L. & Hadly, E.A. (2009) Mammalian Response to Cenozoic Climatic Change. *Annual Review of Earth and Planetary Sciences*, **37**, 181–208.

Blois, J.L., McGuire, J.L., & Hadly, E.A. (2010) Small mammal diversity loss in response to late-Pleistocene climatic change. *Nature*, **465**, 771–4.

Broennimann, O., Valeria, D.C., Petitpierre, B., Breiner, F., D'Amen, M., Randin, C., Engler, R., Hordijk, W., Pottier, J., Di Febbraro, M., Pellissier, L., Pio, D., Dubuis, A., Scherrer, D., Maiorano, L., Psomas, A., Ndiribe, C., Salamin, N., Zimmermann, N., & Guisan, A. (2016) Package ' ecospat . v2.2.0.

Burns, C.E., Johnston, K.M., & Schmitz, O.J. (2003) Global climate change and mammalian species diversity in U.S. national parks. *Proceedings of the National Academy of Sciences of the United States of America*, **100**, 11474–11477.

Chen, I., Hill, J.K., Ohlemüller, R., Roy, D.B., & Thomas, C.D. (2011) Rapid Range Shifts of Species Associated with High Levels of Climate Warming. *Science*, **333**, 1024–1026.

Currie, D.J. (2001) Projected effects of climate change on patterns of vertebrate and tree species richness in the counterminous United States. *Ecosystems*, **4**, 216–225.

Davis, M.B. & Shaw, R.G. (2001) Range shifts and adaptive responses to Quaternary climate change. *Science,* **292**, 673–9.

Dinerstein, E., Olson, D., Joshi, A., et al. (2017) An Ecoregion-Based Approach to Protecting Half the Terrestrial Realm. *Bioscience*, **67**, 534–545.

Elith, J., H. Graham, C., P. Anderson, R., et al. (2006) Novel methods improve prediction of species' distributions from occurrence data. *Ecography*, **29**, 129–151.

Finsinger, W., Giesecke, T., Brewer, S., & Leydet, M. (2017) Emergence patterns of novelty in European vegetation assemblages over the past 15 000 years. *Ecology Letters*, **20**, 336–346.

Fitzpatrick, M.C., Blois, J.L., Williams, J.W., Nieto-Lugilde, D., Maguire, K.C., & Lorenz, D.J. (2018) How will climate novelty influence ecological forecasts? Using the Quaternary to assess future reliability. *Global Change Biology*, **24**, 3575–3586.

Fitzpatrick, M.C. & Hargrove, W.W. (2009) The projection of species distribution models and the problem of non-analog climate. *Biodiversity and Conservation*, **18**, 2255–2261.

Gill, J.L., Williams, J.W., Jackson, S.T., Lininger, K.B., & Robinson, G.S. (2009) Pleistocene Megafaunal Collapse, Novel Plant Communities, and Enhanced Fire Regimes in North America. *Science*, **326**, 1100–1103.

Graham, R.W. (1988) The Role of Climatic Change in the Design of Biological Reserves: The Paleoecological Perspective for Conservation Biology. *Conservation Biology*, **2**, 391–394.

Graham, R., Lundelius, E., Graham, M., Schroeder, E., Toomey, R., Anderson, E., Barnosky, A., Burns, J., Churcher, C., Grayson, D., Guthrie, R., Harington, C., Jefferson, G., Martin, L., McDonald, H., Morlan, R., Semken, H., Webb, S., Werdelin, L., & Wilson, M. (1996) Spatial Response of Mammals to Late Quaternary Environmental Fluctuations. *Science*, **272**, 1601–6.

Guisan, a, Guisan, a, Zimmermann, N.E., & Zimmermann, N.E. (2000) Predictive habitat distribution models in ecology. *Ecological Modelling*, **135**, 147–186.

Hijmans, R.J., Cameron, S.E., Parra, J.L., Jones, P.G., & Jarvis, a (2005) Very High Resolution Interpolated Climate Surface for Global Land Areas. *International Journal of Climatology*, **25,** 1965 – 1978.

Hirzel, A.H., Le Lay, G., Helfer, V., Randin, C., & Guisan, A. (2006) Evaluating the ability of habitat suitability models to predict species presences. *Ecological Modelling*, **199**, 142–152.

Holt, B.G., Lessard, J.-P., Borregaard, M.K., Fritz, S.A., Araújo, M.B., Dimitrov, D., Fabre, P.-H., Graham, C.H., Graves, G.R., Jønsson, K.A., Nogués-Bravo, D., Wang, Z., Whittaker, R.J., Fjeldsa, J., & Rahbek, C. (2013) An update of Wallace's zoogeographic regions of the world. *Science*, **339**, 74–78.

IPCC, (2014) Climate change 2014: synthesis report. Contribution of Working Groups I, II, and III to the Fifth Assessment Report of the Intergovernmental Panel on Climate Change [Core Writing Team, Pachauri, R.K. & Meyer, L.A. (eds.)]. IPCC, Geneva, Switzerland, 151 pp.

Jackson, S.T. & Overpeck, J.T. (2000) Responses of plant populations and communities to environmental changes of the late Quaternary. *Paleobiology*, **26**, 194–220.

Jackson S.T. & Williams J.W. (2004) Modern analogs in Quaternary paleoecology: here today, gone yesterday, gone tomorrow? *Annual Review of Earth and Planetary Sciences*, **32**, 495–537.

Kreft, H. & Jetz, W. (2013) Comment on "An update of Wallace's zoogeographic regions of the world." *Science*, **341**, 343.

La Sorte, F.A. & Jetz, W. (2012) Tracking of climatic niche boundaries under recent climate change. *Journal of Animal Ecology*, **81**, 914–925.

Lawler, J.J., Shafer, S.L., White, D., Kareiva, P., Maurer, E.P., Blaustein, A.R., & Bartlein, P.J. (2009) Projected climate-induced faunal change in the Western Hemisphere. *Ecology*, **90**, 588–597.

Lyons, S.K. (2003) A quantitative assessment of the range shifts of Pleistocene mammals. *Journal of Mammalogy*, **84**, 385-402.

Mahony, C.R., Cannon, A.J., Wang, T., & Aitken, S.N. (2017) A closer look at novel climates: new methods and insights at continental to landscape scales. *Global Change Biology*, **23**, 3934–3955.

Mahony, C.R., MacKenzie Will H., & Aitken, S.N. (2018) Novel climates: Trajectorie of climate chane beyond the boundaries of British Columbia's forest management knowledge system. *Forest Ecology and Management*, **410**, 34–47.

Maguire, K.C., Nieto-Lugilde, D., Blois, J.L., Fitzpatrick, M.C., Williams, J.W., Ferrier, S., & Lorenz, D.J. (2016) Controlled comparison of species- and community-level models across novel climates and communities. *Proceedings of the Royal Society B: Biological Sciences*, **283**, 20152817.

Meinshausen, M., Smith, S.J., Calvin, K., Daniel, J.S., Kainuma, M.L.T., Lamarque, J.-F., Matsumoto, K., Montzka, S.A., Raper, S.C.B., Riahi, K., Thomson, A., Velders, G.J.M., & van Vuuren, D.P.P. (2011) The RCP greenhouse gas concentrations and their extensions from 1765 to 2300. *Climatic Change*, **109**, 213–241.

Moritz, C. & Agudo, R. (2013) The future of species under climate change: resilience or decline? *Science*, **341**, 504–8.

Myers, N., Mittermeler, R.A., Mittermeler, C.G., da Fonseca, G.A.B., & Kent, J. (2000) Biodiversity hotspots for conservation priorities. *Nature*, **403**, 853–8.

Nieto-Lugilde, D., Maguire, K.C., Blois, J.L., Williams, J.W., & Fitzpatrick, M.C. (2018) Multiresponse algorithms for community-level modelling: Review of theory, applications, and comparison to species distribution models. *Methods in Ecology and Evolution*, **9**, 834–848.

Oksanen, J., Blanchet, F.G., Friendly, M., Kindt, R., Legendre, P., McGlinn, D., Minchin, P.R., O'Hara, R.B., Simpson, G.L., Solymos, P., Stevens, M.H.H., Szoecs, E., & Wagner, H. (2017) Package "vegan".

Owens, H.L., Campbell, L.P., Dornak, L.L., Saupe, E.E., Barve, N., Soberón, J., Ingenloff, K., Lira-Noriega, A., Hensz, C.M., Myers, C.E., & Peterson, A.T. (2013) Constraints on interpretation of ecological niche models by limited environmental ranges on calibration areas. *Ecological Modelling*, **263**, 10–18.

Parmesan, C., Yohe, G., & Andrus, J.E. (2003) A globally coherent fingerprint of climate change impacts across natural systems. *Nature*, **421**, 37–42.

Patterson, B.D., Ceballos, G., Sechrest, W., Tognelli, M.F., Brooks, T., Luna, L., Ortega, P., Salazar, I., & Young, B.E. (2007) Digital distribution maps of the mammals of the western hemisphere, version 3.0. Arlington, Virginia, USA: NatureServe.

Pearson, R.G., Raxworthy, C.J., Nakamura, M., & Townsend Peterson, A. (2007) Predicting species distributions from small numbers of occurrence records: a test case using cryptic geckos in Madagascar. *Journal of Biogeography*, **34**, 102–117.

Pinsky, M.L., Worm, B., Fogarty, M.J., Sarmiento, J.L., & Levin, S.A. (2013) Marine taxa track local climate velocities. *Science*, **341**, 1239–42.

Purvis, A. & Hector, A. (2000) Getting the measure of biodiversity. *Nature*, **405**, 212–219.

Radeloff, V.C., Williams, J.W., Bateman, B.L., Burke, K.D., Carter, S.K., Childress, E.S., Cromwell, K.J., Gratton, C., Hasley, A.O., Kraemer, B.M., Latzka, A.W., Marin-Spiotta, E., Meine, C.D., Munoz, S.E., Neeson, T.M., Pidgeon, A.M., Rissman, A.R., Rivera, R.J., Szymanski, L.M., & Usinowicz, J. (2015) The rise of novelty in ecosystems. *Ecological Applications*, **25**, 2051–2068.

Radosavljevic, A. & Anderson, R.P. (2014) Making better Maxent models of species distributions: complexity, overfitting and evaluation. *Journal of Biogeography*, **41**, 629–643.

Sanderson, B.M., Knutti, R., Caldwell, P., Sanderson, B.M., Knutti, R., & Caldwell, P. (2015) A Representative Democracy to Reduce Interdependency in a Multimodel Ensemble. *Journal of Climate,* **28**, 5171–5194.

Schloss, C.A., Nuñez, T.A., & Lawler, J.J. (2012) Dispersal will limit ability of mammals to track climate change in the Western Hemisphere. *Proceedings of the National Academy of Sciences of the United States of America*, **109**, 8606–11.

Smith, J.R., Letten, A.D., Ke, P., Anderson, C.B., Hendershot, J.N., Dhami, M.K., Dlott, G.A., Grainger, T.N., Howard, M.E., Morrison, B.M.L., Routh, D., San Juan, P.A., Mooney, H.A., Mordecai, E.A., Crowther, T.W., & Daily, G.C. (2018) A global test of ecoregions. *Nature Ecology & Evolution*, **2**, 1889 **-** 96.

Spooner, F.E.B., Pearson, R.G., & Freeman, R. (2018) Rapid warming is associated with population decline among terrestrial birds and mammals globally. *Global Change Biology*, **24**, 4521–4531.

Thuiller, W. (2004) Patterns and uncertainties of species’ range shifts under climate change. *Global Change Biology,* **10**, 2020–2027.

Thuiller, W., Lafourcade, B., Engler, R., & Araujo, M.B. (2009) BIOMOD - A platform for ensemble forecasting of species distributions. *Ecography*, **32**, 369–373.

Tingley, M.W., Monahan, W.B., Beissinger, S.R., & Moritz, C. (2009) Birds track their Grinnellian niche through a century of climate change. *Proceedings of the National Academy of Sciences of the United States of America*, **106 Suppl**, 19637–43.

VanDerWal, J., Murphy, H.T., Kutt, A.S., Perkins, G.C., Bateman, B.L., Perry, J.J., & Reside, A.E. (2013) Focus on poleward shifts in species’ distribution underestimates the fingerprint of climate change. *Nature Climate Change,* **3**, 239–243.

Walther, G.-R. (2010) Community and ecosystem responses to recent climate change. *Philosophical transactions of the Royal Society of London. Series B, Biological sciences*, **365**, 2019–24.

Walther, G., Post, E., Convey, P., Menzel, A., Parmesan, C., Beebee, T.J.C., Fromentin, J., Hoegh-Guldberg, O., & Bairlein, F. (2002) Ecological responses to recent climate change. *Nature*, **416**, 389–95.

Webb, T. (1987) The Appearance and Disappearance of Major Vegetational Assemblages: Long-Term Vegetational Dynamics in Eastern North America. *Vegetatio*, **69**, 177–187.

Williams, J.E. & Blois, J.L. (2018) Range shifts in response to past and future climate change: Can climate velocities and species' dispersal capabilities explain variation in mammalian range shifts? *Journal of Biogeography,* **45**, 2175–2189.

Williams, J.W. & Jackson, S.T. (2007) Novel climates, no-analog communities, and ecological surprises. *Frontiers in Ecology and the Environment*, **5**, 475–482.

Williams, J.W., Jackson, S.T., & Kutzbach, J. (2007) Projected distributions of novel and disappearing climates by 2100 AD. *Proceedings of the National Academy of Sciences*, **104**, 5738–5742.

Williams, J.W., Kharouba, H.M., Veloz, S., Vellend, M., McLachlan, J., Liu, Z., Otto-Bliesner, B., & He, F. (2013) The ice age ecologist: testing methods for reserve prioritization during the last global warming. *Global Ecology and Biogeography,* **22**, 289–301.

Williams J.W., Shuman B.N., Webb T. III, Bartlein P., & Leduc P.L. (2004) Late-Quaternary vegetation dynamics in North America: Scaling from taxa to biomes. *Ecological Monographs*, **74**, 309–334.

Wisz, M.S., Pottier, J., Kissling, W.D., et al. (2013) The role of biotic interactions in shaping distributions and realised assemblages of species: Implications for species distribution modelling. *Biological Reviews*, **88**, 15–30.

Wolda, H. (1981) Similarity indices, sample size and diversity. *Oecologia*, **50**, 296–302.

Zhang, L., Liu, S., Sun, P., Wang, T., Wang, G., Zhang, X., & Wang, L. (2015) Consensus forecasting of species distributions: the effects of niche model performance and niche properties. *PloS one*, **10**, e0120056.

4.8 Tables

Table 4.1: Summary statistics of estimated change in species richness through time. Shown are the average species richness, the maximum increase in species richness, the average loss of species richness, the average change of species richness and the average dissimilarity from the contemporary time period to four different future time periods and representative concentration pathways.

	AD 2050 RCP 4.5	**AD 2050 RCP 8.5**	**AD 2070 RCP 4.5**	**AD 2070 RCP 8.5**
Maximum Increase in Species Richness	42.00	48.00	50.00	62.00
Maximum Loss of Species Richness	21.00	22.00	21.00	24.00
Average Loss of Species Richness	3.50	4.00	4.20	5.30
Average Change in Species Richness	8.20	10.80	11.70	21.00
Average Dissimilarity	0.50	0.55	0.56	0.66

4.9 Figures

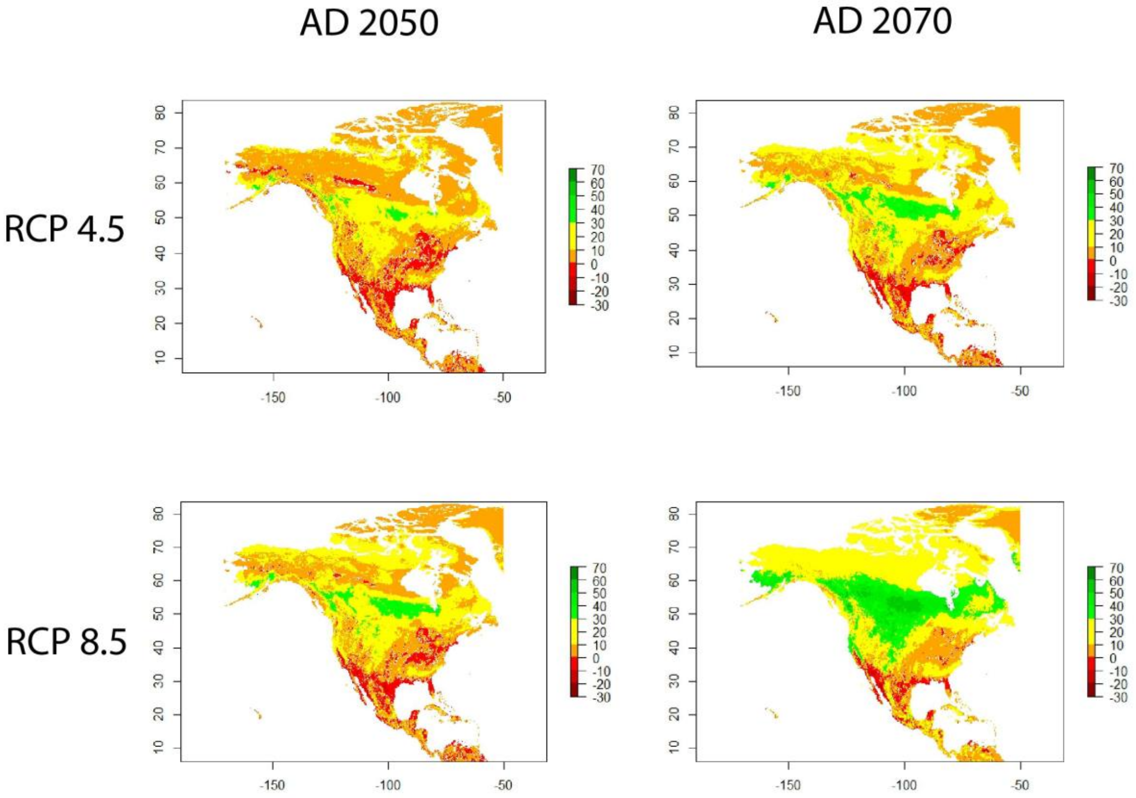

Figure 4.1: Projected change in species richness. Shown are the estimated differences in species richness from the contemporary time period and each associated future time period (columns) and representative concentration pathway (rows).

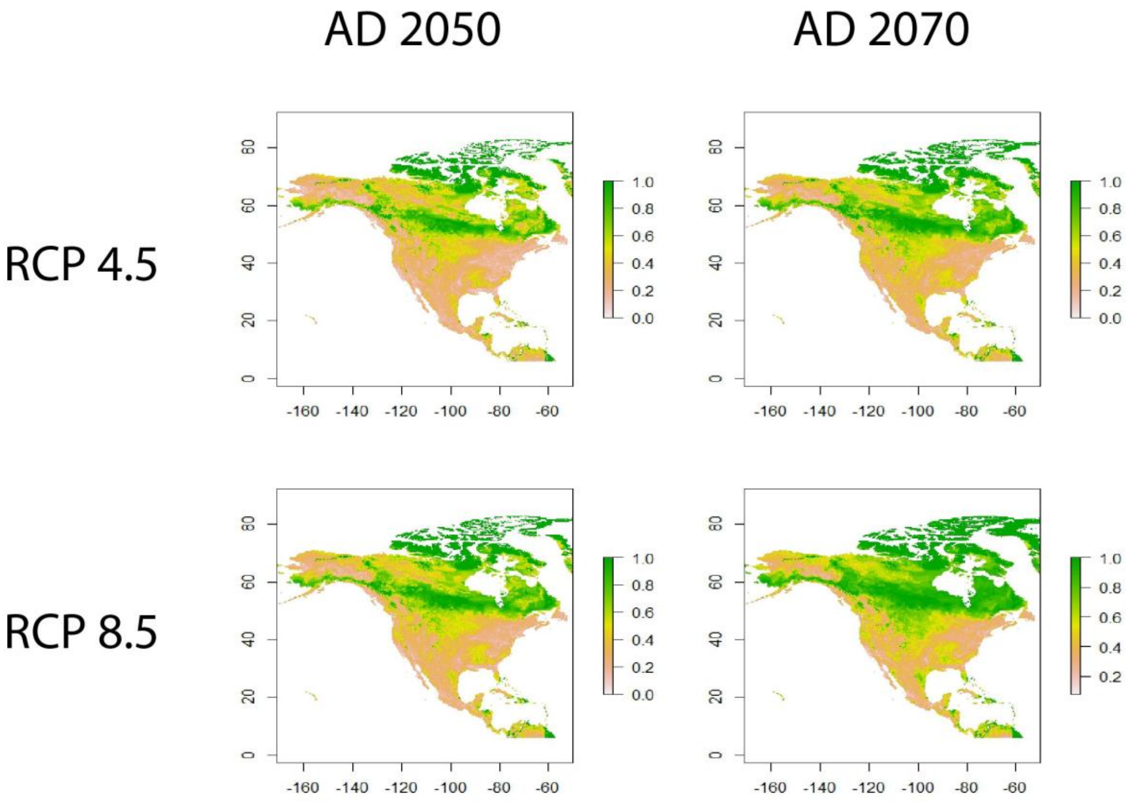

Figure 4.2: Estimated community dissimilarity between contemporary and future communities. Sørenson dissimilarity is calculated between contemporary communities and communities from from each associated future time period (columns) and representative concentration pathway (rows).

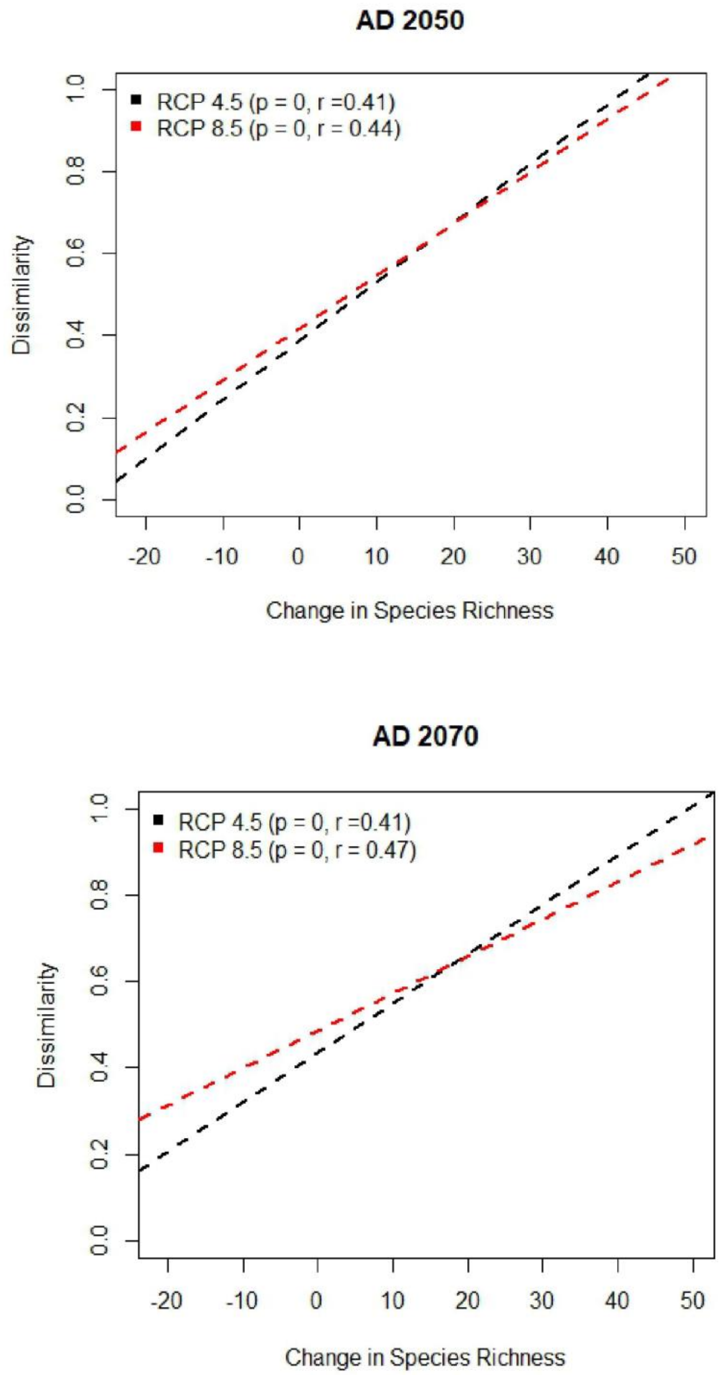

Figure 4.3: Correlation between community dissimilarity and the change in species richness between contemporary communities and the associated future scenarios. The dashed lines represent the correlation trendline for each future scenario.

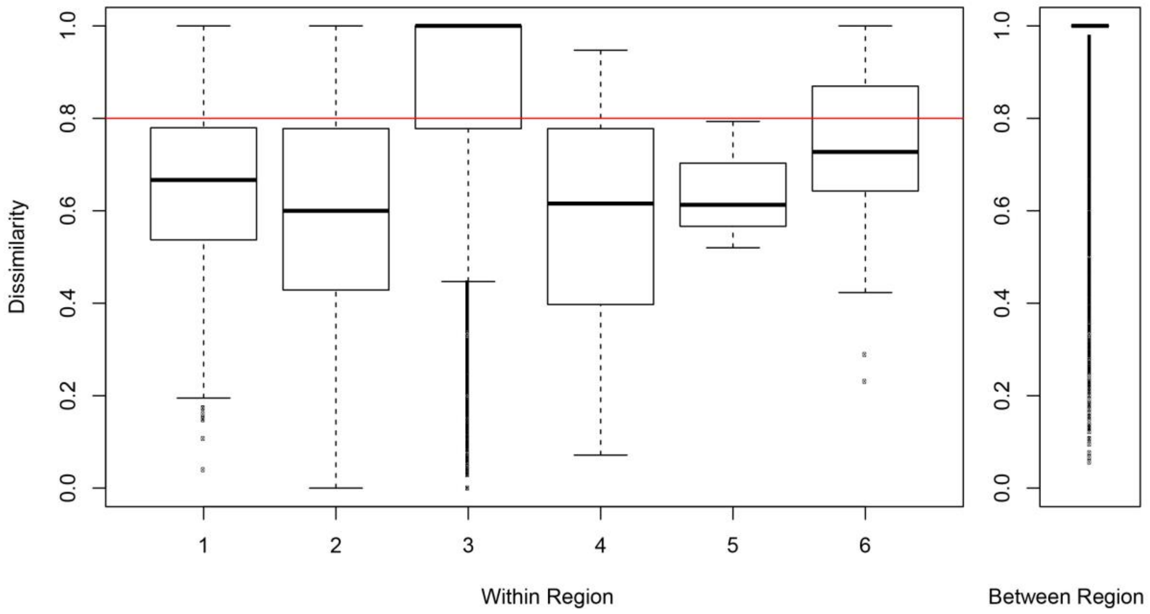

Figure 4.4: Dissimilarity within and between zoogeographic regions. The horizontal red line indicates the dissimilarity threshold of 0.8 used in this study to indicate significantly novel communities, based on the dominant pattern of within-region dissimilarities across regions. See Fig. 4.5 for the spatial location of each region.

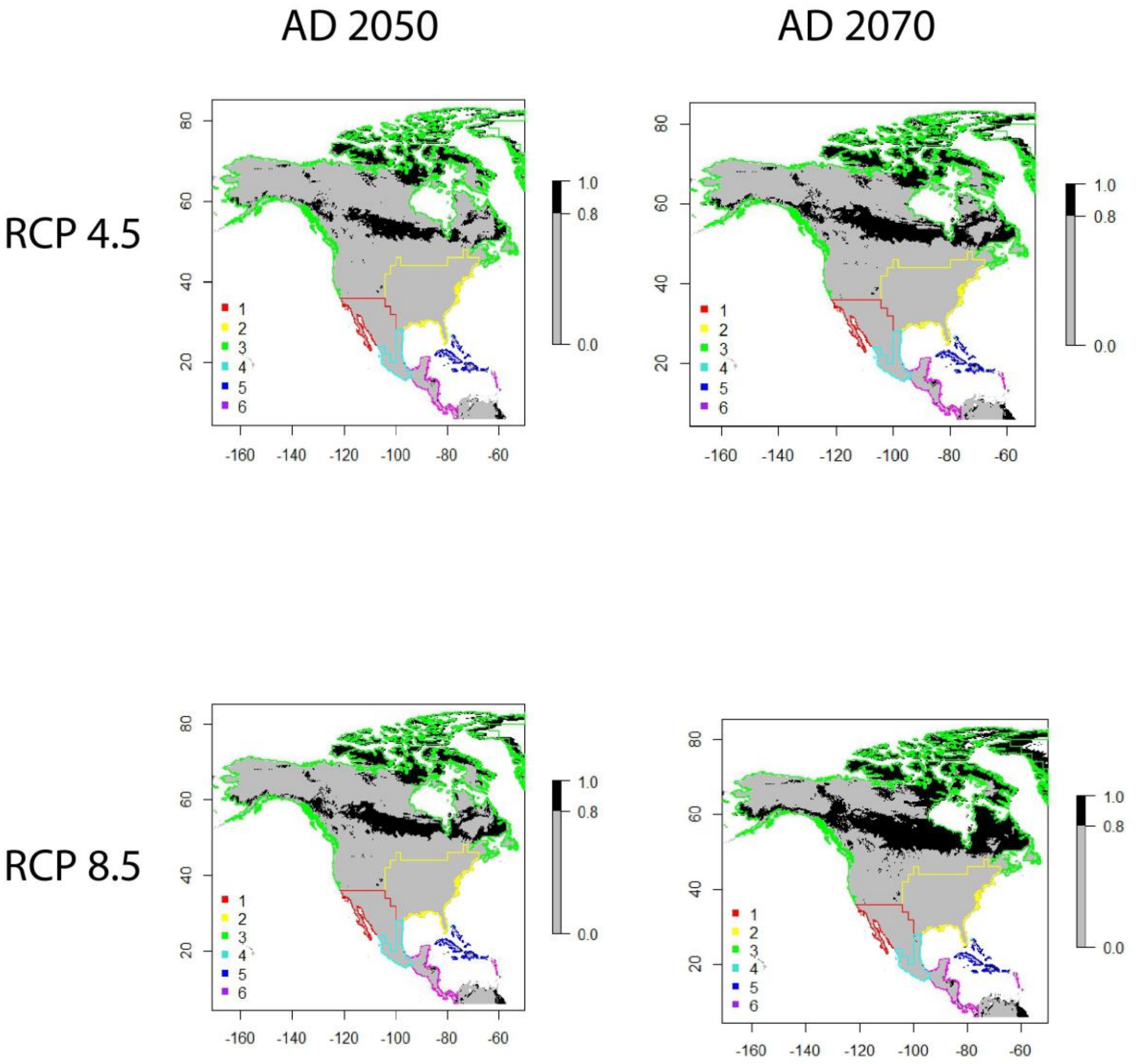

Figure 4.5: Estimated distribution of novel communities and the associated zoogeographic regions. A dissimilarity threshold of 0.80 was used to determine which communities would become novel in the future scenarios. Note: numbers for the zoogeographic regions in this study do not correspond with the associated numbers from Holt et al. (2013).

4.10 Appendix

Table 4.10.1: List of species that models were constructed for in this study. Boyce index values for the contemporary ensemble species distribution models are also shown for each species. Values of 1 indicate that models performed accurately based on the data. Values of 0 indicate the models performed as good as random models and values of -1 indicate that the models performed poorly.

Species	**Boyce Index**
Alces americanus	0.98
Alouatta palliata	0.67
Alouatta pigra	0.87
Ammospermophilus harrisii	0.81
Ammospermophilus interpres	0.88
Ammospermophilus leucurus	0.96
Ammospermophilus nelsoni	0.74
Antilocapra americana	1.00
Aplodontia rufa	0.97
Arborimus albipes	0.92
Arborimus longicaudus	0.93
Ateles geoffroyi	0.91
Baiomys musculus	0.96
Baiomys taylori	0.89
Bassariscus astutus	0.80
Bassariscus sumichrasti	0.75
Blarina carolinensis	0.96
Blarina hylophaga	0.97
Bos bison	0.98
Brachylagus idahoensis	0.92
Caluromys derbianus	0.72
Canis latrans	0.93
Canis lupus	0.98
Canis rufus	0.87
Castor canadensis	0.96
Cervus canadensis	0.99
Chaetodipus arenarius	0.77
Chaetodipus artus	0.65
Chaetodipus baileyi	0.96

Species	**Boyce Index**
Chaetodipus californicus	0.96
Chaetodipus eremicus	0.86
Chaetodipus fallax	0.86
Chaetodipus formosus	0.92
Chaetodipus goldmani	0.78
Chaetodipus hispidus	0.99
Chaetodipus intermedius	0.88
Chaetodipus nelsoni	0.91
Chaetodipus penicillatus	0.93
Chaetodipus pernix	0.90
Chaetodipus rudinoris	0.25
Chaetodipus spinatus	0.45
Condylura cristata	0.98
Conepatus leuconotus	0.96
Conepatus semistriatus	0.76
Cratogeomys castanops	0.97
Cratogeomys merriami	0.92
Cryptotis goldmani	0.74
Cryptotis magna	0.74
Cryptotis mexicana	0.92
Cryptotis parva	0.97
Cuniculus paca	0.91
Cynomys gunnisoni	0.95
Cynomys leucurus	0.96
Cynomys ludovicianus	0.92
Cynomys mexicanus	0.86
Cynomys parvidens	0.93
Dasyprocta mexicana	0.93
Dasyprocta punctata	0.75
Dasypus novemcinctus	0.97
Dicrostonyx groenlandicus	0.96
Didelphis marsupialis	0.93
Didelphis virginiana	0.99
Dipodomys agilis	0.92
Dipodomys californicus	0.92
Dipodomys heermanni	0.89
Dipodomys merriami	0.96
Dipodomys microps	0.94
Dipodomys nelsoni	0.85

Species	**Boyce Index**
Dipodomys nitratoides	0.55
Dipodomys ordii	0.95
Dipodomys panamintinus	0.95
Dipodomys phillipsii	0.95
Dipodomys simulans	0.80
Dipodomys spectabilis	0.92
Dipodomys stephensi	0.36
Dipodomys venustus	0.51
Eira barbara	0.44
Galictis vittata	0.79
Geomys arenarius	0.80
Geomys attwateri	0.51
Geomys breviceps	0.76
Geomys bursarius	0.97
Geomys knoxjonesi	0.78
Geomys personatus	0.81
Geomys pinetis	0.87
Geomys texensis	0.72
Glaucomys sabrinus	0.90
Glaucomys volans	0.99
Gulo gulo	1.00
Habromys lepturus	-0.28
Heteromys desmarestianus	0.73
Heteromys gaumeri	0.77
Lemmiscus curtatus	0.95
Lemmus trimucronatus	0.99
Leopardus pardalis	0.93
Leopardus wiedii	0.91
Lepus alleni	0.84
Lepus americanus	0.96
Lepus californicus	0.98
Lepus callotis	0.93
Lepus othus	0.97
Lepus townsendii	0.98
Liomys irroratus	0.97
Liomys pictus	0.97
Lontra longicaudis	0.83
Lynx canadensis	0.98
Lynx rufus	0.94

Species	**Boyce Index**
Marmosa mexicana	0.91
Marmota broweri	0.95
Marmota caligata	0.98
Marmota flaviventris	0.94
Marmota monax	0.94
Martes pennanti	0.99
Megadontomys cryophilus	0.70
Mephitis macroura	0.96
Mephitis mephitis	0.97
Microdipodops pallidus	0.71
Microtus californicus	0.89
Michrotus chrotorrhinus	0.98
Microtus longicaudus	0.99
Microtus mexicanus	0.87
Microtus miurus	0.99
Microtus mogollonensis	0.96
Microtus montanus	0.95
Microtus ochrogaster	0.98
Microtus oregoni	0.97
Microtus pennsylvanicus	0.99
Microtus pinetorum	0.98
Microtus quasiater	0.89
Microtus richardsoni	0.95
Microtus townsendii	0.82
Microtus xanthognathus	0.96
Mustela erminea	0.94
Mustela frenata	0.97
Mustela nigripes	0.96
Mustela nivalis	0.93
Myocastor coypus	0.93
Myodes californicus	0.95
Myodes gapperi	0.99
Myodes rutilus	0.98
Napaeozapus insignis	0.97
Nasua narica	0.95
Nelsonia neotomodon	0.97
Nelsonia neotomodon	0.97
Neotoma albigula	0.96
Neotoma cinerea	0.99

Species	**Boyce Index**
Neotoma devia	0.86
Neotoma floridana	0.89
Neotoma fuscipes	0.95
Neotoma goldmani	0.94
Neotoma lepida	0.93
Neotoma leucodon	0.94
Neotoma macrotis	0.95
Neotoma magister	0.84
Neotoma mexicana	0.97
Neotoma micropus	0.95
Neotoma phenax	0.86
Neotoma stephensi	0.97
Neotomodon alstoni	0.90
Neovison vison	0.94
Neurotrichus gibbsii	0.92
Notiosorex crawfordi	0.75
Nyctomys sumichrasti	0.91
Ochotona collaris	0.82
Ochotona princeps	0.99
Ochrotomys nuttalli	0.92
Odocoileus hemionus	0.98
Odocoileus virginianus	1.00
Oligoryzomys fulvescens	0.88
Ondatra zibethicus	0.97
Onychomys arenicola	0.93
Onychomys leucogaster	0.98
Onychomys torridus	0.80
Oreamnos americanus	0.90
Orthogeomys grandis	0.83
Orthogeomys hispidus	0.96
Oryzomys alfaroi	0.96
Oryzomys chapmani	0.89
Oryzomys couesi	0.97
Oryzomys melanotis	0.27
Oryzomys palustris	0.98
Oryzomys rostratus	0.80
Osgoodomys banderanus	0.84
Ototylomys phyllotis	0.92
Ovis canadensis	0.98

Species	**Boyce Index**
Ovis dalli	0.95
Panthera onca	0.84
Parascalops breweri	0.96
Pecari tajacu	0.93
Perognathus amplus	0.92
Perognathus fasciatus	0.90
Perognathus flavescens	0.87
Perognathus flavus	0.93
Perognathus inornatus	0.81
Perognathus longimembris	0.97
Perognathus merriami	0.84
Perognathus parvus	0.97
Peromyscus attwateri	0.94
Peromyscus aztecus	0.85
Peromyscus beatae	0.73
Peromyscus boylii	0.95
Peromyscus californicus	0.99
Peromyscus crinitus	0.95
Peromyscus difficilis	0.98
Peromyscus eremicus	0.96
Peromyscus eva	0.62
Peromyscus fraterculus	0.70
Peromyscus furvus	0.79
Peromyscus gossypinus	0.99
Peromyscus gratus	0.94
Peromyscus keeni	0.99
Peromyscus leucopus	1.00
Peromyscus levipes	0.82
Peromyscus maniculatus	0.99
Peromyscus megalops	0.92
Peromyscus melanocarpus	0.69
Peromyscus melanophrys	0.98
Peromyscus melanotis	0.97
Peromyscus merriami	0.62
Peromyscus mexicanus	0.96
Peromyscus nasutus	0.98
Peromyscus pectoralis	0.97
Peromyscus perfulvus	0.19
Peromyscus polionotus	0.95

Species	**Boyce Index**
Peromyscus simulus	0.54
Peromyscus spicilegus	0.81
Peromyscus truei	0.97
Peromyscus zarhynchus	0.80
Phenacomys intermedius	0.96
Philander opossum	0.83
Podomys floridanus	0.96
Potos flavus	0.78
Procyon lotor	0.97
Puma concolor	0.95
Puma yagouaroundi	0.87
Rangifer tarandus	0.96
Reithrodontomys chrysopsis	0.87
Reithrodontomys fulvescens	0.98
Reithrodontomys gracilis	0.79
Reithrodontomys humulis	0.95
Reithrodontomys megalotis	0.98
Reithrodontomys mexicanus	0.81
Reithrodontomys microdon	0.88
Reithrodontomys montanus	0.94
Reithrodontomys raviventris	-0.01
Reithrodontomys sumichrasti	0.92
Romerolagus diazi	0.74
Scalopus aquaticus	0.98
Scapanus latimanus	0.98
Scapanus orarius	0.93
Scapanus townsendii	0.82
Sciurus aberti	0.96
Sciurus alleni	0.82
Sciurus arizonensis	0.95
Sciurus aureogaster	0.93
Sciurus carolinensis	0.99
Sciurus colliaei	0.87
Sciurus deppei	0.98
Sciurus griseus	0.95
Sciurus nayaritensis	0.89
Sciurus niger	0.99
Sciurus oculatus	0.71
Sciurus yucatanensis	0.93

Species	**Boyce Index**
Sigmodon alleni	0.83
Sigmodon arizonae	0.68
Sigmodon fulviventer	0.93
Sigmodon hispidus	0.97
Sigmodon leucotis	0.87
Sigmodon mascotensis	0.75
Sigmodon ochrognathus	0.91
Sorex arcticus	0.97
Sorex bendirii	0.93
Sorex cinereus	0.96
Sorex dispar	0.84
Sorex fumeus	0.97
Sorex haydeni	0.94
Sorex hoyi	0.99
Sorex merriami	0.87
Sorex monticolus	0.99
Sorex nanus	0.96
Sorex ornatus	0.91
Sorex pacificus	0.81
Sorex palustris	0.99
Sorex preblei	0.91
Sorex rohweri	0.55
Sorex saussurei	0.43
Sorex trowbridgii	0.98
Sorex tundrensis	0.99
Sorex ugyunak	0.89
Sorex vagrans	0.98
Sorex ventralis	0.46
Spermophilus beecheyi	0.91
Spermophilus beldingi	0.92
Spermophilus columbianus	0.90
Spermophilus franklinii	0.81
Spermophilus lateralis	0.92
Spermophilus madrensis	0.83
Spermophilus mexicanus	0.95
Spermophilus mohavensis	0.77
Spermophilus parryii	0.98
Spermophilus richardsonii	0.90
Spermophilus spilosoma	0.94

Species	**Boyce Index**
Spermophilus tereticaudus	0.75
Spermophilus tridecemlineatus	0.97
Spermophilus variegatus	0.93
Spermophilus washingtoni	0.93
Spilogale gracilis	0.97
Spilogale putorius	0.89
Spilogale pygmaea	0.64
Sylvilagus aquaticus	0.94
Sylvilagus audubonii	0.99
Sylvilagus bachmani	0.92
Sylvilagus brasiliensis	0.94
Sylvilagus cunicularius	0.88
Sylvilagus floridanus	0.96
Sylvilagus nuttallii	0.89
Sylvilagus obscurus	0.80
Sylvilagus palustris	0.95
Sylvilagus transitionalis	0.66
Synaptomys borealis	0.95
Synaptomys cooperi	0.90
Tamandua mexicana	0.88
Tamias striatus	1.00
Tamiasciurus douglasii	0.98
Tamiasciurus hudsonicus	0.99
Tapirus bairdii	0.69
Taxidea taxus	0.95
Tayassu pecari	0.89
Thomomys bottae	0.99
Thomomys bulbivorus	0.38
Thomomys idahoensis	0.94
Thomomys mazama	0.92
Thomomys monticola	0.87
Thomomys talpoides	0.98
Thomomys townsendii	0.95
Thomomys umbrinus	0.90
Tlacuatzin canescens	0.72
Tylomys nudicaudus	0.88
Urocyon cinereoargenteus	0.98
Ursus americanus	1.00

Species	**Boyce Index**
Ursus arctos	0.97
Vulpes lagopus	0.98
Vulpes macrotis	0.90
Vulpes velox	0.80
Vulpes vulpes	0.95
Zapus hudsonius	0.99
Zapus princeps	0.99
Zapus trinotatus	0.87